

PDF hosted at the Radboud Repository of the Radboud University Nijmegen

The following full text is a preprint version which may differ from the publisher's version.

For additional information about this publication click this link.

<http://hdl.handle.net/2066/92383>

Please be advised that this information was generated on 2021-06-22 and may be subject to change.

Study of Jet Shapes in Inclusive Jet Production in pp Collisions at $\sqrt{s} = 7$ TeV using the ATLAS Detector

(The ATLAS Collaboration)
(Dated: January 4, 2011)

Jet shapes have been measured in inclusive jet production in proton-proton collisions at $\sqrt{s} = 7$ TeV using 3 pb^{-1} of data recorded by the ATLAS experiment at the LHC. Jets are reconstructed using the anti- k_t algorithm with transverse momentum $30 \text{ GeV} < p_T < 600 \text{ GeV}$ and rapidity in the region $|y| < 2.8$. The data are corrected for detector effects and compared to several leading-order QCD matrix elements plus parton shower Monte Carlo predictions, including different sets of parameters tuned to model fragmentation processes and underlying event contributions in the final state. The measured jets become narrower with increasing jet transverse momentum and the jet shapes present a moderate jet rapidity dependence. Within QCD, the data test a variety of perturbative and non-perturbative effects. In particular, the data show sensitivity to the details of the parton shower, fragmentation, and underlying event models in the Monte Carlo generators. For an appropriate choice of the parameters used in these models, the data are well described.

PACS numbers: 13.85.Ni, 13.85.Qk, 14.65.Ha, 87.18.Sn

I. INTRODUCTION

The study of the jet shapes [1] in proton-proton collisions provides information about the details of the parton-to-jet fragmentation process, leading to collimated flows of particles in the final state. The internal structure of sufficiently energetic jets is mainly dictated by the emission of multiple gluons from the primary parton, calculable in perturbative QCD (pQCD) [2]. The shape of the jet depends on the type of partons (quark or gluon) that give rise to jets in the final state [3], and is also sensitive to non-perturbative fragmentation effects and underlying event (UE) contributions from the interaction between proton remnants. A proper modeling of the soft contributions is crucial for the understanding of jet production in hadron-hadron collisions and for the comparison of the jet cross section measurements with pQCD theoretical predictions [4, 5]. In addition, jet shape related observables have been recently proposed [6] to search for new physics in event topologies with highly boosted particles in the final state decaying into multiple jets of particles.

Jet shape measurements have previously been performed in $p\bar{p}$ [7], $e^\pm p$ [8], and e^+e^- [9] collisions. In this paper, measurements of differential and integrated jet shapes in proton-proton collisions at $\sqrt{s} = 7$ TeV are presented for the first time. The study uses data collected by the ATLAS experiment corresponding to 3 pb^{-1} of total integrated luminosity. The measurements are corrected for detector effects and compared to several Monte Carlo (MC) predictions based on pQCD leading-order (LO) matrix elements plus parton showers, and including different phenomenological models to describe fragmentation processes and UE contributions.

The paper is organised as follows. The detector is described in the next section. Section 3 discusses the simulations used in the measurements, while Section 4 and Section 5 provide details on jet reconstruction and event selection, respectively. Jet shape observables are defined in Section 6. The procedure used to correct the measurements for detector effects is explained in Section 7, and the study of systematic uncertainties is discussed in Section 8. The jet shape measurements are presented in Section 9. Finally, Section 10 is devoted to summary and conclusions.

II. EXPERIMENTAL SETUP

The ATLAS detector [10] covers nearly the entire solid angle around the collision point with layers of tracking detectors, calorimeters, and muon chambers. For the measurements presented in this paper, the tracking system and calorimeters are of particular importance.

The ATLAS inner detector has full coverage in ϕ [11] and covers the pseudorapidity range $|\eta| < 2.5$. It consists of a silicon pixel detector, a silicon microstrip detector and a transition radiation tracker, all immersed in a 2 Tesla magnetic field. High granularity liquid-argon (LAr) electromagnetic sampling calorimeters cover the pseudorapidity range $|\eta| < 3.2$. The hadronic calorimetry in the range $|\eta| < 1.7$ is provided by a scintillator-tile calorimeter, which is separated into a large barrel and two smaller extended barrel cylinders, one on either side of the central barrel. In the end-caps ($|\eta| > 1.5$), LAr hadronic calorimeters match the outer $|\eta|$ limits of the end-cap electromagnetic calorimeters. The LAr forward calorimeters provide both electromagnetic and hadronic energy measurements, and they extend the coverage to $|\eta| < 4.9$.

The trigger system uses three consecutive trigger levels to select events. The Level-1 (L1) trigger is based on custom-built hardware to process the incoming data with a fixed latency of $2.5 \mu\text{s}$. This is the only trigger level used in this analysis. The events studied here are selected either by the system of minimum-bias trigger scintillators (MBTS) or by the calorimeter trigger. The MBTS detector [12] consists of 32 scintillator counters of thickness 2 cm organized in two disks. The disks are installed on the inner face of the end-cap calorimeter cryostats at $z = \pm 356$ cm, such that the disk surface is perpendicular to the beam direction. This leads to a coverage of $2.09 < |\eta| < 3.84$. The jet trigger is based on the selection of jets according to their transverse energy, E_T . The L1 jet reconstruction uses the so called jet elements, which are made of electromagnetic and hadronic cells grouped together with a granularity of $\Delta\phi \times \Delta\eta = 0.2 \times 0.2$ for $|\eta| < 3.2$. The jet finding is based on a sliding window algorithm with steps of one jet element, and the jet E_T is computed in a window of configurable size around the jet.

III. MONTE CARLO SIMULATION

Monte Carlo simulated samples are used to determine and correct for detector effects, and to estimate part of the systematic uncertainties on the measured jet shapes. Samples of inclusive jet events in proton-proton collisions at $\sqrt{s} = 7$ TeV are produced using both PYTHIA 6.4.21 [13] and HERWIG++ 2.4.2 [14] event generators. These MC programs implement LO pQCD matrix elements for $2 \rightarrow 2$ processes plus parton shower in the leading logarithmic approximation, and the string [15] and cluster [16] models for fragmentation into hadrons, respectively. In the case of PYTHIA, different MC samples with slightly different parton shower and UE modeling in the final state are considered. The samples are generated using three tuned sets of parameters denoted as ATLAS-MC09 [17], DW [18], and Perugia2010 [19]. In addition, a special PYTHIA-Perugia2010 sample without UE contributions is generated. Finally, inclusive jet samples are also produced using the ALPGEN 2.13 [20] event generator interfaced with HERWIG 6.5 [21] and JIMMY 3.41 [22] to model the UE contributions. HERWIG++ and PYTHIA-MC09 samples are generated with MRST2007LO* [23] parton density functions (PDFs) inside the proton, PYTHIA-Perugia2010 and PYTHIA-DW with CTEQ5L [24] PDFs, and ALPGEN with CTEQ61L [25] PDFs.

The MC generated samples are passed through a full simulation [26] of the ATLAS detector and trigger, based on GEANT4 [27]. The Quark Gluon String Precompound (QGSP) model [28] is used for the fragmentation of the nucleus, and the Bertini cascade (BERT) model [29] for the description of the interactions of the hadrons in the medium of the nucleus. Test-beam measurements for single pions have shown that these simulation settings best describe the response and resolution in the barrel [30] and end-cap [31] calorimeters. The simulated events are then reconstructed and analyzed with the same analysis chain as for the data, and the same trigger and event selection criteria.

IV. JET RECONSTRUCTION

Jets are defined using the anti- k_t jet algorithm [32] with distance parameter (in $y-\phi$ space) $R = 0.6$, and the energy depositions in calorimeter clusters as input in both data and MC events. Topological clusters [5] are built around seed calorimeter cells with $|E_{\text{cell}}| > 4\sigma$, where σ is defined as the RMS of the cell energy noise distribution, to which all directly neighboring cells are added. Further neighbors of neighbors are iteratively added for all cells with signals above a secondary threshold $|E_{\text{cell}}| > 2\sigma$, and the clusters are set massless. In addition, in the simulated events jets are also defined at the particle level [33] using as input all the final state particles from the MC generation.

The anti- k_t algorithm constructs, for each input object (either energy cluster or particle) i , the quantities d_{ij} and d_{iB} as follows:

$$d_{ij} = \min(k_{ti}^{-2}, k_{tj}^{-2}) \frac{(\Delta R)_{ij}^2}{R^2}, \quad (1)$$

$$d_{iB} = k_{ti}^{-2}, \quad (2)$$

where

$$(\Delta R)_{ij}^2 = (y_i - y_j)^2 + (\phi_i - \phi_j)^2, \quad (3)$$

k_{ti} is the transverse momentum of object i with respect to the beam direction, ϕ_i its azimuthal angle, and y_i its rapidity. A list containing all the d_{ij} and d_{iB} values is compiled. If the smallest entry is a d_{ij} , objects i and j are combined (their four-vectors are added) and the list is updated. If the smallest entry is a d_{iB} , this object is considered a complete ‘‘jet’’ and is removed from the list. As defined above, d_{ij} is a distance measure between two objects, and

Trigger Information		
p_T (GeV)	trigger configurations	integrated luminosity (nb ⁻¹)
30 - 60	MBTS	0.7
60 - 80	L1_5/MBTS	17
80 - 110	L1_10/L1_5/MBTS	96
110 - 160	L1_15/L1_10/L1_5/MBTS	545
160 - 210	L1_30/L1_15/L1_10/L1_5/MBTS	1878
210 - 600	L1_55/L1_30/L1_15/L1_10/L1_5/MBTS	2993

TABLE I: For the various jet p_T ranges, the trigger configurations used to collect the data and the corresponding total integrated luminosity. MBTS denotes the use of the minimum-bias trigger scintillators, while L1_5, L1_10, L1_15, L1_30, and L1_55 correspond to L1 calorimeter triggers with 5, 10, 15, 30, and 55 GeV thresholds, respectively.

d_{iB} is a similar distance between the object and the beam. Thus the variable R is a resolution parameter which sets the relative distance at which jets are resolved from each other as compared to the beam. The anti- k_t algorithm is theoretically well-motivated [32] and produces geometrically well-defined (“cone-like”) jets.

According to MC simulation, the measured jet angular variables, y and ϕ , are reconstructed with a resolution of better than 0.05 units, which improves as the jet transverse momentum, p_T , increases. The measured jet p_T is corrected to the particle level scale [5] using an average correction, computed as a function of jet transverse momentum and pseudorapidity, and extracted from MC simulation.

V. EVENT SELECTION

The data were collected during the first LHC run at $\sqrt{s} = 7$ TeV with the ATLAS tracking detectors, calorimeters and magnets operating at nominal conditions. Events are selected online using different L1 trigger configurations in such a way that, in the kinematic range for the jets considered in this study (see below), the trigger selection is fully efficient and does not introduce any significant bias in the measured jet shapes. Table 1 presents the trigger configurations employed in each p_T region and the corresponding integrated luminosity. The unrescaled trigger thresholds were increased with time to keep pace with the LHC instantaneous luminosity evolution. For jet p_T smaller than 60 GeV, the data are selected using the signals from the MBTS detectors on either side of the interaction point. Only events in which the MBTS recorded one or more counters above threshold on at least one side are retained. For larger p_T , the events are selected using either MBTS or L1 calorimeter based triggers (see Section 2) with a minimum transverse energy threshold at the electromagnetic scale [34] that varies between 5 GeV (L1_5) and 55 GeV (L1_55), depending on when the data were collected and the p_T range considered (see Table 1).

The events are required to have one and only one reconstructed primary vertex with a z -position within 10 cm of the origin of the coordinate system, which suppresses pile-up contributions from multiple proton-proton interactions in the same bunch crossing, beam-related backgrounds and cosmic rays. In this analysis, events are required to have at least one jet with corrected transverse momentum $p_T > 30$ GeV and rapidity $|y| < 2.8$. This corresponds approximately to the kinematic region, in the absolute four momentum transfer squared Q^2 - Bjorken- x plane, of $10^3 \text{ GeV}^2 < Q^2 < 4 \times 10^5 \text{ GeV}^2$ and $6 \times 10^{-4} < x < 2 \times 10^{-2}$. Additional quality criteria are applied to ensure that jets are not produced by noisy calorimeter cells, and to avoid problematic detector regions.

VI. JET SHAPE DEFINITION

The internal structure of the jet is studied in terms of the differential and integrated jet shapes, as reconstructed using the uncorrected energy clusters in the calorimeter associated with the jet. The differential jet shape $\rho(r)$ as a function of the distance $r = \sqrt{\Delta y^2 + \Delta \phi^2}$ to the jet axis is defined as the average fraction of the jet p_T that lies inside an annulus of inner radius $r - \Delta r/2$ and outer radius $r + \Delta r/2$ around the jet axis:

$$\rho(r) = \frac{1}{\Delta r} \frac{1}{N^{\text{jet}}} \sum_{\text{jets}} \frac{p_T(r - \Delta r/2, r + \Delta r/2)}{p_T(0, R)}, \quad \Delta r/2 \leq r \leq R - \Delta r/2, \quad (4)$$

where $p_T(r_1, r_2)$ denotes the summed p_T of the clusters in the annulus between radius r_1 and r_2 , N^{jet} is the number of

jets, and $R = 0.6$ and $\Delta r = 0.1$ are used. The points from the differential jet shape at different r values are correlated since, by definition, $\sum_0^R \rho(r) \Delta r = 1$. Alternatively, the integrated jet shape $\Psi(r)$ is defined as the average fraction of the jet p_T that lies inside a cone of radius r concentric with the jet cone:

$$\Psi(r) = \frac{1}{N_{\text{jet}}} \sum_{\text{jets}} \frac{p_T(0, r)}{p_T(0, R)}, \quad 0 \leq r \leq R, \quad (5)$$

where, by definition, $\Psi(r = R) = 1$, and the points at different r values are correlated. The same definitions apply to simulated calorimeter clusters and final-state particles in the MC generated events to define differential and integrated jet shapes at the calorimeter and particle levels, respectively. The jet shape measurements are performed in different regions of jet p_T and $|y|$, and a minimum of 100 jets in data are required in each region to limit the statistical fluctuations on the measured values.

VII. CORRECTION FOR DETECTOR EFFECTS

The measured differential and integrated jet shapes, as determined by using calorimeter topological clusters, are corrected for detector effects back to the particle level. This is done using MC simulated events and a bin-by-bin correction procedure that also accounts for the efficiency of the selection criteria and of the jet reconstruction in the calorimeter. PYTHIA-Perugia2010 provides a reasonable description of the measured jet shapes in all regions of jet p_T and $|y|$, and is therefore used to compute the correction factors. Here, the method is described in detail for the differential case. A similar procedure is employed to correct independently the integrated measurements. The correction factors $U(r, p_T, |y|)$ are computed separately in each jet p_T and $|y|$ region. They are defined as the ratio between the jet shapes at the particle level $\rho(r)_{mc}^{par}$, obtained using particle-level jets in the kinematic range under consideration, and the reconstructed jet shapes at the calorimeter level $\rho(r)_{mc}^{cal}$, after the selection criteria are applied and using calorimeter-level jets in the given p_T and $|y|$ range. The correction factors $U(r, p_T, |y|) = \rho(r)_{mc}^{par} / \rho(r)_{mc}^{cal}$ present a moderate p_T and $|y|$ dependence and vary between 0.95 and 1.1 as r increases. For the integrated jet shapes, the correction factors differ from unity by less than 5%. The corrected jet shape measurements in each p_T and $|y|$ region are computed by multiplying bin-by-bin the measured uncorrected jet shapes in data by the corresponding correction factors.

VIII. SYSTEMATIC UNCERTAINTIES

A detailed study of systematic uncertainties on the measured differential and integrated jet shapes has been performed. The impact on the differential measurements is described here in detail.

- The absolute energy scale of the individual clusters belonging to the jet is varied in the data according to studies using isolated tracks [5], which parametrize the uncertainty on the calorimeter cluster energy as a function of p_T and η of the cluster. This introduces a systematic uncertainty on the measured differential jet shapes that varies between 3% to 15% as r increases and constitutes the dominant systematic uncertainty in this analysis.
- The systematic uncertainty on the measured jet shapes arising from the details of the model used to simulate calorimeter showers in the MC events is studied. A different simulated sample is considered, where the FRITIOF [35] plus BERT showering model is employed instead of the QGSP plus BERT model. FRITOF+BERT provides the second best description of the test-beam results [30] after QGSP+BERT. This introduces an uncertainty on the measured differential jet shapes that varies between 1% to 4%, and is approximately independent of p_T and $|y|$.
- The measured jet p_T is varied by 2% to 8%, depending on p_T and $|y|$, to account for the remaining uncertainty on the absolute jet energy scale [5], after removing contributions already accounted for and related to the energy of the single clusters and the calorimeter shower modeling, as discussed above. This introduces an uncertainty of about 3% to 5% in the measured differential jet shapes.
- The 14% uncertainty on the jet energy resolution [5] translates into a smaller than 2% effect on the measured differential jet shapes.

- The correction factors are recomputed using HERWIG++, which implements different parton shower, fragmentation and UE models than PYTHIA, and compared to PYTHIA-Perugia2010. In addition, the correction factors are also computed using ALPGEN and PYTHIA-DW for $p_T < 110$ GeV, where these MC samples provide a reasonable description of the uncorrected shapes in the data. The results from HERWIG++ encompass the variations obtained using all the above generators and are conservatively adopted in all p_T and $|y|$ ranges to compute systematic uncertainties on the differential jet shapes. These uncertainties increase between 2% and 10% with increasing r .
- An additional 1% uncertainty on the differential measurements is included to account for deviations from unity (non-closure) in the bin-by-bin correction procedure when applied to a statistically independent MC sample.
- No significant dependence on instantaneous luminosity is observed in the measured jet shapes, indicating that residual pile-up contributions are negligible after selecting events with only one reconstructed primary vertex.
- It was verified that the presence of small dead calorimeter regions in the data does not affect the measured jet shapes.

The different systematic uncertainties are added in quadrature to the statistical uncertainty to obtain the final result. The total uncertainty for differential jet shapes decreases with increasing p_T and varies typically between 3% and 10% (10% and 20%) at $r = 0.05$ ($r = 0.55$). The total uncertainty is dominated by the systematic uncertainty, except at very large p_T where the measurements are still statistically limited. In the case of the integrated measurements, the total systematic uncertainty varies between 10% and 2% (4% and 1%) at $r = 0.1$ ($r = 0.3$) as p_T increases, and vanishes as r approaches the edge of the jet cone.

Finally, the jet shape analysis is also performed using either tracks from the inner detector inside the jet cone, as reconstructed using topological clusters; or calorimeter towers of fixed size 0.1×0.1 ($y - \phi$ space) instead of topological clusters as input to the jet reconstruction algorithm. For the former, the measurements are limited to jets with $|y| < 1.9$, as dictated by the tracking coverage and the chosen size of the jet. After the data are corrected back to particle level, the results from these alternative analyses are consistent with the nominal results, with maximum deviations in the differential measurements of about 2% (5%) at $r=0.05$ ($r=0.55$), well within the quoted systematic uncertainties.

IX. RESULTS

The measurements presented in this article refer to differential and integrated jet shapes, $\rho(r)$ and $\Psi(r)$, corrected at the particle level and obtained for anti- k_t jets with distance parameter $R = 0.6$ in the region $|y| < 2.8$ and $30 \text{ GeV} < p_T < 600 \text{ GeV}$. The measurements are presented in separate bins of p_T and $|y|$. Tabulated values of the results are available in the Appendix and in Ref. [36].

Figures 1 to 3 show the measured differential jet shapes as a function of r in different p_T ranges. The dominant peak at small r indicates that the majority of the jet momentum is concentrated close to the jet axis. At low p_T , more than 80% of the transverse momentum is contained within a cone of radius $r = 0.3$ around the jet direction. This fraction increases up to 95% at very high p_T , showing that jets become narrower as p_T increases. This is also observed in Fig. 4, where the measured $1 - \Psi(0.3)$, the fraction of the jet transverse momentum outside a fixed radius $r = 0.3$, decreases as a function of p_T .

The data are compared to predictions from HERWIG++, ALPGEN, PYTHIA-Perugia2010, and PYTHIA-MC09 in Fig. 1 to Fig. 4(a); and to predictions from PYTHIA-DW and PYTHIA-Perugia2010 with and without UE contributions in Fig. 4(b). The jet shapes predicted by PYTHIA-Perugia2010 provide a reasonable description of the data, while HERWIG++ predicts broader jets than the data at low and very high p_T . The PYTHIA-DW predictions are in between PYTHIA-Perugia2010 and HERWIG++ at low p_T and produce jets which are slightly narrower at high p_T . ALPGEN is similar to PYTHIA-Perugia2010 at low p_T , but produces jets significantly narrower than the data at high p_T . PYTHIA-MC09 tends to produce narrower jets than the data in the whole kinematic range under study. The latter may be attributed to an inadequate modeling of the soft gluon radiation and UE contributions in PYTHIA-MC09 samples, in agreement with previous observations of the particle flow activity in the final state [12]. Finally, Fig. 4(b) shows that PYTHIA-Perugia2010 without UE contributions predicts jets much narrower than the data at low p_T . This confirms the sensitivity of jet shape observables in the region $p_T < 160 \text{ GeV}$ to a proper description of the UE activity in the final state.

The dependence on $|y|$ is shown in Fig. 5, where the measured jet shapes are presented separately in five different jet rapidity regions and different p_T bins, for jets with $p_T < 400 \text{ GeV}$. At high p_T , the measured $1 - \Psi(0.3)$ shape presents a mild $|y|$ dependence, indicating that the jets become slightly narrower in the forward regions. This tendency is

observed also in the various MC samples. Similarly, Figs. 6 and 7 present the measured $1 - \Psi(0.3)$ as a function of p_T in the different $|y|$ regions compared to PYTHIA-Perugia2010 predictions. The result of χ^2 tests to the data in Fig. 7 with respect to the predictions from the different MC generators are reported in Table 7, for each of the five rapidity regions. Here the different sources of systematic uncertainty are considered independent and fully correlated across p_T bins (see Appendix). As already discussed, PYTHIA-Perugia2010 provides the best overall description of the data, while PYTHIA-Perugia2010 without UE contributions and ALPGEN show the largest discrepancies.

Finally, and only for illustration, the typical shapes of quark- and gluon-initiated jets, as determined using events generated with PYTHIA-Perugia2010, are also shown in Figs. 6 and 7. For this purpose, MC events are selected with at least two particle-level jets with $p_T > 30$ GeV and $|y| < 2.8$ in the final state. The two leading jets in this dijet sample are classified as quark-initiated or gluon-initiated jets by matching (in $y - \phi$ space) their direction with one of the outgoing partons from the QCD $2 \rightarrow 2$ hard process. At low p_T the measured jet shapes are similar to those from gluon-initiated jets, as expected from the dominance of hard processes with gluons in the final state. At high p_T , where the impact of the UE contributions becomes smaller (see Fig. 4(b)), the observed trend with p_T in the data is mainly attributed to a changing quark- and gluon-jet mixture in the final state, convoluted with perturbative QCD effects related to the running of the strong coupling.

X. SUMMARY AND CONCLUSIONS

In summary, jet shapes have been measured in inclusive jet production in proton-proton collisions at $\sqrt{s} = 7$ TeV using 3 pb^{-1} of data recorded by the ATLAS experiment at the LHC. Jets are reconstructed using the anti- k_t algorithm with distance parameter $R = 0.6$ in the kinematic region $30 \text{ GeV} < p_T < 600 \text{ GeV}$ and $|y| < 2.8$. The data are corrected for detector effects and compared to different leading-order matrix elements plus parton shower MC predictions. The measured jets become narrower as the jet transverse momentum and rapidity increase, although with a rather mild rapidity dependence. The data are reasonably well described by PYTHIA-Perugia2010. HERWIG++ predicts jets slightly broader than the data, whereas ALPGEN interfaced with HERWIG and JIMMY, PYTHIA-DW, and PYTHIA-MC09 all predict jets narrower than the data. Within QCD, the data show sensitivity to a variety of perturbative and non-perturbative effects. The results reported in this paper indicate the potential of jet shape measurements at the LHC to constrain the current phenomenological models for soft gluon radiation, UE activity, and non-perturbative fragmentation processes in the final state.

XI. ACKNOWLEDGEMENTS

We wish to thank CERN for the efficient commissioning and operation of the LHC during this initial high-energy data-taking period as well as the support staff from our institutions without whom ATLAS could not be operated efficiently.

We acknowledge the support of ANPCyT, Argentina; YerPhI, Armenia; ARC, Australia; BMWF, Austria; ANAS, Azerbaijan; SSTC, Belarus; CNPq and FAPESP, Brazil; NSERC, NRC and CFI, Canada; CERN; CONICYT, Chile; CAS, MOST and NSFC, China; COLCIENCIAS, Colombia; MSMT CR, MPO CR and VSC CR, Czech Republic; DNRF, DNSRC and Lundbeck Foundation, Denmark; ARTEMIS, European Union; IN2P3-CNRS, CEA-DSM/IRFU, France; GNAS, Georgia; BMBF, DFG, HGF, MPG and AvH Foundation, Germany; GSRT, Greece; ISF, MINERVA, GIF, DIP and Benoziyo Center, Israel; INFN, Italy; MEXT and JSPS, Japan; CNRST, Morocco; FOM and NWO, Netherlands; RCN, Norway; MNiSW, Poland; GRICES and FCT, Portugal; MERYS (MECTS), Romania; MES of Russia and ROSATOM, Russian Federation; JINR; MSTB, Serbia; MSSR, Slovakia; ARRS and MVZT, Slovenia; DST/NRF, South Africa; MICINN, Spain; SRC and Wallenberg Foundation, Sweden; SER, SNSF and Cantons of Bern and Geneva, Switzerland; NSC, Taiwan; TAEK, Turkey; STFC, the Royal Society and Leverhulme Trust, United Kingdom; DOE and NSF, United States of America.

The crucial computing support from all WLCG partners is acknowledged gratefully, in particular from CERN and the ATLAS Tier-1 facilities at TRIUMF (Canada), NDGF (Denmark, Norway, Sweden), CC-IN2P3 (France), KIT/GridKA (Germany), INFN-CNAF (Italy), NL-T1 (Netherlands), PIC (Spain), ASGC (Taiwan), RAL (UK) and BNL (USA) and in the Tier-2 facilities worldwide.

-
- [1] S. D. Ellis, Z. Kunszt and D. E. Soper, Phys. Rev. Lett. **69** 3615 (1992).
 [2] D. J. Gross and F. Wilczek, Phys. Rev. D **8** 3633 (1973).

- [3] Inclusive jet shape studies have a very limited sensitivity to the presence of a small contribution from heavy-flavor quarks in the final state.
- [4] The CDF Collaboration, A. Abulencia *et al.*, Phys. Rev. D **75** 092006 (2007).
The D0 Collaboration, V. M. Abazov *et al.*, Phys. Rev. Lett. **101** 062001 (2008).
The CDF Collaboration, T. Aaltonen *et al.*, Phys. Rev. D **78** 052006 (2008).
- [5] The ATLAS Collaboration, G. Aad *et al.*, CERN-PH-EP-2010-034; arXiv:1009.5908 (2010); accepted for publication in Eur. Phys. J. C, and references therein.
- [6] J. M. Butterworth, A. R. Davison, M. Rubin and G. P. Salam, Phys. Rev. Lett. **100** 242001 (2008).
D. Kaplan *et al.*, Phys. Rev. Lett. **101** 142001 (2008).
G. Salam, Eur. Phys. J. C **67** 637 (2010).
- [7] The CDF Collaboration, D. Acosta *et al.*, Phys. Rev. D **71** 112002 (2005).
The CDF Collaboration, F. Abe *et al.*, Phys. Rev. Lett. **70** 713 (1993).
The D0 Collaboration, S. Abachi *et al.*, Phys. Lett. B **357** 500 (1995).
- [8] The ZEUS Collaboration, S. Chekanov *et al.*, Nucl. Phys. B **700** 3 (2004).
The ZEUS Collaboration, J. Breitweg *et al.*, Eur. Phys. J. C **8** 3 367 (1999).
The H1 Collaboration, C. Adloff *et al.*, Nucl. Phys. B **545** 3 (1999).
The ZEUS Collaboration, J. Breitweg *et al.*, Eur. Phys. J. C **2** 1 61 (1998).
- [9] The OPAL Collaboration, R. Akers *et al.*, Z. Phys. C **63** 197 (1994).
The OPAL Collaboration, K. Ackerstaff *et al.*, Eur. Phys. J. C **1** 479 (1998).
- [10] The ATLAS Collaboration, G. Aad *et al.*, JINST **3** S08003 (2008).
- [11] The ATLAS reference system is a Cartesian right-handed coordinate system, with the nominal collision point at the origin. The anti-clockwise beam direction defines the positive z -axis, while the positive x -axis is defined as pointing from the collision point to the centre of the LHC ring and the positive y -axis points upwards. The azimuthal angle ϕ is measured around the beam axis, and the polar angle θ is measured with respect to the z -axis. The pseudorapidity is defined as $\eta = -\ln(\tan(\theta/2))$. The rapidity is defined as $y = 0.5 \times \ln[(E + p_z)/(E - p_z)]$, where E denotes the energy and p_z is the component of the momentum along the beam direction.
- [12] The ATLAS Collaboration, G. Aad *et al.*, Phys. Lett. B **688** 21 (2010).
- [13] T. Sjöstrand *et al.*, JHEP **05** 026 (2006).
- [14] M. Bahr *et al.*, HERWIG++ Physics and Manual, Eur. Phys. J. C **58** 639 (2008).
- [15] B. Andersson *et al.*, Phys. Rep. **97** 31 (1983).
- [16] B.R. Webber, Nucl. Phys. B **238** 492 (1984).
- [17] ATLAS Collaboration, ATLAS MC tunes for MC09, ATL-PHYS-PUB-2010-002 (2010).
- [18] The CDF Collaboration, T. Aaltonen *et al.*, Phys. Rev. D **82** 034001 (2010).
- [19] P. Z. Skands, CERN-PH-TH-2010-113, arXiv:hep-ph/1005.3457 (2010).
- [20] M.L. Mangano *et al.*, JHEP **01** 0307 (2003).
- [21] G. Corcella *et al.*, JHEP **0101** 010 (2001).
- [22] J. Butterworth, J. Forshaw and M. Seymour, Z. Phys. C **72** 637 (1996).
- [23] A. D. Martin, W. J. Stirling, R. S. Thorne and G. Watt, Eur. Phys. J. C **63** 189 (2009).
A. Sherstnev and R. S. Thorne, Eur. Phys. J. C **55** 553 (2008).
- [24] J. Pumplin *et al.*, JHEP **0207** 012 (2002).
- [25] D. Stump *et al.*, JHEP **0310** 046 (2003).
- [26] The ATLAS Collaboration, G. Aad *et al.*, Eur. Phys. J. C **70** 823 (2010).
- [27] S. Agostinelli *et al.*, Nucl. Instrum. and Meth. **A506** 250 (2003).
- [28] G. Folger and J.P. Wellisch, arXiv:nucl-th/0306007 (2003).
- [29] H. Bertini, Phys. Rev. **188** 1711 (1969).
- [30] E. Abat *et al.*, Tech. Rep. ATL-CAL-PUB-2010-001, CERN, Geneva, (2010).
P. Adragna *et al.*, CERN-PH-EP-2009-019; ATL-TILECAL-PUB-2009-009 (2009).
E. Abat *et al.*, Nucl. Instrum. and Meth. **A607** 372 (2009).
E. Abat *et al.*, Nucl. Instrum. and Meth. **A615** 158 (2010).
E. Abat *et al.*, Nucl. Instrum. and Meth. **A621** 134 (2010).
- [31] J. Pinfold *et al.*, Nucl. Instrum. Meth. **A593** 324 (2008).
D. M. Gingrich *et al.*, J. Inst. **2** no. 05 P05005 (2007).
- [32] M. Cacciari, G. P. Salam and G. Soyez, JHEP 0804 063 (2008).
- [33] The final state in the MC generators is defined using all particles (including muons and neutrinos) with lifetime above 10^{-11} s.
- [34] The electromagnetic scale is the appropriate scale for the reconstruction of the energy deposited by electrons or photons in the calorimeter.
- [35] B. Andersson, G. Gustafson and B. Nilsson-Almqvist, Nucl. Phys. B **281** 289 (1987).
- [36] A complete set of tables for differential and integrated measurements as a function of p_T and $|y|$ are available at the Durham HepData repository (<http://hepdata.cedar.ac.uk>).

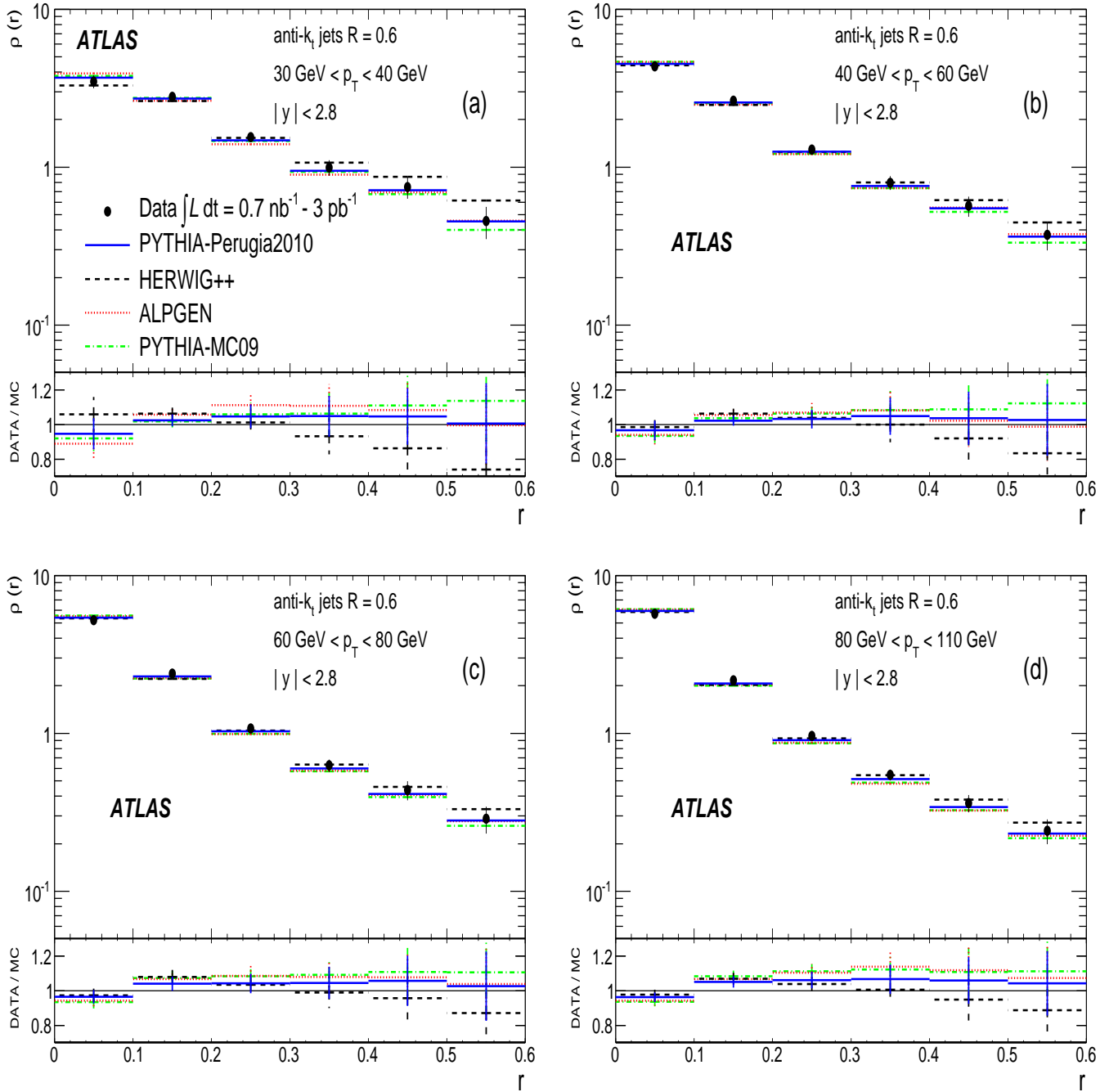


FIG. 1: The measured differential jet shape, $\rho(r)$, in inclusive jet production for jets with $|y| < 2.8$ and $30 \text{ GeV} < p_T < 110 \text{ GeV}$ is shown in different p_T regions. Error bars indicate the statistical and systematic uncertainties added in quadrature. The predictions of PYTHIA-Perugia2010 (solid lines), HERWIG++ (dashed lines), ALPGEN interfaced with HERWIG and JIMMY (dotted lines), and PYTHIA-MC09 (dashed-dotted lines) are shown for comparison.

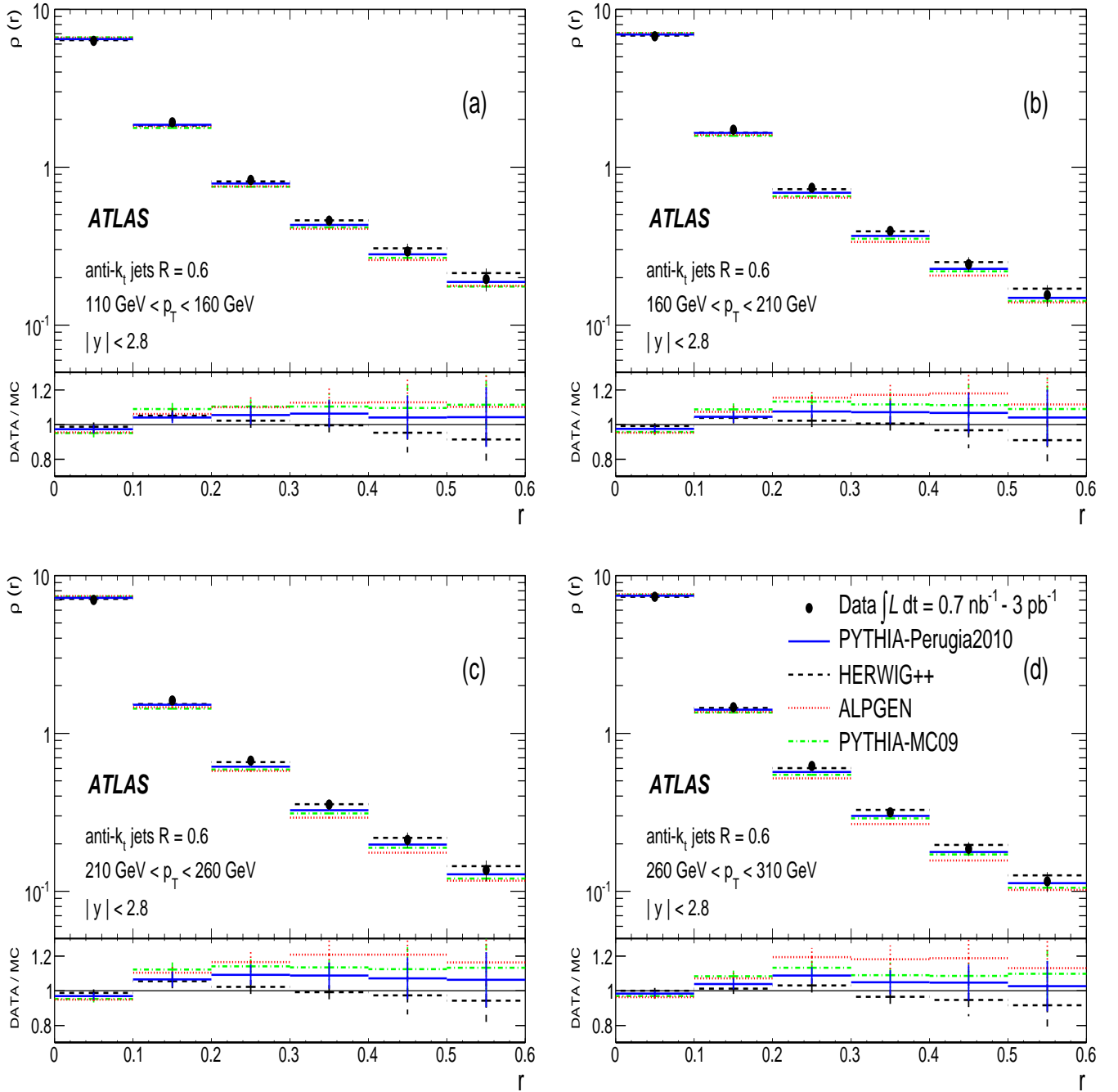


FIG. 2: The measured differential jet shape, $\rho(r)$, in inclusive jet production for jets with $|y| < 2.8$ and $110 \text{ GeV} < p_T < 310 \text{ GeV}$ is shown in different p_T regions. Error bars indicate the statistical and systematic uncertainties added in quadrature. The predictions of PYTHIA-Perugia2010 (solid lines), HERWIG++ (dashed lines), ALPGEN interfaced with HERWIG and JIMMY (dotted lines), and PYTHIA-MC09 (dashed-dotted lines) are shown for comparison.

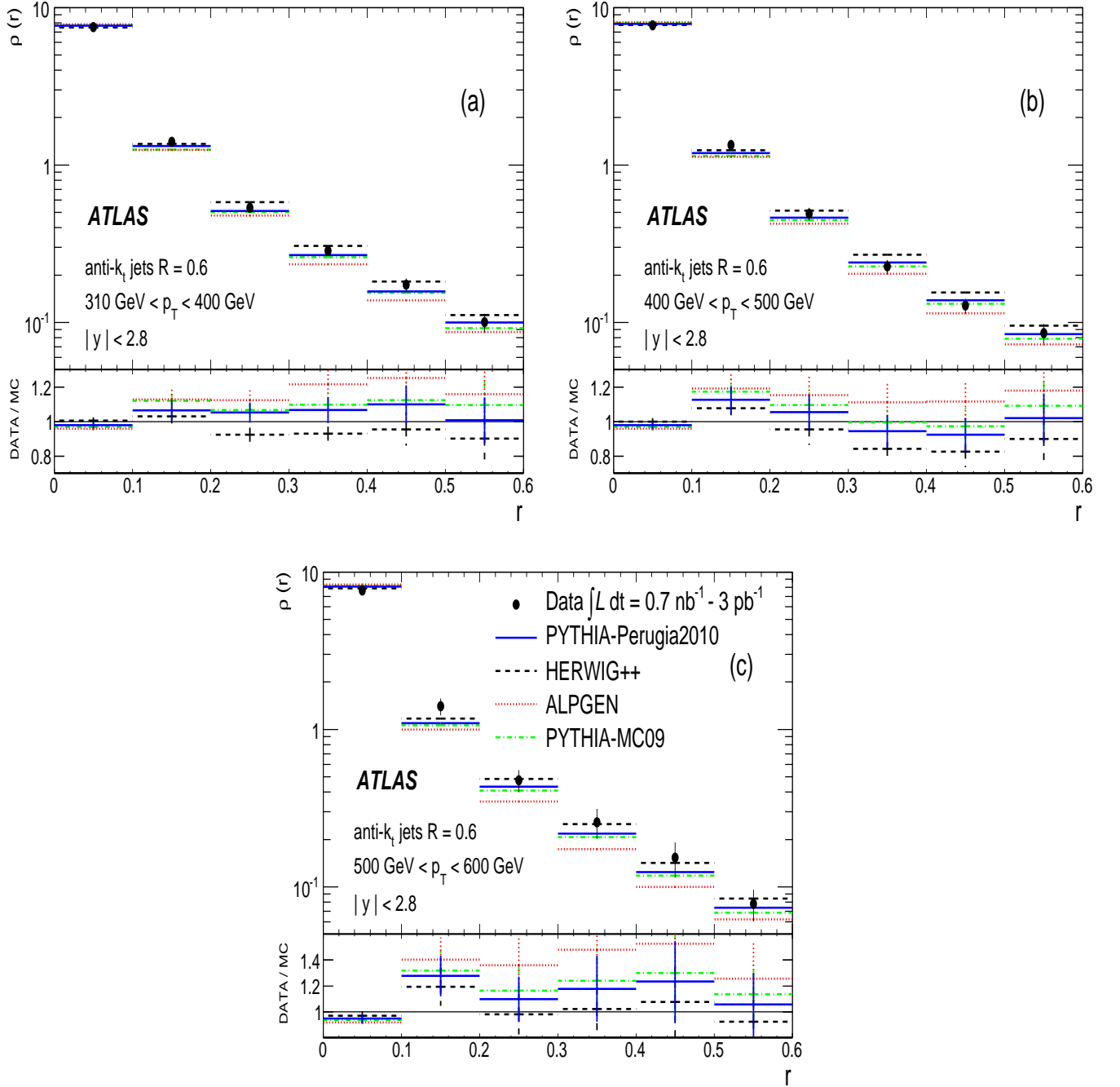


FIG. 3: The measured differential jet shape, $\rho(r)$, in inclusive jet production for jets with $|y| < 2.8$ and $310 \text{ GeV} < p_T < 600 \text{ GeV}$ is shown in different p_T regions. Error bars indicate the statistical and systematic uncertainties added in quadrature. The predictions of PYTHIA-Perugia2010 (solid lines), HERWIG++ (dashed lines), ALPGEN interfaced with HERWIG and JIMMY (dotted lines), and PYTHIA-MC09 (dashed-dotted lines) are shown for comparison.

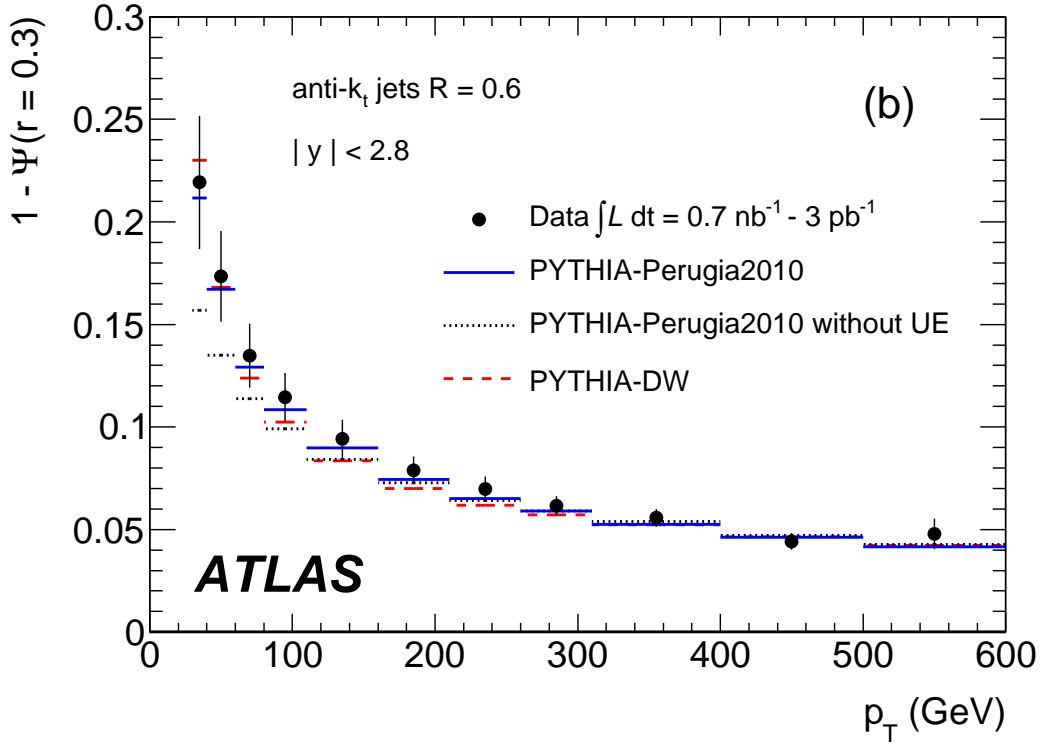
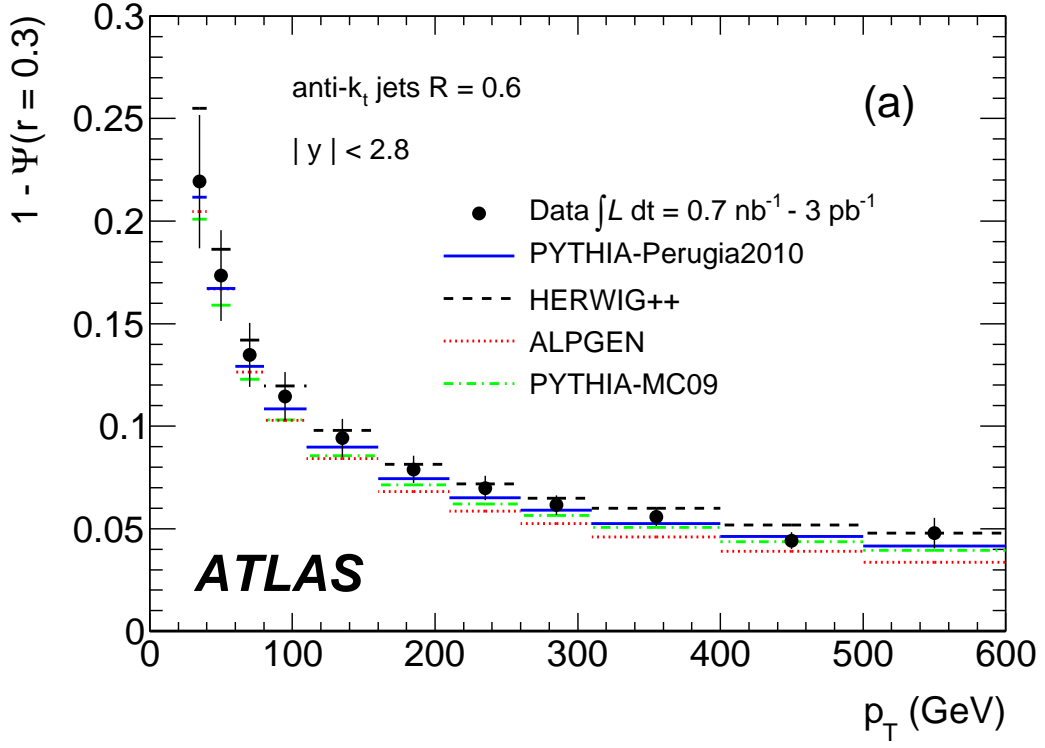


FIG. 4: The measured integrated jet shape, $1 - \Psi(r = 0.3)$, as a function of p_T for jets with $|y| < 2.8$ and $30 \text{ GeV} < p_T < 600 \text{ GeV}$. Error bars indicate the statistical and systematic uncertainties added in quadrature. The data are compared to the predictions of: (a) PYTHIA-Perugia2010 (solid lines), HERWIG++ (dashed lines), ALPGEN interfaced with HERWIG and JIMMY (dotted lines), and PYTHIA-MC09 (dashed-dotted lines); (b) PYTHIA-Perugia2010 (solid lines), PYTHIA-Perugia2010 without UE (dotted lines), and PYTHIA-DW (dashed lines).

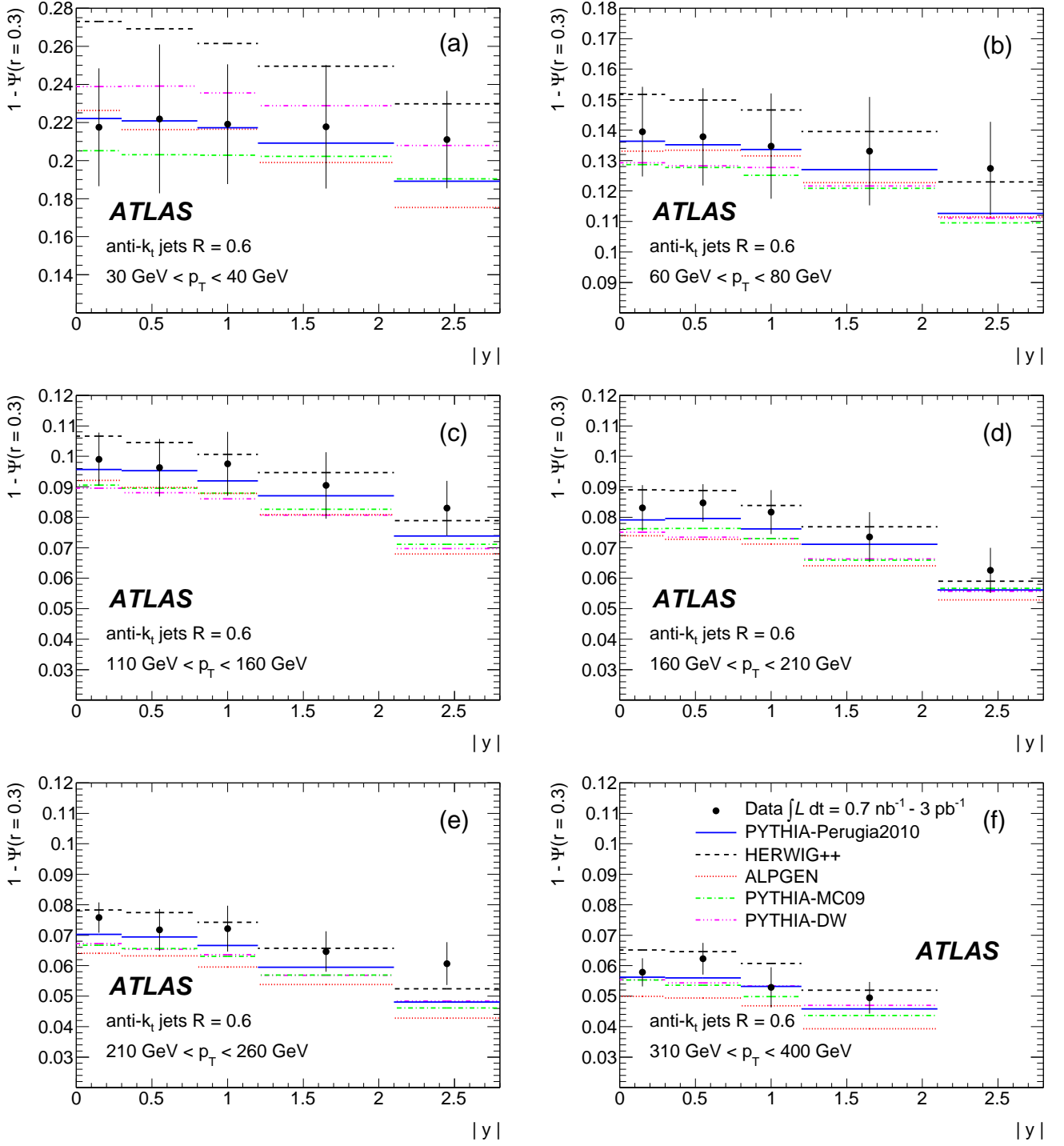


FIG. 5: The measured integrated jet shape, $1 - \Psi(r = 0.3)$, as a function of $|y|$ for jets with $|y| < 2.8$ and $30 \text{ GeV} < p_T < 400 \text{ GeV}$. Error bars indicate the statistical and systematic uncertainties added in quadrature. The predictions of PYTHIA-Perugia2010 (solid lines), HERWIG++ (dashed lines), ALPGEN interfaced with HERWIG and JIMMY (dotted lines), PYTHIA-MC09 (dashed-dotted lines), and PYTHIA-DW (dashed-dotted-dotted lines) are shown for comparison.

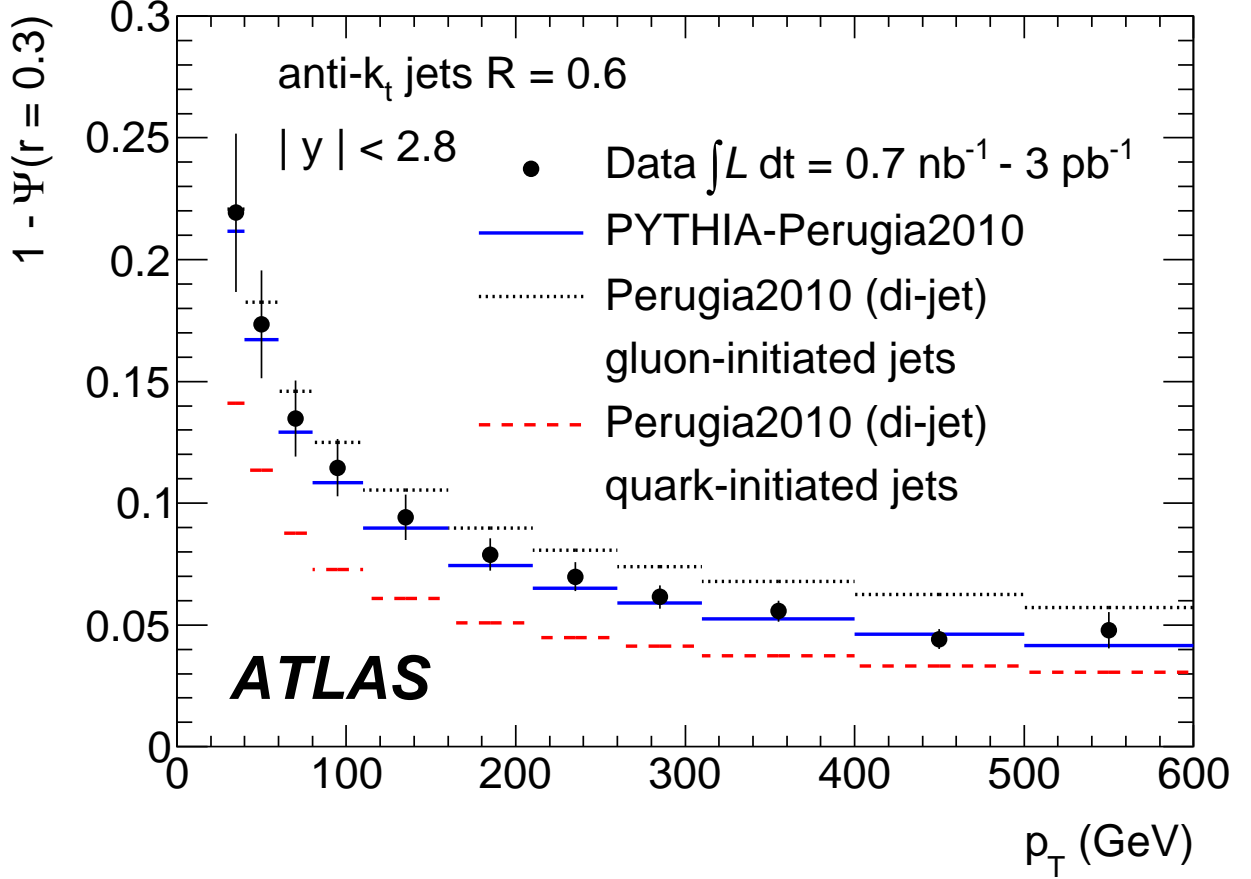


FIG. 6: The measured integrated jet shape, $1 - \Psi(r = 0.3)$, as a function of p_T for jets with $|y| < 2.8$ and $30 \text{ GeV} < p_T < 600 \text{ GeV}$. Error bars indicate the statistical and systematic uncertainties added in quadrature. The predictions of PYTHIA-Perugia2010 (solid line) are shown for comparison, together with the prediction separately for quark-initiated (dashed lines) and gluon-initiated jets (dotted lines) in dijet events.

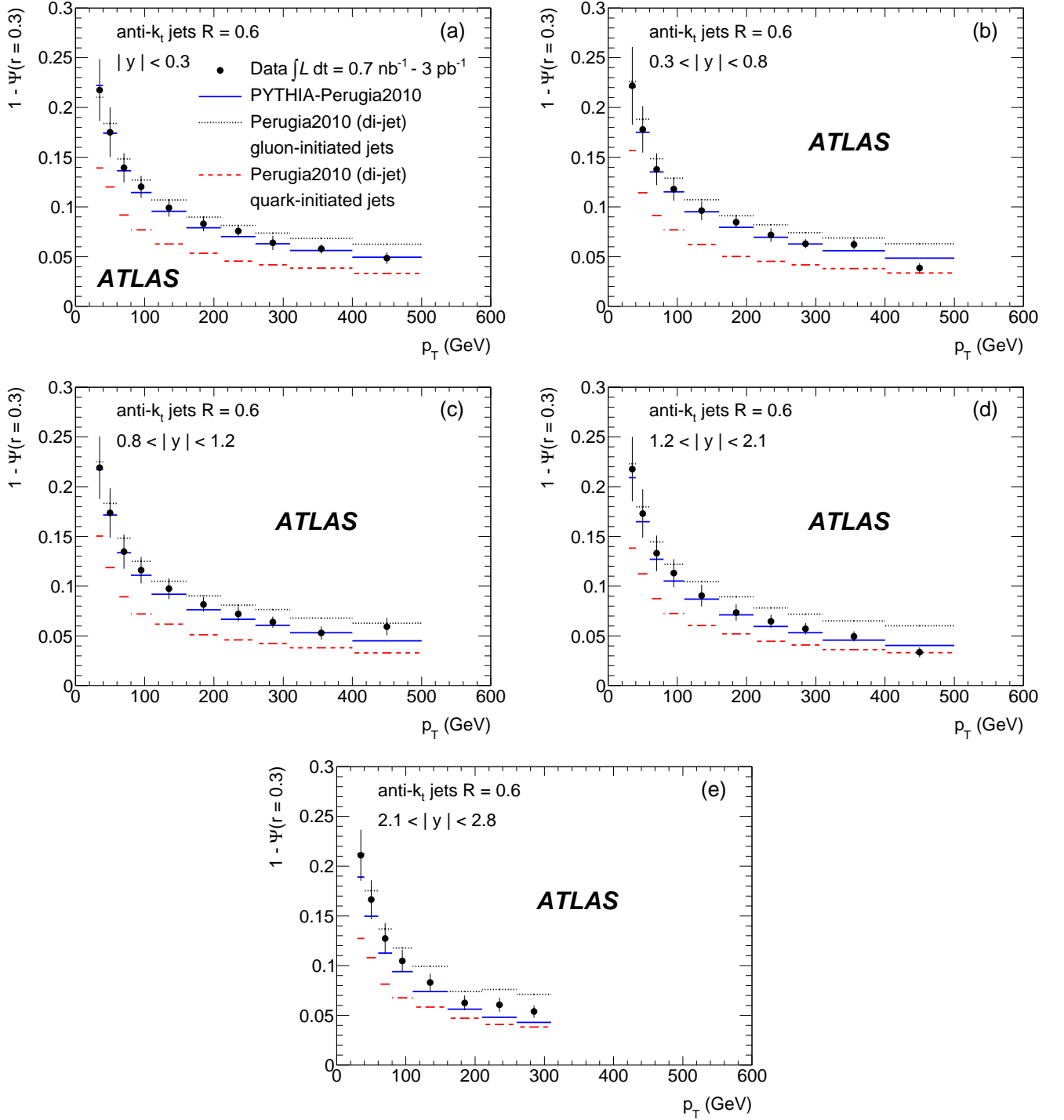


FIG. 7: The measured integrated jet shape, $1 - \Psi(r = 0.3)$, as a function of p_T in different jet rapidity regions for jets with $|y| < 2.8$ and $30 \text{ GeV} < p_T < 500 \text{ GeV}$. Error bars indicate the statistical and systematic uncertainties added in quadrature. The predictions of PYTHIA-Perugia2010 (solid line) are shown for comparison, together with the prediction separately for quark-initiated (dashed lines) and gluon-initiated jets (dotted lines) in dijet events.

Appendix A: Data Points and Correlation of Systematic Uncertainties

Data for differential and integrated measurements are collected in Tables 2 to 6, which include a detailed description of the contributions from the different sources of systematic uncertainty, as discussed in Section 8.

A χ^2 test is performed to the data points in Tables 5 and 6 with respect to a given MC prediction, separately in each rapidity region. The systematic uncertainties are considered independent and fully correlated across p_T bins, and the test is carried out according to the formula

$$\chi^2 = \sum_{j=1}^{p_T \text{ bins}} \frac{[d_j - mc_j(\bar{s})]^2}{[\delta d_j]^2 + [\delta mc_j(\bar{s})]^2} + \sum_{i=1}^5 [s_i]^2, \quad (\text{A1})$$

where d_j is the measured data point j , $mc_j(\bar{s})$ is the corresponding MC prediction, and \bar{s} denotes the vector of standard deviations, s_i , for the different independent sources of systematic uncertainty. For each rapidity region considered, the sums above run over the total number of data points in p_T and five independent sources of systematic uncertainty, and the χ^2 is minimized with respect to \bar{s} . Correlations among systematic uncertainties are taken into account in $mc_j(\bar{s})$. The χ^2 results for the different MC predictions are collected in Table 7, and indicate that PYTHIA-Perugia2010 provides the overall best description of the data.

$\rho(r) \ (0 < y < 2.8)$							
30 GeV < p_T < 40 GeV							
r	$\rho \pm (\text{stat.}) \pm (\text{syst.})$	cluster e-scale	shower model	jet e-scale	resolution	correction	non-closure
0.05	$3.486 \pm 0.011 \pm 0.331$	∓ 0.202	± 0.024	∓ 0.168	± 0.102	± 0.169	± 0.035
0.15	$2.787 \pm 0.009 \pm 0.093$	∓ 0.034	∓ 0.024	± 0.022	± 0.015	± 0.074	± 0.028
0.25	$1.550 \pm 0.006 \pm 0.102$	± 0.048	∓ 0.005	± 0.076	± 0.041	∓ 0.019	± 0.015
0.35	$0.995 \pm 0.004 \pm 0.112$	± 0.072	∓ 0.007	± 0.058	± 0.032	∓ 0.054	± 0.010
0.45	$0.748 \pm 0.003 \pm 0.117$	± 0.088	± 0.005	± 0.044	± 0.022	∓ 0.059	± 0.007
0.55	$0.455 \pm 0.002 \pm 0.105$	± 0.082	± 0.002	± 0.019	± 0.009	∓ 0.062	± 0.005
40 GeV < p_T < 60 GeV							
r	$\rho \pm (\text{stat.}) \pm (\text{syst.})$	cluster e-scale	shower model	jet e-scale	resolution	correction	non-closure
0.05	$4.350 \pm 0.018 \pm 0.250$	∓ 0.180	± 0.043	∓ 0.133	± 0.058	± 0.075	± 0.043
0.15	$2.631 \pm 0.014 \pm 0.072$	∓ 0.026	∓ 0.038	± 0.032	± 0.001	± 0.036	± 0.026
0.25	$1.292 \pm 0.009 \pm 0.068$	± 0.040	∓ 0.021	± 0.043	± 0.020	∓ 0.011	± 0.013
0.35	$0.797 \pm 0.006 \pm 0.081$	± 0.064	± 0.004	± 0.034	± 0.024	∓ 0.026	± 0.008
0.45	$0.567 \pm 0.004 \pm 0.084$	± 0.069	∓ 0.001	± 0.030	± 0.011	∓ 0.035	± 0.006
0.55	$0.372 \pm 0.003 \pm 0.075$	± 0.065	± 0.004	± 0.014	± 0.009	∓ 0.034	± 0.004
60 GeV < p_T < 80 GeV							
r	$\rho \pm (\text{stat.}) \pm (\text{syst.})$	cluster e-scale	shower model	jet e-scale	resolution	correction	non-closure
0.05	$5.193 \pm 0.011 \pm 0.210$	∓ 0.149	± 0.076	∓ 0.087	± 0.048	± 0.058	± 0.052
0.15	$2.383 \pm 0.007 \pm 0.093$	∓ 0.015	∓ 0.069	± 0.038	± 0.020	± 0.034	± 0.024
0.25	$1.074 \pm 0.005 \pm 0.058$	± 0.033	∓ 0.026	± 0.020	± 0.014	∓ 0.029	± 0.011
0.35	$0.626 \pm 0.003 \pm 0.056$	± 0.050	± 0.003	± 0.017	± 0.007	∓ 0.015	± 0.006
0.45	$0.437 \pm 0.002 \pm 0.060$	± 0.055	± 0.006	± 0.014	± 0.010	∓ 0.015	± 0.004
0.55	$0.288 \pm 0.001 \pm 0.056$	± 0.049	± 0.002	± 0.009	± 0.001	∓ 0.026	± 0.003
80 GeV < p_T < 110 GeV							
r	$\rho \pm (\text{stat.}) \pm (\text{syst.})$	cluster e-scale	shower model	jet e-scale	resolution	correction	non-closure
0.05	$5.719 \pm 0.010 \pm 0.169$	∓ 0.122	± 0.075	∓ 0.061	± 0.014	± 0.031	± 0.057
0.15	$2.166 \pm 0.006 \pm 0.068$	∓ 0.009	∓ 0.054	± 0.026	± 0.001	± 0.021	± 0.022
0.25	$0.962 \pm 0.004 \pm 0.043$	± 0.026	∓ 0.023	± 0.014	± 0.007	∓ 0.019	± 0.010
0.35	$0.547 \pm 0.002 \pm 0.044$	± 0.041	∓ 0.007	± 0.013	± 0.002	∓ 0.001	± 0.005
0.45	$0.361 \pm 0.002 \pm 0.046$	± 0.043	∓ 0.002	± 0.010	± 0.001	∓ 0.013	± 0.004
0.55	$0.241 \pm 0.001 \pm 0.043$	± 0.040	± 0.002	± 0.006	± 0.006	∓ 0.014	± 0.002
110 GeV < p_T < 160 GeV							
r	$\rho \pm (\text{stat.}) \pm (\text{syst.})$	cluster e-scale	shower model	jet e-scale	resolution	correction	non-closure
0.05	$6.292 \pm 0.009 \pm 0.160$	∓ 0.095	± 0.067	∓ 0.056	± 0.018	± 0.067	± 0.063
0.15	$1.925 \pm 0.005 \pm 0.060$	∓ 0.008	∓ 0.049	± 0.020	± 0.012	∓ 0.015	± 0.019
0.25	$0.830 \pm 0.003 \pm 0.043$	± 0.020	∓ 0.023	± 0.016	± 0.001	∓ 0.024	± 0.008
0.35	$0.458 \pm 0.002 \pm 0.034$	± 0.031	∓ 0.003	± 0.010	± 0.001	∓ 0.009	± 0.005
0.45	$0.292 \pm 0.001 \pm 0.035$	± 0.033	∓ 0.003	± 0.008	± 0.002	∓ 0.009	± 0.003
0.55	$0.195 \pm 0.001 \pm 0.032$	± 0.031	± 0.001	± 0.005	± 0.002	∓ 0.009	± 0.002
160 GeV < p_T < 210 GeV							
r	$\rho \pm (\text{stat.}) \pm (\text{syst.})$	cluster e-scale	shower model	jet e-scale	resolution	correction	non-closure
0.05	$6.738 \pm 0.012 \pm 0.124$	∓ 0.074	± 0.050	∓ 0.037	± 0.001	± 0.040	± 0.067
0.15	$1.722 \pm 0.007 \pm 0.055$	∓ 0.002	∓ 0.046	± 0.018	± 0.002	∓ 0.019	± 0.017
0.25	$0.742 \pm 0.005 \pm 0.026$	± 0.015	∓ 0.015	± 0.010	± 0.006	∓ 0.007	± 0.007
0.35	$0.394 \pm 0.003 \pm 0.025$	± 0.024	± 0.003	± 0.004	± 0.003	± 0.001	± 0.004
0.45	$0.243 \pm 0.002 \pm 0.026$	± 0.025	± 0.003	± 0.005	± 0.003	∓ 0.005	± 0.002
0.55	$0.155 \pm 0.001 \pm 0.024$	± 0.023	± 0.002	± 0.002	± 0.002	∓ 0.007	± 0.002

TABLE II: The measured differential jet shape, $\rho(r)$, as a function of r in different p_T regions, for jets with $|y| < 2.8$ and $30 \text{ GeV} < p_T < 210 \text{ GeV}$ (see Figs. 1 and 2). The contributions from the different sources of systematic uncertainty are listed separately.

$\rho(r) (0 < y < 2.8)$							
210 GeV < p_T < 260 GeV							
r	$\rho \pm (\text{stat.}) \pm (\text{syst.})$	cluster e-scale	shower model	jet e-scale	resolution	correction	non-closure
0.05	$7.004 \pm 0.021 \pm 0.146$	∓ 0.061	± 0.084	∓ 0.037	± 0.055	± 0.035	± 0.070
0.15	$1.612 \pm 0.012 \pm 0.066$	∓ 0.001	∓ 0.050	± 0.019	± 0.033	∓ 0.012	± 0.016
0.25	$0.672 \pm 0.008 \pm 0.035$	± 0.012	∓ 0.027	± 0.011	± 0.013	∓ 0.005	± 0.007
0.35	$0.353 \pm 0.005 \pm 0.024$	± 0.019	∓ 0.010	± 0.007	± 0.006	∓ 0.005	± 0.004
0.45	$0.212 \pm 0.003 \pm 0.024$	± 0.020	∓ 0.007	± 0.005	± 0.004	∓ 0.008	± 0.002
0.55	$0.136 \pm 0.001 \pm 0.020$	± 0.019	∓ 0.001	± 0.003	± 0.003	∓ 0.005	± 0.001
260 GeV < p_T < 310 GeV							
r	$\rho \pm (\text{stat.}) \pm (\text{syst.})$	cluster e-scale	shower model	jet e-scale	resolution	correction	non-closure
0.05	$7.300 \pm 0.036 \pm 0.113$	∓ 0.053	± 0.055	∓ 0.027	± 0.030	∓ 0.001	± 0.073
0.15	$1.463 \pm 0.021 \pm 0.038$	± 0.001	∓ 0.030	± 0.016	± 0.009	± 0.004	± 0.015
0.25	$0.619 \pm 0.014 \pm 0.024$	± 0.011	∓ 0.013	± 0.008	± 0.013	± 0.001	± 0.006
0.35	$0.315 \pm 0.008 \pm 0.019$	± 0.016	∓ 0.010	± 0.002	± 0.003	± 0.003	± 0.003
0.45	$0.186 \pm 0.004 \pm 0.018$	± 0.017	∓ 0.005	± 0.003	± 0.002	± 0.002	± 0.002
0.55	$0.115 \pm 0.002 \pm 0.016$	± 0.015	∓ 0.001	± 0.002	± 0.004	∓ 0.004	± 0.001
310 GeV < p_T < 400 GeV							
r	$\rho \pm (\text{stat.}) \pm (\text{syst.})$	cluster e-scale	shower model	jet e-scale	resolution	correction	non-closure
0.05	$7.495 \pm 0.052 \pm 0.128$	∓ 0.043	± 0.059	∓ 0.034	± 0.033	± 0.056	± 0.075
0.15	$1.405 \pm 0.031 \pm 0.070$	∓ 0.001	∓ 0.056	± 0.019	± 0.026	∓ 0.024	± 0.014
0.25	$0.536 \pm 0.018 \pm 0.023$	± 0.008	∓ 0.008	± 0.006	± 0.001	∓ 0.019	± 0.005
0.35	$0.285 \pm 0.011 \pm 0.016$	± 0.013	± 0.002	± 0.006	± 0.004	∓ 0.005	± 0.003
0.45	$0.173 \pm 0.006 \pm 0.016$	± 0.014	∓ 0.001	± 0.003	± 0.005	∓ 0.004	± 0.002
0.55	$0.101 \pm 0.003 \pm 0.013$	± 0.012	± 0.001	± 0.002	± 0.001	∓ 0.003	± 0.001
400 GeV < p_T < 500 GeV							
r	$\rho \pm (\text{stat.}) \pm (\text{syst.})$	cluster e-scale	shower model	jet e-scale	resolution	correction	non-closure
0.05	$7.720 \pm 0.114 \pm 0.106$	∓ 0.034	± 0.043	∓ 0.031	± 0.011	± 0.036	± 0.077
0.15	$1.339 \pm 0.075 \pm 0.054$	± 0.001	∓ 0.047	± 0.020	± 0.010	∓ 0.003	± 0.013
0.25	$0.489 \pm 0.039 \pm 0.023$	± 0.006	± 0.001	± 0.008	± 0.005	∓ 0.020	± 0.005
0.35	$0.226 \pm 0.019 \pm 0.012$	± 0.009	∓ 0.003	± 0.003	± 0.003	∓ 0.005	± 0.002
0.45	$0.128 \pm 0.009 \pm 0.011$	± 0.010	± 0.001	± 0.002	± 0.002	∓ 0.003	± 0.001
0.55	$0.086 \pm 0.006 \pm 0.011$	± 0.010	± 0.001	± 0.001	± 0.001	∓ 0.003	± 0.001
500 GeV < p_T < 600 GeV							
r	$\rho \pm (\text{stat.}) \pm (\text{syst.})$	cluster e-scale	shower model	jet e-scale	resolution	correction	non-closure
0.05	$7.638 \pm 0.261 \pm 0.093$	∓ 0.026	± 0.001	∓ 0.022	± 0.009	± 0.040	± 0.076
0.15	$1.400 \pm 0.168 \pm 0.037$	± 0.001	∓ 0.011	± 0.013	± 0.003	∓ 0.030	± 0.014
0.25	$0.475 \pm 0.074 \pm 0.017$	± 0.006	± 0.008	± 0.009	± 0.010	∓ 0.003	± 0.005
0.35	$0.257 \pm 0.054 \pm 0.012$	± 0.010	∓ 0.004	± 0.004	± 0.001	∓ 0.002	± 0.003
0.45	$0.153 \pm 0.037 \pm 0.012$	± 0.011	± 0.002	± 0.004	± 0.001	∓ 0.002	± 0.002
0.55	$0.078 \pm 0.015 \pm 0.010$	± 0.009	± 0.004	± 0.002	± 0.001	∓ 0.003	± 0.001

TABLE III: The measured differential jet shape, $\rho(r)$, as a function of r in different p_T regions, for jets with $|y| < 2.8$ and $210 \text{ GeV} < p_T < 600 \text{ GeV}$ (see Fig. 3). The contributions from the different sources of systematic uncertainty are listed separately.

$1 - \Psi(r = 0.3)$								
$(0 < y < 2.8)$								
p_T (GeV)	$1 - \Psi(r = 0.3) \pm (\text{stat.}) \pm (\text{syst.})$	cluster e-scale	shower model	jet e-scale	resolution	correction	non-closure	
30 - 40	$0.2193 \pm 0.0006 \pm 0.0325$	± 0.0212	± 0.0001	± 0.0105	± 0.0057	± 0.0216	-	-
40 - 60	$0.1733 \pm 0.0008 \pm 0.0221$	± 0.0177	± 0.0006	± 0.0070	± 0.0041	± 0.0104	-	-
60 - 80	$0.1347 \pm 0.0004 \pm 0.0157$	± 0.0138	± 0.0010	± 0.0035	± 0.0017	± 0.0064	-	-
80 - 110	$0.1146 \pm 0.0003 \pm 0.0117$	± 0.0109	± 0.0005	± 0.0025	± 0.0007	± 0.0033	-	-
110 - 160	$0.0942 \pm 0.0003 \pm 0.0092$	± 0.0084	± 0.0001	± 0.0021	± 0.0005	± 0.0030	-	-
160 - 210	$0.0789 \pm 0.0004 \pm 0.0067$	± 0.0063	± 0.0007	± 0.0010	± 0.0008	± 0.0015	-	-
210 - 260	$0.0698 \pm 0.0006 \pm 0.0059$	± 0.0051	± 0.0015	± 0.0013	± 0.0011	± 0.0020	-	-
260 - 310	$0.0615 \pm 0.0010 \pm 0.0046$	± 0.0042	± 0.0014	± 0.0006	± 0.0008	± 0.0003	-	-
310 - 400	$0.0556 \pm 0.0015 \pm 0.0041$	± 0.0035	± 0.0001	± 0.0010	± 0.0007	± 0.0016	-	-
400 - 500	$0.0442 \pm 0.0024 \pm 0.0033$	± 0.0028	± 0.0001	± 0.0006	± 0.0006	± 0.0016	-	-
500 - 600	$0.0479 \pm 0.0070 \pm 0.0026$	± 0.0022	± 0.0002	± 0.0008	± 0.0001	± 0.0012	-	-

TABLE IV: The measured integrated jet shape, $1 - \Psi(r = 0.3)$, as a function of p_T , for jets with $|y| < 2.8$ and $30 \text{ GeV} < p_T < 600 \text{ GeV}$ (see Fig. 4). The contributions from the different sources of systematic uncertainty are listed separately.

$1 - \Psi(r = 0.3)$								
$(0 < y < 0.3)$								
p_T (GeV)	$1 - \Psi(r = 0.3) \pm (\text{stat.}) \pm (\text{syst.})$	cluster e-scale	shower model	jet e-scale	resolution	correction	non-closure	
30 - 40	$0.2175 \pm 0.0016 \pm 0.0309$	± 0.0149	± 0.0050	± 0.0112	± 0.0057	± 0.0234	-	
40 - 60	$0.1751 \pm 0.0023 \pm 0.0249$	± 0.0133	± 0.0002	± 0.0074	± 0.0041	± 0.0192	-	
60 - 80	$0.1395 \pm 0.0011 \pm 0.0147$	± 0.0105	± 0.0070	± 0.0039	± 0.0017	± 0.0062	-	
80 - 110	$0.1203 \pm 0.0009 \pm 0.0110$	± 0.0086	± 0.0035	± 0.0022	± 0.0007	± 0.0055	-	
110 - 160	$0.0990 \pm 0.0007 \pm 0.0087$	± 0.0067	± 0.0025	± 0.0017	± 0.0005	± 0.0047	-	
160 - 210	$0.0831 \pm 0.0010 \pm 0.0074$	± 0.0051	± 0.0004	± 0.0008	± 0.0008	± 0.0053	-	
210 - 260	$0.0758 \pm 0.0015 \pm 0.0047$	± 0.0042	± 0.0017	± 0.0008	± 0.0011	± 0.0006	-	
260 - 310	$0.0639 \pm 0.0024 \pm 0.0068$	± 0.0035	± 0.0032	± 0.0003	± 0.0008	± 0.0049	-	
310 - 400	$0.0578 \pm 0.0031 \pm 0.0034$	± 0.0030	± 0.0002	± 0.0013	± 0.0007	± 0.0007	-	
400 - 500	$0.0486 \pm 0.0044 \pm 0.0037$	± 0.0024	± 0.0022	± 0.0006	± 0.0006	± 0.0017	-	
$(0.3 < y < 0.8)$								
p_T (GeV)	$1 - \Psi(r = 0.3) \pm (\text{stat.}) \pm (\text{syst.})$	cluster e-scale	shower model	jet e-scale	resolution	correction	non-closure	
30 - 40	$0.2219 \pm 0.0012 \pm 0.0390$	± 0.0173	± 0.0036	± 0.0109	± 0.0057	± 0.0326	-	
40 - 60	$0.1779 \pm 0.0017 \pm 0.0233$	± 0.0145	± 0.0051	± 0.0059	± 0.0041	± 0.0160	-	
60 - 80	$0.1378 \pm 0.0008 \pm 0.0159$	± 0.0117	± 0.0021	± 0.0041	± 0.0017	± 0.0097	-	
80 - 110	$0.1179 \pm 0.0007 \pm 0.0116$	± 0.0093	± 0.0002	± 0.0025	± 0.0007	± 0.0063	-	
110 - 160	$0.0963 \pm 0.0006 \pm 0.0094$	± 0.0073	± 0.0006	± 0.0018	± 0.0005	± 0.0056	-	
160 - 210	$0.0847 \pm 0.0007 \pm 0.0061$	± 0.0055	± 0.0017	± 0.0017	± 0.0008	± 0.0011	-	
210 - 260	$0.0718 \pm 0.0012 \pm 0.0067$	± 0.0045	± 0.0023	± 0.0016	± 0.0011	± 0.0039	-	
260 - 310	$0.0631 \pm 0.0019 \pm 0.0042$	± 0.0038	± 0.0009	± 0.0008	± 0.0008	± 0.0010	-	
310 - 400	$0.0623 \pm 0.0030 \pm 0.0042$	± 0.0031	± 0.0016	± 0.0011	± 0.0007	± 0.0019	-	
400 - 500	$0.0384 \pm 0.0033 \pm 0.0042$	± 0.0025	± 0.0005	± 0.0007	± 0.0006	± 0.0031	-	
$(0.8 < y < 1.2)$								
p_T (GeV)	$1 - \Psi(r = 0.3) \pm (\text{stat.}) \pm (\text{syst.})$	cluster e-scale	shower model	jet e-scale	resolution	correction	non-closure	
30 - 40	$0.2191 \pm 0.0014 \pm 0.0314$	± 0.0233	± 0.0030	± 0.0102	± 0.0057	± 0.0172	-	
40 - 60	$0.1736 \pm 0.0020 \pm 0.0247$	± 0.0192	± 0.0030	± 0.0090	± 0.0041	± 0.0116	-	
60 - 80	$0.1347 \pm 0.0009 \pm 0.0173$	± 0.0151	± 0.0013	± 0.0052	± 0.0017	± 0.0063	-	
80 - 110	$0.1161 \pm 0.0008 \pm 0.0133$	± 0.0118	± 0.0001	± 0.0034	± 0.0007	± 0.0051	-	
110 - 160	$0.0975 \pm 0.0007 \pm 0.0105$	± 0.0092	± 0.0001	± 0.0024	± 0.0005	± 0.0043	-	
160 - 210	$0.0817 \pm 0.0009 \pm 0.0071$	± 0.0069	± 0.0007	± 0.0014	± 0.0008	± 0.0010	-	
210 - 260	$0.0721 \pm 0.0016 \pm 0.0073$	± 0.0054	± 0.0010	± 0.0015	± 0.0011	± 0.0044	-	
260 - 310	$0.0639 \pm 0.0022 \pm 0.0051$	± 0.0046	± 0.0010	± 0.0016	± 0.0008	± 0.0002	-	
310 - 400	$0.0529 \pm 0.0031 \pm 0.0058$	± 0.0038	± 0.0001	± 0.0009	± 0.0007	± 0.0042	-	
400 - 500	$0.0593 \pm 0.0079 \pm 0.0037$	± 0.0030	± 0.0014	± 0.0011	± 0.0006	± 0.0012	-	

TABLE V: The measured integrated jet shape, $1 - \Psi(r = 0.3)$, as a function of p_T , for jets with $30 \text{ GeV} < p_T < 500 \text{ GeV}$ in different jet rapidity regions (see Fig. 7). The contributions from the different sources of systematic uncertainty are listed separately.

$1 - \Psi(r = 0.3)$								
$(1.2 < y < 2.1)$								
p_T (GeV)	$1 - \Psi(r = 0.3) \pm (\text{stat.}) \pm (\text{syst.})$	cluster e-scale	shower model	jet e-scale	resolution	correction	non-closure	
30 - 40	$0.2177 \pm 0.0010 \pm 0.0325$	± 0.0263	± 0.0017	± 0.0114	± 0.0057	± 0.0140	-	-
40 - 60	$0.1731 \pm 0.0014 \pm 0.0244$	± 0.0217	± 0.0014	± 0.0066	± 0.0041	± 0.0077	-	-
60 - 80	$0.1331 \pm 0.0007 \pm 0.0178$	± 0.0168	± 0.0001	± 0.0035	± 0.0017	± 0.0045	-	-
80 - 110	$0.1130 \pm 0.0006 \pm 0.0140$	± 0.0133	± 0.0029	± 0.0029	± 0.0007	± 0.0012	-	-
110 - 160	$0.0904 \pm 0.0005 \pm 0.0109$	± 0.0103	± 0.0010	± 0.0019	± 0.0005	± 0.0029	-	-
160 - 210	$0.0735 \pm 0.0007 \pm 0.0082$	± 0.0077	± 0.0011	± 0.0015	± 0.0008	± 0.0019	-	-
210 - 260	$0.0646 \pm 0.0011 \pm 0.0066$	± 0.0061	± 0.0007	± 0.0014	± 0.0011	± 0.0014	-	-
260 - 310	$0.0573 \pm 0.0021 \pm 0.0053$	± 0.0051	± 0.0007	± 0.0011	± 0.0008	± 0.0002	-	-
310 - 400	$0.0495 \pm 0.0026 \pm 0.0045$	± 0.0043	± 0.0005	± 0.0008	± 0.0007	± 0.0009	-	-
400 - 500	$0.0335 \pm 0.0033 \pm 0.0037$	± 0.0035	± 0.0006	± 0.0007	± 0.0006	± 0.0006	-	-
$(2.1 < y < 2.8)$								
p_T (GeV)	$1 - \Psi(r = 0.3) \pm (\text{stat.}) \pm (\text{syst.})$	cluster e-scale	shower model	jet e-scale	resolution	correction	non-closure	
30 - 40	$0.2110 \pm 0.0014 \pm 0.0256$	± 0.0209	± 0.0094	± 0.0098	± 0.0057	± 0.0003	-	-
40 - 60	$0.1664 \pm 0.0021 \pm 0.0193$	± 0.0169	± 0.0048	± 0.0066	± 0.0042	± 0.0023	-	-
60 - 80	$0.1274 \pm 0.0011 \pm 0.0153$	± 0.0126	± 0.0062	± 0.0057	± 0.0017	± 0.0012	-	-
80 - 110	$0.1048 \pm 0.0009 \pm 0.0110$	± 0.0099	± 0.0031	± 0.0033	± 0.0007	± 0.0004	-	-
110 - 160	$0.0830 \pm 0.0008 \pm 0.0090$	± 0.0076	± 0.0026	± 0.0034	± 0.0005	± 0.0019	-	-
160 - 210	$0.0626 \pm 0.0010 \pm 0.0074$	± 0.0058	± 0.0030	± 0.0026	± 0.0008	± 0.0020	-	-
210 - 260	$0.0607 \pm 0.0023 \pm 0.0066$	± 0.0048	± 0.0018	± 0.0027	± 0.0011	± 0.0029	-	-
260 - 310	$0.0538 \pm 0.0040 \pm 0.0047$	± 0.0040	± 0.0022	± 0.0007	± 0.0009	± 0.0006	-	-

TABLE VI: The measured integrated jet shape, $1 - \Psi(r = 0.3)$, as a function of p_T , for jets with $30 \text{ GeV} < p_T < 500 \text{ GeV}$ in different jet rapidity regions (see Fig. 7). The contributions from the different sources of systematic uncertainty are listed separately.

$\chi^2/d.o.f$					
	$0 < y < 0.3$	$0.3 < y < 0.8$	$0.8 < y < 1.2$	$1.2 < y < 2.1$	$2.1 < y < 2.8$
degrees of freedom (d.o.f)	10	10	10	10	8
PYTHIA-Perugia2010	0.6	1.8	2.4	1.4	1.4
HERWIG++	2.2	2.3	3.1	1.8	4.0
PYTHIA-MC09	1.0	2.5	2.4	1.5	3.2
PYTHIA-DW	2.4	3.4	6.9	4.0	5.2
ALPGEN	3.8	9.8	7.4	6.7	6.0
PYTHIA-Perugia2010 (no UE)	4.2	9.7	4.9	8.6	4.8

TABLE VII: Results of χ^2 tests to the data in Fig. 7 with respect to the different MC predictions. As discussed in the text, the different sources of systematic uncertainty are considered independent and fully correlated across p_T bins.

The ATLAS Collaboration

G. Aad⁴⁸, B. Abbott¹¹¹, J. Abdallah¹¹, A.A. Abdelalim⁴⁹, A. Abdesselam¹¹⁸, O. Abidinov¹⁰, B. Abi¹¹², M. Abolins⁸⁸, H. Abramowicz¹⁵³, H. Abreu¹¹⁵, E. Acerbi^{89a,89b}, B.S. Acharya^{164a,164b}, M. Ackers²⁰, D.L. Adams²⁴, T.N. Addy⁵⁶, J. Adelman¹⁷⁵, M. Aderholz⁹⁹, S. Adomeit⁹⁸, P. Adragna⁷⁵, T. Adye¹²⁹, S. Aefsky²², J.A. Aguilar-Saavedra^{124b,a}, M. Aharrouche⁸¹, S.P. Ahlen²¹, F. Ahles⁴⁸, A. Ahmad¹⁴⁸, M. Ahsan⁴⁰, G. Aielli^{133a,133b}, T. Akdogan^{18a}, T.P.A. Åkesson⁷⁹, G. Akimoto¹⁵⁵, A.V. Akimov⁹⁴, M.S. Alam¹, M.A. Alam⁷⁶, S. Albrand⁵⁵, M. Aleksa²⁹, I.N. Aleksandrov⁶⁵, M. Aleppo^{89a,89b}, F. Alessandria^{89a}, C. Alexa^{25a}, G. Alexander¹⁵³, G. Alexandre⁴⁹, T. Alexopoulos⁹, M. Alhroob²⁰, M. Aliev¹⁵, G. Alimonti^{89a}, J. Alison¹²⁰, M. Aliyev¹⁰, P.P. Allport⁷³, S.E. Allwood-Spiers⁵³, J. Almond⁸², A. Aloisio^{102a,102b}, R. Alon¹⁷¹, A. Alonso⁷⁹, J. Alonso¹⁴, M.G. Alvigi^{102a,102b}, K. Amako⁶⁶, P. Amaral²⁹, C. Amelung²², V.V. Ammosov¹²⁸, A. Amorim^{124a,b}, G. Amorós¹⁶⁷, N. Amram¹⁵³, C. Anastopoulos¹³⁹, T. Andeen³⁴, C.F. Anders²⁰, K.J. Anderson³⁰, A. Andreazza^{89a,89b}, V. Andrei^{58a}, M-L. Andrieux⁵⁵, X.S. Anduaga⁷⁰, A. Angerami³⁴, F. Anghinolfi²⁹, N. Anjos^{124a}, A. Annovi⁴⁷, A. Antonaki⁸, M. Antonelli⁴⁷, S. Antonelli^{19a,19b}, J. Antos^{144b}, F. Anulli^{132a}, S. Aoun⁸³, L. Aperio Bella⁴, R. Apolle¹¹⁸, G. Arabidze⁸⁸, I. Aracena¹⁴³, Y. Arai⁶⁶, A.T.H. Arce⁴⁴, J.P. Archambault²⁸, S. Arfaoui^{29,c}, J-F. Arguin¹⁴, E. Arik^{18a,*}, M. Arik^{18a}, A.J. Armbruster⁸⁷, K.E. Arms¹⁰⁹, S.R. Armstrong²⁴, O. Arnaez⁴, C. Arnault¹¹⁵, A. Artamonov⁹⁵, G. Artoni^{132a,132b}, D. Arutinov²⁰, S. Asai¹⁵⁵, J. Silva^{124a,d}, R. Asfandiyarov¹⁷², S. Ask²⁷, B. Åsman^{146a,146b}, L. Asquith⁵, K. Assamagan²⁴, A. Astbury¹⁶⁹, A. Astvatsatourov⁵², G. Atoian¹⁷⁵, B. Aubert⁴, B. Auerbach¹⁷⁵, E. Auge¹¹⁵, K. Augsten¹²⁷, M. Auresseau⁴, N. Austin⁷³, R. Avramidou⁹, D. Axen¹⁶⁸, C. Ay⁵⁴, G. Azuelos^{93,e}, Y. Azuma¹⁵⁵, M.A. Baak²⁹, G. Baccaglioni^{25a}, C. Bacci^{134a,134b}, A.M. Bach¹⁴, H. Bachacou¹³⁶, K. Bachas²⁹, G. Bachy²⁹, M. Backes⁴⁹, E. Badescu^{25a}, P. Bagnaia^{132a,132b}, S. Bahinipati², Y. Bai^{32a}, D.C. Bailey¹⁵⁸, T. Bain¹⁵⁸, J.T. Baines¹²⁹, O.K. Baker¹⁷⁵, S. Baker⁷⁷, F. Baltasar Dos Santos Pedrosa²⁹, E. Banas³⁸, P. Banerjee⁹³, Sw. Banerjee¹⁶⁹, D. Banfi^{89a,89b}, A. Bangert¹³⁷, V. Bansal¹⁶⁹, H.S. Bansil¹⁷, L. Barak¹⁷¹, S.P. Baranov⁹⁴, A. Barashkou⁶⁵, A. Barbaro Galtieri¹⁴, T. Barber²⁷, E.L. Barberio⁸⁶, D. Barberis^{50a,50b}, M. Barbero²⁰, D.Y. Bardin⁶⁵, T. Barillari⁹⁹, M. Barisonzi¹⁷⁴, T. Barklow¹⁴³, N. Barlow²⁷, B.M. Barnett¹²⁹, R.M. Barnett¹⁴, A. Baroncelli^{134a}, A.J. Barr¹¹⁸, F. Barreiro⁸⁰, J. Barreiro Guimarães da Costa⁵⁷, P. Barrillon¹¹⁵, R. Bartoldus¹⁴³, A.E. Barton⁷¹, D. Bartsch²⁰, R.L. Bates⁵³, L. Batkova^{144a}, J.R. Batley²⁷, A. Battaglia¹⁶, M. Battistin²⁹, G. Battistoni^{89a}, F. Bauer¹³⁶, H.S. Bawa¹⁴³, B. Beare¹⁵⁸, T. Beau⁷⁸, P.H. Beauchemin¹¹⁸, R. Beccherle^{50a}, P. Bechtel⁴¹, H.P. Beck¹⁶, M. Beckingham⁴⁸, K.H. Becks¹⁷⁴, A.J. Beddall^{18c}, A. Beddall^{18c}, V.A. Bednyakov⁶⁵, C. Bee⁸³, M. Beegle²⁴, S. Behar Harpaz¹⁵², P.K. Behera⁶³, M. Beimforde⁹⁹, C. Belanger-Champagne¹⁶⁶, P.J. Bell⁴⁹, W.H. Bell⁴⁹, G. Bella¹⁵³, L. Bellagamba^{19a}, F. Bellina²⁹, G. Bellomo^{89a,89b}, M. Bellomo^{119a}, A. Belloni⁵⁷, K. Belotskiy⁹⁶, O. Beltramello²⁹, S. Ben Ami¹⁵², O. Benary¹⁵³, D. Benchekroun^{135a}, C. Bouchouk⁸³, M. Bendel⁸¹, B.H. Benedict¹⁶³, N. Benekos¹⁶⁵, Y. Benhammou¹⁵³, D.P. Benjamin⁴⁴, M. Benoit¹¹⁵, J.R. Bensinger²², K. Benslama¹³⁰, S. Bentvelsen¹⁰⁵, D. Berge²⁹, E. Bergeas Kuutmann⁴¹, N. Berger⁴, F. Berghaus¹⁶⁹, E. Berghlund⁴⁹, J. Beringer¹⁴, K. Bernardet⁸³, P. Bernat¹¹⁵, R. Bernhard⁴⁸, C. Bernius²⁴, T. Berry⁷⁶, A. Bertin^{19a,19b}, F. Bertinelli²⁹, F. Bertolucci^{122a,122b}, M.I. Besana^{89a,89b}, N. Besson¹³⁶, S. Bethke⁹⁹, W. Bhimji⁴⁵, R.M. Bianchi²⁹, M. Bianco^{72a,72b}, O. Biebel⁹⁸, J. Biesiada¹⁴, M. Biglietti^{132a,132b}, H. Bilokon⁴⁷, M. Bindi^{19a,19b}, A. Bingul^{18c}, C. Bini^{132a,132b}, C. Biscarat¹⁷⁷, U. Bitenc⁴⁸, K.M. Black²¹, R.E. Blair⁵, J-B Blanchard¹¹⁵, G. Blanchot²⁹, C. Blocker²², J. Blocki³⁸, A. Blondel⁴⁹, W. Blum⁸¹, U. Blumenschein⁵⁴, G.J. Bobbink¹⁰⁵, V.B. Bobrovnikov¹⁰⁷, A. Bocci⁴⁴, R. Bock²⁹, C.R. Boddy¹¹⁸, M. Boehler⁴¹, J. Boek¹⁷⁴, N. Boelaert³⁵, S. Böser⁷⁷, J.A. Bogaerts²⁹, A. Bogdanchikov¹⁰⁷, A. Bogouch^{90,*}, C. Bohm^{146a}, V. Boisvert⁷⁶, T. Bold^{163,f}, V. Boldea^{25a}, M. Boonekamp¹³⁶, G. Boorman⁷⁶, C.N. Booth¹³⁹, P. Booth¹³⁹, J.R.A. Booth¹⁷, S. Bordini⁷⁸, C. Borer¹⁶, A. Borisov¹²⁸, G. Borissov⁷¹, I. Borjanovic^{12a}, S. Borroni^{132a,132b}, K. Bos¹⁰⁵, D. Boscherini^{19a}, M. Bosman¹¹, H. Boterenbrood¹⁰⁵, D. Botterill¹²⁹, J. Bouchami⁹³, J. Boudreau¹²³, E.V. Bouhova-Thacker⁷¹, C. Boulahouache¹²³, C. Bourdarios¹¹⁵, N. Bousson⁸³, A. Boveia³⁰, J. Boyd²⁹, I.R. Boyko⁶⁵, N.I. Bozhko¹²⁸, I. Bozovic-Jelisavcic^{12b}, J. Bracinik¹⁷, A. Braem²⁹, E. Brambilla^{72a,72b}, P. Branchini^{134a}, G.W. Brandenburg⁵⁷, A. Brandt⁷, G. Brandt⁴¹, O. Brandt⁵⁴, U. Bratzler¹⁵⁶, B. Brau⁸⁴, J.E. Brau¹¹⁴, H.M. Braun¹⁷⁴, B. Brelvi¹⁵⁸, J. Bremer²⁹, R. Brenner¹⁶⁶, S. Bressler¹⁵², D. Breton¹¹⁵, N.D. Brett¹¹⁸, P.G. Bright-Thomas¹⁷, D. Britton⁵³, F.M. Brochu²⁷, I. Brock²⁰, R. Brock⁸⁸, T.J. Brodbeck⁷¹, E. Brodet¹⁵³, F. Broggi^{89a}, C. Bromberg⁸⁸, G. Brooijmans³⁴, W.K. Brooks^{31b}, G. Brown⁸², E. Brubaker³⁰, P.A. Bruckman de Renstrom³⁸, D. Bruncko^{144b}, R. Brunelieri⁴⁸, S. Brunet⁶¹, A. Bruni^{19a}, G. Bruni^{19a}, M. Bruschi^{19a}, T. Buanes¹³, F. Bucci⁴⁹, J. Buchanan¹¹⁸, N.J. Buchanan², P. Buchholz¹⁴¹, R.M. Buckingham¹¹⁸, A.G. Buckley⁴⁵, S.I. Buda^{25a}, I.A. Budagov⁶⁵, B. Budick¹⁰⁸, V. Büscher⁸¹, L. Bugge¹¹⁷, D. Buirra-Clark¹¹⁸, E.J. Buis¹⁰⁵, O. Bulekov⁹⁶, M. Bunse⁴², T. Buran¹¹⁷, H. Burckhart²⁹, S. Burdin⁷³, T. Burgess¹³, S. Burke¹²⁹, E. Busato³³, P. Bussey⁵³, C.P. Buszello¹⁶⁶, F. Butin²⁹, B. Butler¹⁴³, J.M. Butler²¹, C.M. Buttar⁵³, J.M. Butterworth⁷⁷, W. Buttinger²⁷, T. Byatt⁷⁷, S. Cabrera Urbán¹⁶⁷, M. Caccia^{89a,89b,g}, D. Caforio^{19a,19b}, O. Cakir^{3a}, P. Calafiura¹⁴, G. Calderini⁷⁸, P. Calfayan⁹⁸, R. Calkins¹⁰⁶, L.P. Caloba^{23a}, R. Caloi^{132a,132b}, D. Calvet³³, S. Calvet³³, A. Camard⁷⁸, P. Camarri^{133a,133b}, M. Cambiaghi^{119a,119b}, D. Cameron¹¹⁷, J. Cammin²⁰, S. Campana²⁹, M. Campanelli⁷⁷, V. Canale^{102a,102b}, F. Canelli³⁰, A. Canepa^{159a}, J. Cantero⁸⁰, L. Capasso^{102a,102b},

M.D.M. Capeans Garrido²⁹, I. Caprini^{25a}, M. Caprini^{25a}, D. Capriotti⁹⁹, M. Capua^{36a,36b}, R. Caputo¹⁴⁸, C. Caramarcu^{25a}, R. Cardarelli^{133a}, T. Carli²⁹, G. Carlino^{102a}, L. Carminati^{89a,89b}, B. Caron^{159a}, S. Caron⁴⁸, C. Carpentieri⁴⁸, G.D. Carrillo Montoya¹⁷², S. Carron Montero¹⁵⁸, A.A. Carter⁷⁵, J.R. Carter²⁷, J. Carvalho^{124a,h}, D. Casadei¹⁰⁸, M.P. Casado¹¹, M. Cascella^{122a,122b}, C. Caso^{50a,50b,*}, A.M. Castaneda Hernandez¹⁷², E. Castaneda-Miranda¹⁷², V. Castillo Gimenez¹⁶⁷, N.F. Castro^{124b,a}, G. Cataldi^{72a}, F. Cataneo²⁹, A. Catinaccio²⁹, J.R. Catmore⁷¹, A. Cattai²⁹, G. Cattani^{133a,133b}, S. Caughron⁸⁸, A. Cavallari^{132a,132b}, P. Cavalleri⁷⁸, D. Cavalli^{89a}, M. Cavalli-Sforza¹¹, V. Cavasinni^{122a,122b}, A. Cazzato^{72a,72b}, F. Ceradini^{134a,134b}, C. Cerna⁸³, A.S. Cerqueira^{23a}, A. Cerri²⁹, L. Cerrito⁷⁵, F. Cerutti⁴⁷, S.A. Cetin^{18b}, F. Cevenini^{102a,102b}, A. Chafaq^{135a}, D. Chakraborty¹⁰⁶, K. Chan², B. Chapleau⁸⁵, J.D. Chapman²⁷, J.W. Chapman⁸⁷, E. Chareyre⁷⁸, D.G. Charlton¹⁷, V. Chavda⁸², S. Cheatham⁷¹, S. Chekanov⁵, S.V. Chekulaev^{159a}, G.A. Chelkov⁶⁵, H. Chen²⁴, L. Chen², S. Chen^{32c}, T. Chen^{32c}, X. Chen¹⁷², S. Cheng^{32a}, A. Cheplakov⁶⁵, V.F. Chepurinov⁶⁵, R. Cherkaoui El Moursli^{135d}, V. Tcherniatine²⁴, E. Cheu⁶, S.L. Cheung¹⁵⁸, L. Chevalier¹³⁶, F. Chevallier¹³⁶, G. Chiefari^{102a,102b}, L. Chikovani⁵¹, J.T. Childers^{58a}, A. Chilingarov⁷¹, G. Chiodini^{72a}, M.V. Chizhov⁶⁵, G. Choudalakis³⁰, S. Chouridou¹³⁷, I.A. Christidi⁷⁷, A. Christov⁴⁸, D. Chromek-Burckhart²⁹, M.L. Chu¹⁵¹, J. Chudoba¹²⁵, G. Ciapetti^{132a,132b}, A.K. Ciftci^{3a}, R. Ciftci^{3a}, D. Cinca³³, V. Cindro⁷⁴, M.D. Ciobotaru¹⁶³, C. Ciocca^{19a,19b}, A. Ciocio¹⁴, M. Cirilli^{87,i}, M. Ciubancan^{25a}, A. Clark⁴⁹, P.J. Clark⁴⁵, W. Cleland¹²³, J.C. Clemens⁸³, B. Clement⁵⁵, C. Clement^{146a,146b}, R.W. Clift¹²⁹, Y. Coadou⁸³, M. Cobal^{164a,164c}, A. Cocco^{50a,50b}, J. Cochran⁶⁴, P. Coe¹¹⁸, J.G. Cogan¹⁴³, J. Coggeshall¹⁶⁵, E. Cogneras¹⁷⁷, C.D. Cojocar²⁸, J. Colas⁴, A.P. Colijn¹⁰⁵, C. Collard¹¹⁵, N.J. Collins¹⁷, C. Collins-Tooth⁵³, J. Collot⁵⁵, G. Colon⁸⁴, R. Coluccia^{72a,72b}, G. Comune⁸⁸, P. Conde Muño^{124a}, E. Coniavitis¹¹⁸, M.C. Conidi¹¹, M. Consonni¹⁰⁴, S. Constantinescu^{25a}, C. Conta^{119a,119b}, F. Conventi^{102a,j}, J. Cook²⁹, M. Cooke¹⁴, B.D. Cooper⁷⁵, A.M. Cooper-Sarkar¹¹⁸, N.J. Cooper-Smith⁷⁶, K. Copic³⁴, T. Cornelissen^{50a,50b}, M. Corradi^{19a}, S. Correard⁸³, F. Corriveau^{85,k}, A. Cortes-Gonzalez¹⁶⁵, G. Cortiana⁹⁹, G. Costa^{89a}, M.J. Costa¹⁶⁷, D. Costanzo¹³⁹, T. Costin³⁰, D. Côté²⁹, R. Coura Torres^{23a}, L. Courneyea¹⁶⁹, G. Cowan⁷⁶, C. Cowden²⁷, B.E. Cox⁸², K. Cranmer¹⁰⁸, M. Crinziani²⁰, G. Crosetti^{36a,36b}, R. Crupi^{72a,72b}, S. Crépe-Renaudin⁵⁵, C. Cuenca Almenar¹⁷⁵, T. Cuhadar Donszelmann¹³⁹, S. Cuneo^{50a,50b}, M. Curatolo⁴⁷, C.J. Curtis¹⁷, P. Cwetanski⁶¹, H. Cziri¹⁴¹, Z. Czyczula¹¹⁷, S. D'Auria⁵³, M. D'Onofrio⁷³, A. D'Orazio^{132a,132b}, A. Da Rocha Gesualdi Mello^{23a}, P.V.M. Da Silva^{23a}, C. Da Via⁸², W. Dabrowski³⁷, A. Dahlhoff⁴⁸, T. Dai⁸⁷, C. Dallapiccola⁸⁴, S.J. Dallison^{129,*}, M. Dam³⁵, M. Dameri^{50a,50b}, D.S. Damiani¹³⁷, H.O. Danielsson²⁹, R. Dankers¹⁰⁵, D. Dannheim⁹⁹, V. Dao⁴⁹, G. Darbo^{50a}, G.L. Darlea^{25b}, C. Daum¹⁰⁵, J.P. Dauvergne²⁹, W. Davey⁸⁶, T. Davidek¹²⁶, N. Davidson⁸⁶, R. Davidson⁷¹, M. Davies⁹³, A.R. Davison⁷⁷, E. Dawe¹⁴², I. Dawson¹³⁹, J.W. Dawson^{5,*}, R.K. Daya³⁹, K. De⁷, R. de Asmundis^{102a}, S. De Castro^{19a,19b}, S. De Cecco⁷⁸, J. de Graat⁹⁸, N. De Groot¹⁰⁴, P. de Jong¹⁰⁵, E. De La Cruz-Burelo⁸⁷, C. De La Taille¹¹⁵, B. De Lotto^{164a,164c}, L. De Mora⁷¹, L. De Nooij¹⁰⁵, M. De Oliveira Branco²⁹, D. De Pedis^{132a}, P. de Saintignon⁵⁵, A. De Salvo^{132a}, U. De Sanctis^{164a,164c}, A. De Santo¹⁴⁹, J.B. De Vivie De Regie¹¹⁵, S. Dean⁷⁷, G. Dedes⁹⁹, D.V. Dedovich⁶⁵, J. Degenhardt¹²⁰, M. Dehchar¹¹⁸, M. Deile⁹⁸, C. Del Papa^{164a,164c}, J. Del Peso⁸⁰, T. Del Prete^{122a,122b}, A. Dell'Acqua²⁹, L. Dell'Asta^{89a,89b}, M. Della Pietra^{102a,l}, D. della Volpe^{102a,102b}, M. Delmastro²⁹, P. Delpierre⁸³, N. Delruelle²⁹, P.A. Delsart⁵⁵, C. Deluca¹⁴⁸, S. Demers¹⁷⁵, M. Demichev⁶⁵, B. Demirkoz¹¹, J. Deng¹⁶³, S.P. Denisov¹²⁸, C. Dennis¹¹⁸, D. Derendarz³⁸, J.E. Derkaoui^{135c}, F. Derue⁷⁸, P. Dervan⁷³, K. Desch²⁰, E. Devetak¹⁴⁸, P.O. Deviveiros¹⁵⁸, A. Dewhurst¹²⁹, B. DeWilde¹⁴⁸, S. Dhaliwal¹⁵⁸, R. Dhullipudi^{24,m}, A. Di Ciaccio^{133a,133b}, L. Di Ciaccio⁴, A. Di Girolamo²⁹, B. Di Girolamo²⁹, S. Di Luise^{134a,134b}, A. Di Mattia⁸⁸, R. Di Nardo^{133a,133b}, A. Di Simone^{133a,133b}, R. Di Sipio^{19a,19b}, M.A. Diaz^{31a}, F. Diblen^{18c}, E.B. Diehl⁸⁷, H. Dietl⁹⁹, J. Dietrich⁴⁸, T.A. Dietzsch^{58a}, S. Diglio¹¹⁵, K. Dindar Yagci³⁹, J. Dingfelder²⁰, C. Dionisi^{132a,132b}, P. Dita^{25a}, S. Dita^{25a}, F. Dittus²⁹, F. Djama⁸³, R. Djilkibaev¹⁰⁸, T. Djobava⁵¹, M.A.B. do Vale^{23a}, A. Do Valle Wemans^{124a}, T.K.O. Doan⁴, M. Dobbs⁸⁵, R. Dobinson^{29,*}, D. Dobos⁴², E. Dobson²⁹, M. Dobson¹⁶³, J. Dodd³⁴, O.B. Dogan^{18a,*}, C. Doglioni¹¹⁸, T. Doherty⁵³, Y. Doi^{66,*}, J. Dolejsi¹²⁶, I. Dolenc⁷⁴, Z. Dolezal¹²⁶, B.A. Dolgoshein⁹⁶, T. Dohmae¹⁵⁵, M. Donadelli^{23b}, M. Donega¹²⁰, J. Donini⁵⁵, J. Dopke¹⁷⁴, A. Doria^{102a}, A. Dos Anjos¹⁷², M. Dosil¹¹, A. Dotti^{122a,122b}, M.T. Dova⁷⁰, J.D. Dowell¹⁷, A.D. Doxiadis¹⁰⁵, A.T. Doyle⁵³, Z. Drasal¹²⁶, J. Drees¹⁷⁴, N. Dressnandt¹²⁰, H. Drevermann²⁹, C. Driouichi³⁵, M. Dris⁹, J.G. Drohan⁷⁷, J. Dubbert⁹⁹, T. Dubbs¹³⁷, S. Dube¹⁴, E. Duchovni¹⁷¹, G. Duckeck⁹⁸, A. Dudarev²⁹, F. Dudziak¹¹⁵, M. Dührssen²⁹, I.P. Duerdoth⁸², L. Duflot¹¹⁵, M-A. Dufour⁸⁵, M. Dunford²⁹, H. Duran Yildiz^{3b}, R. Duxfield¹³⁹, M. Dwuznik³⁷, F. Dydak²⁹, D. Dzahini⁵⁵, M. Düren⁵², J. Ebke⁹⁸, S. Eckert⁴⁸, S. Eckweiler⁸¹, K. Edmonds⁸¹, C.A. Edwards⁷⁶, I. Efthymiopoulos⁴⁹, W. Ehrenfeld⁴¹, T. Ehrich⁹⁹, T. Eifert²⁹, G. Eigen¹³, K. Einsweiler¹⁴, E. Eisenhandler⁷⁵, T. Ekelof¹⁶⁶, M. El Kacimi⁴, M. Ellert¹⁶⁶, S. Elles⁴, F. Ellinghaus⁸¹, K. Ellis⁷⁵, N. Ellis²⁹, J. Elmsheuser⁹⁸, M. Elsing²⁹, R. Ely¹⁴, D. Emeliyanov¹²⁹, R. Engelmann¹⁴⁸, A. Engl⁹⁸, B. Epp⁶², A. Eppig⁸⁷, J. Erdmann⁵⁴, A. Ereditato¹⁶, D. Eriksson^{146a}, J. Ernst¹, M. Ernst²⁴, J. Ernwein¹³⁶, D. Errede¹⁶⁵, S. Errede¹⁶⁵, E. Ertel⁸¹, M. Escalier¹¹⁵, C. Escobar¹⁶⁷, X. Espinal Curull¹¹, B. Esposito⁴⁷, F. Etienne⁸³, A.I. Etienvre¹³⁶, E. Etzion¹⁵³, D. Evangelakou⁵⁴, H. Evans⁶¹, L. Fabbri^{19a,19b}, C. Fabre²⁹, K. Facius³⁵, R.M. Fakhrudinov¹²⁸, S. Falciano^{132a}, A.C. Falou¹¹⁵, Y. Fang¹⁷², M. Fanti^{89a,89b}, A. Farbin⁷, A. Farilla^{134a}, J. Farley¹⁴⁸, T. Farooque¹⁵⁸,

S.M. Farrington¹¹⁸, P. Farthouat²⁹, D. Fasching¹⁷², P. Fassnacht²⁹, D. Fassouliotis⁸, B. Fatholahzadeh¹⁵⁸, A. Favaretto^{89a,89b}, L. Fayard¹¹⁵, S. Fazio^{36a,36b}, R. Febbraro³³, P. Federic^{144a}, O.L. Fedin¹²¹, I. Fedorko²⁹, W. Fedorko⁸⁸, M. Fehling-Kaschek⁴⁸, L. Feligioni⁸³, D. Fellmann⁵, C.U. Felzmann⁸⁶, C. Feng^{32d}, E.J. Feng³⁰, A.B. Fenyuk¹²⁸, J. Ferencei^{144b}, D. Ferguson¹⁷², J. Ferland⁹³, B. Fernandes^{124a,n}, W. Fernando¹⁰⁹, S. Ferrag⁵³, J. Ferrari¹¹⁸, V. Ferrara⁴¹, A. Ferrari¹⁶⁶, P. Ferrari¹⁰⁵, R. Ferrari^{119a}, A. Ferrer¹⁶⁷, M.L. Ferrer⁴⁷, D. Ferrere⁴⁹, C. Ferretti⁸⁷, A. Ferretto Parodi^{50a,50b}, M. Fiascaris³⁰, F. Fiedler⁸¹, A. Filipčić⁷⁴, A. Filippas⁹, F. Filthaut¹⁰⁴, M. Fincke-Keeler¹⁶⁹, M.C.N. Fiolhais^{124a,h}, L. Fiorini¹¹, A. Firan³⁹, G. Fischer⁴¹, P. Fischer²⁰, M.J. Fisher¹⁰⁹, S.M. Fisher¹²⁹, J. Flammer²⁹, M. Flechl⁴⁸, I. Fleck¹⁴¹, J. Fleckner⁸¹, P. Fleischmann¹⁷³, S. Fleischmann²⁰, T. Flick¹⁷⁴, L.R. Flores Castillo¹⁷², M.J. Flowerdew⁹⁹, F. Föhlich^{58a}, M. Fokitis⁹, T. Fonseca Martin¹⁶, D.A. Forbush¹³⁸, A. Formica¹³⁶, A. Forti⁸², D. Fortin^{159a}, J.M. Foster⁸², D. Fournier¹¹⁵, A. Foussat²⁹, A.J. Fowler⁴⁴, K. Fowler¹³⁷, H. Fox⁷¹, P. Francavilla^{122a,122b}, S. Franchino^{119a,119b}, D. Francis²⁹, T. Frank¹⁷¹, M. Franklin⁵⁷, S. Franz²⁹, M. Fraternali^{119a,119b}, S. Fratina¹²⁰, S.T. French²⁷, R. Froeschl²⁹, D. Froidevaux²⁹, J.A. Frost²⁷, C. Fukunaga¹⁵⁶, E. Fullana Torregrosa²⁹, J. Fuster¹⁶⁷, C. Gabaldon²⁹, O. Gabizon¹⁷¹, T. Gadfort²⁴, S. Gadowski⁴⁹, G. Gagliardi^{50a,50b}, P. Gagnon⁶¹, C. Galea⁹⁸, E.J. Gallas¹¹⁸, M.V. Gallas²⁹, V. Gallo¹⁶, B.J. Gallop¹²⁹, P. Gallus¹²⁵, E. Galyaev⁴⁰, K.K. Gan¹⁰⁹, Y.S. Gao^{143,o}, V.A. Gapienko¹²⁸, A. Gaponenko¹⁴, F. Garberson¹⁷⁵, M. Garcia-Sciveres¹⁴, C. García¹⁶⁷, J.E. García Navarro⁴⁹, R.W. Gardner³⁰, N. Garelli²⁹, H. Garitaonandia¹⁰⁵, V. Garonne²⁹, J. Garvey¹⁷, C. Gatti⁴⁷, G. Gaudio^{119a}, O. Gaumer⁴⁹, B. Gaur¹⁴¹, L. Gauthier¹³⁶, I.L. Gavrilenko⁹⁴, C. Gay¹⁶⁸, G. Gaycken²⁰, J-C. Gayde²⁹, E.N. Gazis⁹, P. Ge^{32d}, C.N.P. Gee¹²⁹, Ch. Geich-Gimbel²⁰, K. Gellerstedt^{146a,146b}, C. Gemme^{50a}, M.H. Genest⁹⁸, S. Gentile^{132a,132b}, F. Georgatos⁹, S. George⁷⁶, P. Gerlach¹⁷⁴, A. Gershon¹⁵³, C. Geweniger^{58a}, H. Ghazlane^{135d}, P. Ghez⁴, N. Ghodbane³³, B. Giacobbe^{19a}, S. Giagu^{132a,132b}, V. Giakoumopoulou⁸, V. Giangiobbe^{122a,122b}, F. Gianotti²⁹, B. Gibbard²⁴, A. Gibson¹⁵⁸, S.M. Gibson²⁹, G.F. Gieraltowski⁵, L.M. Gilbert¹¹⁸, M. Gilchriese¹⁴, O. Gildemeister²⁹, V. Gilevsky⁹¹, D. Gillberg²⁸, A.R. Gillman¹²⁹, D.M. Gingrich^{2,p}, J. Ginzburg¹⁵³, N. Giokaris⁸, R. Giordano^{102a,102b}, F.M. Giorgi¹⁵, P. Giovannini⁹⁹, P.F. Giraud¹³⁶, D. Giugni^{89a}, P. Giusti^{19a}, B.K. Gjelsten¹¹⁷, L.K. Gladilin⁹⁷, C. Glasman⁸⁰, J. Glatzer⁴⁸, A. Glazov⁴¹, K.W. Glitza¹⁷⁴, G.L. Glonti⁶⁵, J. Godfrey¹⁴², J. Godlewski²⁹, M. Goebel⁴¹, T. Göpfert⁴³, C. Goeringer⁸¹, C. Gössling⁴², T. Göttfert⁹⁹, S. Goldfarb⁸⁷, D. Goldin³⁹, T. Golling¹⁷⁵, N.P. Gollub²⁹, S.N. Golovnia¹²⁸, A. Gomes^{124a,q}, L.S. Gomez Fajardo⁴¹, R. Gonçalo⁷⁶, L. Gonella²⁰, C. Gong^{32b}, A. Gonidec²⁹, S. Gonzalez¹⁷², S. González de la Hoz¹⁶⁷, M.L. Gonzalez Silva²⁶, S. Gonzalez-Sevilla⁴⁹, J.J. Goodson¹⁴⁸, L. Goossens²⁹, P.A. Gorbounov⁹⁵, H.A. Gordon²⁴, I. Gorelov¹⁰³, G. Gorfine¹⁷⁴, B. Gorini²⁹, E. Gorini^{72a,72b}, A. Gorišek⁷⁴, E. Gornicki³⁸, S.A. Gorokhov¹²⁸, B.T. Gorski²⁹, V.N. Goryachev¹²⁸, B. Godzik⁴¹, M. Gosselink¹⁰⁵, M.I. Gostkin⁶⁵, M. Gouanère⁴, I. Gough Eschrich¹⁶³, M. Goughri^{135a}, D. Goujdami^{135a}, M.P. Goulette⁴⁹, A.G. Goussiou¹³⁸, C. Goy⁴, I. Grabowska-Bold^{163,r}, V. Grabski¹⁷⁶, P. Grafström²⁹, C. Grah¹⁷⁴, K-J. Grah¹⁴⁷, F. Grancagnolo^{72a}, S. Grancagnolo¹⁵, V. Grassi¹⁴⁸, V. Gratchev¹²¹, N. Grau³⁴, H.M. Gray^{34,s}, J.A. Gray¹⁴⁸, E. Graziani^{134a}, O.G. Grebenyuk¹²¹, D. Greenfield¹²⁹, T. Greenshaw⁷³, Z.D. Greenwood^{24,t}, I.M. Gregor⁴¹, P. Grenier¹⁴³, E. Griesmayer⁴⁶, J. Griffiths¹³⁸, N. Grigalashvili⁶⁵, A.A. Grillo¹³⁷, K. Grimm¹⁴⁸, S. Grinstein¹¹, P.L.Y. Gris³³, Y.V. Grishkevich⁹⁷, J.-F. Grivaz¹¹⁵, J. Grognuz²⁹, M. Groh⁹⁹, E. Gross¹⁷¹, J. Grosse-Knetter⁵⁴, J. Groth-Jensen⁷⁹, M. Gruwe²⁹, K. Grybel¹⁴¹, V.J. Guarino⁵, C. Guichenev³³, A. Guida^{72a,72b}, T. Guillemain⁴, S. Guindon⁵⁴, H. Guler^{85,u}, J. Gunther¹²⁵, B. Guo¹⁵⁸, J. Guo³⁴, A. Gupta³⁰, Y. Gusakov⁶⁵, V.N. Gushchin¹²⁸, A. Gutierrez⁹³, P. Gutierrez¹¹¹, N. Guttman¹⁵³, O. Gutzwiller¹⁷², C. Guyot¹³⁶, C. Gwenlan¹¹⁸, C.B. Gwilliam⁷³, A. Haas¹⁴³, S. Haas²⁹, C. Haber¹⁴, R. Hackenburg²⁴, H.K. Hadavand³⁹, D.R. Hadley¹⁷, P. Haefner⁹⁹, F. Hahn²⁹, S. Haider²⁹, Z. Hajduk³⁸, H. Hakobyan¹⁷⁶, J. Haller⁵⁴, K. Hamacher¹⁷⁴, A. Hamilton⁴⁹, S. Hamilton¹⁶¹, H. Han^{32a}, L. Han^{32b}, K. Hanagaki¹¹⁶, M. Hance¹²⁰, C. Handel⁸¹, P. Hanke^{58a}, C.J. Hansen¹⁶⁶, J.R. Hansen³⁵, J.B. Hansen³⁵, J.D. Hansen³⁵, P.H. Hansen³⁵, P. Hansson¹⁴³, K. Hara¹⁶⁰, G.A. Hare¹³⁷, T. Harenberg¹⁷⁴, D. Harper⁸⁷, R.D. Harrington²¹, O.M. Harris¹³⁸, K. Harrison¹⁷, J.C. Hart¹²⁹, J. Hartert⁴⁸, F. Hartjes¹⁰⁵, T. Haruyama⁶⁶, A. Harvey⁵⁶, S. Hasegawa¹⁰¹, Y. Hasegawa¹⁴⁰, S. Hassani¹³⁶, M. Hatch²⁹, D. Hauff⁹⁹, S. Haug¹⁶, M. Hauschild²⁹, R. Hauser⁸⁸, M. Havranek¹²⁵, B.M. Hawes¹¹⁸, C.M. Hawkes¹⁷, R.J. Hawkins²⁹, D. Hawkins¹⁶³, T. Hayakawa⁶⁷, D. Hayden⁷⁶, H.S. Hayward⁷³, S.J. Hayward¹²⁹, E. Hazen²¹, M. He^{32d}, S.J. Head¹⁷, V. Hedberg⁷⁹, L. Heelan²⁸, S. Heim⁸⁸, B. Heinemann¹⁴, S. Heisterkamp³⁵, L. Helary⁴, M. Heldmann⁴⁸, M. Heller¹¹⁵, S. Hellman^{146a,146b}, C. Hensens¹¹, R.C.W. Henderson⁷¹, M. Henke^{58a}, A. Henrichs⁵⁴, A.M. Henriques Correia²⁹, S. Henrot-Versille¹¹⁵, F. Henry-Couannier⁸³, C. Hensel⁵⁴, T. Henß¹⁷⁴, Y. Hernández Jiménez¹⁶⁷, R. Herrberg¹⁵, A.D. Hershenhorn¹⁵², G. Herten⁴⁸, R. Hertenberger⁹⁸, L. Hervas²⁹, N.P. Hessey¹⁰⁵, A. Hidvegi^{146a}, E. Higón-Rodríguez¹⁶⁷, D. Hill^{5,*}, J.C. Hill²⁷, N. Hill⁵, K.H. Hiller⁴¹, S. Hillert²⁰, S.J. Hillier¹⁷, I. Hinchliffe¹⁴, E. Hines¹²⁰, M. Hirose¹¹⁶, F. Hirsch⁴², D. Hirschebuehl¹⁷⁴, J. Hobbs¹⁴⁸, N. Hod¹⁵³, M.C. Hodgkinson¹³⁹, P. Hodgson¹³⁹, A. Hoecker²⁹, M.R. Hoferkamp¹⁰³, J. Hoffman³⁹, D. Hoffmann⁸³, M. Hohlfeld⁸¹, M. Holder¹⁴¹, A. Holmes¹¹⁸, S.O. Holmgren^{146a}, T. Holy¹²⁷, J.L. Holzbauer⁸⁸, R.J. Homer¹⁷, Y. Homma⁶⁷, T. Horazdovsky¹²⁷, C. Horn¹⁴³, S. Horner⁴⁸, K. Horton¹¹⁸, J-Y. Hostachy⁵⁵, T. Hott⁹⁹, S. Hou¹⁵¹, M.A. Houlden⁷³, A. Hoummada^{135a}, J. Howarth⁸², D.F. Howell¹¹⁸, I. Hristova⁴¹, J. Hrivnac¹¹⁵, I. Hruska¹²⁵, T. Hryn'ova⁴, P.J. Hsu¹⁷⁵, S.-C. Hsu¹⁴, G.S. Huang¹¹¹, Z. Hubacek¹²⁷, F. Hubaut⁸³, F. Huegging²⁰, T.B. Huffman¹¹⁸, E.W. Hughes³⁴, G. Hughes⁷¹, R.E. Hughes-Jones⁸², M. Huhtinen²⁹,

P. Hurst⁵⁷, M. Hurwitz¹⁴, U. Husemann⁴¹, N. Huseynov¹⁰, J. Huston⁸⁸, J. Huth⁵⁷, G. Iacobucci^{102a}, G. Iakovidis⁹, M. Ibbotson⁸², I. Ibragimov¹⁴¹, R. Ichimiya⁶⁷, L. Iconomidou-Fayard¹¹⁵, J. Idarraga¹¹⁵, M. Idzik³⁷, P. Iengo⁴, O. Igonkina¹⁰⁵, Y. Ikegami⁶⁶, M. Ikeno⁶⁶, Y. Ilchenko³⁹, D. Iliadis¹⁵⁴, D. Imbault⁷⁸, M. Imhaeuser¹⁷⁴, M. Imori¹⁵⁵, T. Ince²⁰, J. Inigo-Golfin²⁹, P. Ioannou⁸, M. Iodice^{134a}, G. Ionescu⁴, A. Irls Quiles¹⁶⁷, K. Ishii⁶⁶, A. Ishikawa⁶⁷, M. Ishino⁶⁶, R. Ishmukhametov³⁹, T. Isobe¹⁵⁵, C. Issever¹¹⁸, S. Istin^{18a}, Y. Itoh¹⁰¹, A.V. Ivashin¹²⁸, W. Iwanski³⁸, H. Iwasaki⁶⁶, J.M. Izen⁴⁰, V. Izzo^{102a}, B. Jackson¹²⁰, J.N. Jackson⁷³, P. Jackson¹⁴³, M.R. Jaekel²⁹, V. Jain⁶¹, K. Jakobs⁴⁸, S. Jakobsen³⁵, J. Jakubek¹²⁷, D.K. Jana¹¹¹, E. Jankowski¹⁵⁸, E. Jansen⁷⁷, A. Jantsch⁹⁹, M. Janus²⁰, G. Jarlskog⁷⁹, L. Jeanty⁵⁷, K. Jelen³⁷, I. Jen-La Plante³⁰, P. Jenni²⁹, A. Jeremie⁴, P. Jez³⁵, S. Jézéquel⁴, H. Ji¹⁷², W. Ji⁸¹, J. Jia¹⁴⁸, Y. Jiang^{32b}, M. Jimenez Belenguer²⁹, G. Jin^{32b}, S. Jin^{32a}, O. Jinnouchi¹⁵⁷, M.D. Joergensen³⁵, D. Joffe³⁹, L.G. Johansen¹³, M. Johansen^{146a,146b}, K.E. Johansson^{146a}, P. Johansson¹³⁹, S. Johnert⁴¹, K.A. Johns⁶, K. Jon-And^{146a,146b}, G. Jones⁸², R.W.L. Jones⁷¹, T.W. Jones⁷⁷, T.J. Jones⁷³, O. Jonsson²⁹, K.K. Joo^{158,v}, C. Joram²⁹, P.M. Jorge^{124a,b}, J. Joseph¹⁴, X. Ju¹³⁰, V. Juraneck¹²⁵, P. Jussel⁶², V.V. Kabachenko¹²⁸, S. Kabana¹⁶, M. Kaci¹⁶⁷, A. Kaczmarek³⁸, P. Kadlecik³⁵, M. Kado¹¹⁵, H. Kagan¹⁰⁹, M. Kagan⁵⁷, S. Kaiser⁹⁹, E. Kajomovitz¹⁵², S. Kalinin¹⁷⁴, L.V. Kalinovskaya⁶⁵, S. Kama³⁹, N. Kanaya¹⁵⁵, M. Kaneda¹⁵⁵, T. Kanno¹⁵⁷, V.A. Kantserov⁹⁶, J. Kanzaki⁶⁶, B. Kaplan¹⁷⁵, A. Kapliy³⁰, J. Kaplon²⁹, D. Kar⁴³, M. Karagoz¹¹⁸, M. Karneviskiy⁴¹, K. Karr⁵, V. Kartvelishvili⁷¹, A.N. Karyukhin¹²⁸, L. Kashif⁵⁷, A. Kasmi³⁹, R.D. Kass¹⁰⁹, A. Kastanas¹³, M. Kataoka⁴, Y. Kataoka¹⁵⁵, E. Katsoufis⁹, J. Katzy⁴¹, V. Kaushik⁶, K. Kawagoe⁶⁷, T. Kawamoto¹⁵⁵, G. Kawamura⁸¹, M.S. Kayl¹⁰⁵, V.A. Kazanin¹⁰⁷, M.Y. Kazarinov⁶⁵, S.I. Kazi⁸⁶, J.R. Keates⁸², R. Keeler¹⁶⁹, R. Kehoe³⁹, M. Keil⁵⁴, G.D. Kekelidze⁶⁵, M. Kelly⁸², J. Kennedy⁹⁸, C.J. Kenney¹⁴³, M. Kenyon⁵³, O. Kepka¹²⁵, N. Kerschen²⁹, B.P. Kerševan⁷⁴, S. Kersten¹⁷⁴, K. Kessoku¹⁵⁵, C. Ketterer⁴⁸, M. Khakzad²⁸, F. Khalil-zada¹⁰, H. Khandanyan¹⁶⁵, A. Khanov¹¹², D. Kharchenko⁶⁵, A. Khodinov¹⁴⁸, A.G. Kholodenko¹²⁸, A. Khomich^{58a}, T.J. Khoo²⁷, G. Khoriali²⁰, N. Khovanskiy⁶⁵, V. Khovanskiy⁹⁵, E. Khramov⁶⁵, J. Klubua⁵¹, G. Kilvington⁷⁶, H. Kim⁷, M.S. Kim², P.C. Kim¹⁴³, S.H. Kim¹⁶⁰, N. Kimura¹⁷⁰, O. Kind¹⁵, B.T. King⁷³, M. King⁶⁷, R.S.B. King¹¹⁸, J. Kirk¹²⁹, G.P. Kirsch¹¹⁸, L.E. Kirsch²², A.E. Kiryunin⁹⁹, D. Kisieleska³⁷, T. Kittelmann¹²³, A.M. Kiver¹²⁸, H. Kiyamura⁶⁷, E. Kladiva^{144b}, J. Kläiber-Lodewigs⁴², M. Klein⁷³, U. Klein⁷³, K. Kleinknecht⁸¹, M. Klemetti⁸⁵, A. Klier¹⁷¹, A. Klimentov²⁴, R. Klingenberg⁴², E.B. Klinkby³⁵, T. Kliutchnikova²⁹, P.F. Klok¹⁰⁴, S. Klous¹⁰⁵, E.-E. Kluge^{58a}, T. Kluge⁷³, P. Kluit¹⁰⁵, S. Kluth⁹⁹, E. Kneringer⁶², J. Knobloch²⁹, A. Knue⁵⁴, B.R. Ko⁴⁴, T. Kobayashi¹⁵⁵, M. Kobel⁴³, B. Koblitz²⁹, M. Kocian¹⁴³, A. Kocnar¹¹³, P. Kodys¹²⁶, K. Köneke²⁹, A.C. König¹⁰⁴, S. Koenig⁸¹, S. König⁴⁸, L. Köpke⁸¹, F. Koetsveld¹⁰⁴, P. Koevesarki²⁰, T. Koffas²⁹, E. Koffeman¹⁰⁵, F. Kohn⁵⁴, Z. Kohout¹²⁷, T. Kohriki⁶⁶, T. Koi¹⁴³, T. Kokott²⁰, G.M. Kolachev¹⁰⁷, H. Kolanoski¹⁵, V. Kolesnikov⁶⁵, I. Koletsou^{89a,89b}, J. Koll⁸⁸, D. Kollar²⁹, M. Kollefrath⁴⁸, S.D. Kolya⁸², A.A. Komar⁹⁴, J.R. Komaragiri¹⁴², T. Kondo⁶⁶, T. Kono^{41,w}, A.I. Kononov⁴⁸, R. Konoplich^{108,x}, N. Konstantinidis⁷⁷, A. Kootz¹⁷⁴, S. Koperny³⁷, S.V. Kopikov¹²⁸, K. Korcyl³⁸, K. Kordas¹⁵⁴, V. Koreshev¹²⁸, A. Korn¹⁴, A. Korol¹⁰⁷, I. Korolkov¹¹, E.V. Korolkova¹³⁹, V.A. Korotkov¹²⁸, O. Kortner⁹⁹, S. Kortner⁹⁹, V.V. Kostyukhin²⁰, M.J. Kotamäki²⁹, S. Kotov⁹⁹, V.M. Kotov⁶⁵, C. Kourkoumelis⁸, A. Koutsman¹⁰⁵, R. Kowalewski¹⁶⁹, T.Z. Kowalski³⁷, W. Kozanecki¹³⁶, A.S. Kozhin¹²⁸, V. Kral¹²⁷, V.A. Kramarenko⁹⁷, G. Kramberger⁷⁴, O. Krasel⁴², M.W. Krasny⁷⁸, A. Krasznahorkay¹⁰⁸, J. Kraus⁸⁸, A. Kreisel¹⁵³, F. Krejci¹²⁷, J. Kretzschmar⁷³, N. Krieger⁵⁴, P. Krieger¹⁵⁸, K. Kroeninger⁵⁴, H. Kroha⁹⁹, J. Kroll¹²⁰, J. Kroseberg²⁰, J. Krstic^{12a}, U. Kruchonak⁶⁵, H. Krüger²⁰, Z.V. Krumshteyn⁶⁵, A. Kruth²⁰, T. Kubota¹⁵⁵, S. Kuehn⁴⁸, A. Kugel^{58c}, T. Kuhl¹⁷⁴, D. Kuhn⁶², V. Kukhtin⁶⁵, Y. Kulchitsky⁹⁰, S. Kuleshov^{31b}, C. Kummer⁹⁸, M. Kuna⁸³, N. Kundu¹¹⁸, J. Kunkle¹²⁰, A. Kupco¹²⁵, H. Kurashige⁶⁷, M. Kurata¹⁶⁰, Y.A. Kurochkin⁹⁰, V. Kus¹²⁵, W. Kuykendall¹³⁸, M. Kuze¹⁵⁷, P. Kuzhir⁹¹, O. Kvasnicka¹²⁵, R. Kwee¹⁵, A. La Rosa²⁹, L. La Rotonda^{36a,36b}, L. Labarga⁸⁰, J. Labbe⁴, C. Lacasta¹⁶⁷, F. Lacava^{132a,132b}, H. Lacker¹⁵, D. Lacour⁷⁸, V.R. Lacuesta¹⁶⁷, E. Ladygin⁶⁵, R. Lafaye⁴, B. Laforge⁷⁸, T. Lagouri⁸⁰, S. Lai⁴⁸, E. Laisne⁵⁵, M. Lamanna²⁹, C.L. Lampen⁶, W. Lampl⁶, E. Lancon¹³⁶, U. Landgraf⁴⁸, M.P.J. Landon⁷⁵, H. Landsman¹⁵², J.L. Lane⁸², C. Lange⁴¹, A.J. Lankford¹⁶³, F. Lanni²⁴, K. Lantzsck²⁹, V.V. Lapin^{128,*}, S. Laplace⁴, C. Lapoire²⁰, J.F. Laporte¹³⁶, T. Lari^{89a}, A.V. Larionov¹²⁸, A. Larner¹¹⁸, C. Lasseur²⁹, M. Lassnig²⁹, W. Lau¹¹⁸, P. Laurelli⁴⁷, A. Lavorato¹¹⁸, W. Lavrijsen¹⁴, P. Laycock⁷³, A.B. Lazarev⁶⁵, A. Lazzaro^{89a,89b}, O. Le Dortz⁷⁸, E. Le Guirriec⁸³, C. Le Maner¹⁵⁸, E. Le Menedeu¹³⁶, M. Leahu²⁹, A. Lebedev⁶⁴, C. Lebel⁹³, T. LeCompte⁵, F. Ledroit-Guillon⁵⁵, H. Lee¹⁰⁵, J.S.H. Lee¹⁵⁰, S.C. Lee¹⁵¹, L. Lee JR¹⁷⁵, M. Lefebvre¹⁶⁹, M. Legendre¹³⁶, A. Leger⁴⁹, B.C. LeGeyt¹²⁰, F. Legger⁹⁸, C. Leggett¹⁴, M. Lehmacher²⁰, G. Lehmann Miotto²⁹, M. Lehto¹³⁹, X. Lei⁶, M.A.L. Leite^{23b}, R. Leitner¹²⁶, D. Lellouch¹⁷¹, J. Lellouch⁷⁸, M. Leltchouk³⁴, V. Lendermann^{58a}, K.J.C. Leney^{145b}, T. Lenz¹⁷⁴, G. Lenzen¹⁷⁴, B. Lenzi¹³⁶, K. Leonhardt⁴³, S. Leontsinis⁹, C. Leroy⁹³, J.-R. Lessard¹⁶⁹, J. Lesser^{146a}, C.G. Lester²⁷, A. Leung Fook Cheong¹⁷², J. Levêque⁸³, D. Levin⁸⁷, L.J. Levinson¹⁷¹, M.S. Levitski¹²⁸, M. Lewandowska²¹, M. Leyton¹⁵, B. Li⁸³, H. Li¹⁷², S. Li^{32b}, X. Li⁸⁷, Z. Liang³⁹, Z. Liang^{118,y}, B. Liberti^{133a}, P. Lichard²⁹, M. Lichtnecker⁹⁸, K. Lie¹⁶⁵, W. Liebig¹³, R. Lifshitz¹⁵², J.N. Lilley¹⁷, A. Limosani⁸⁶, M. Limper⁶³, S.C. Lin^{151,z}, F. Linde¹⁰⁵, J.T. Linnemann⁸⁸, E. Lipeles¹²⁰, L. Lipinsky¹²⁵, A. Lipniacka¹³, T.M. Liss¹⁶⁵, A. Lister⁴⁹, A.M. Litke¹³⁷, C. Liu²⁸, D. Liu^{151,aa}, H. Liu⁸⁷, J.B. Liu⁸⁷, M. Liu^{32b}, S. Liu², Y. Liu^{32b}, M. Livan^{119a,119b}, S.S.A. Livermore¹¹⁸, A. Lleres⁵⁵, S.L. Lloyd⁷⁵, E. Lobodzinska⁴¹, P. Loch⁶, W.S. Lockman¹³⁷, S. Lockwitz¹⁷⁵, T. Loddenkoetter²⁰, F.K. Loebinger⁸², A. Loginov¹⁷⁵, C.W. Loh¹⁶⁸,

T. Lohse¹⁵, K. Lohwasser⁴⁸, M. Lokajicek¹²⁵, J. Loken¹¹⁸, V.P. Lombardo^{89a,89b}, R.E. Long⁷¹, L. Lopes^{124a,b}, D. Lopez Mateos^{34,ab}, M. Losada¹⁶², P. Loscutoff¹⁴, F. Lo Sterzo^{132a,132b}, M.J. Losty^{159a}, X. Lou⁴⁰, A. Lounis¹¹⁵, K.F. Loureiro¹⁶², J. Love²¹, P.A. Love⁷¹, A.J. Lowe¹⁴³, F. Lu^{32a}, J. Lu², L. Lu³⁹, H.J. Lubatti¹³⁸, C. Luci^{132a,132b}, A. Lucotte⁵⁵, A. Ludwig⁴³, D. Ludwig⁴¹, I. Ludwig⁴⁸, J. Ludwig⁴⁸, F. Luehring⁶¹, G. Luijckx¹⁰⁵, D. Lumb⁴⁸, L. Luminari^{132a}, E. Lund¹¹⁷, B. Lund-Jensen¹⁴⁷, B. Lundberg⁷⁹, J. Lundberg²⁹, J. Lundquist³⁵, M. Lungwitz⁸¹, A. Lupi^{122a,122b}, G. Lutz⁹⁹, D. Lynn²⁴, J. Lys¹⁴, E. Lytken⁷⁹, H. Ma²⁴, L.L. Ma¹⁷², M. Maaßen⁴⁸, J.A. Macana Goia⁹³, G. Maccarrone⁴⁷, A. Macchiolo⁹⁹, B. Maček⁷⁴, J. Machado Miguens^{124a,b}, D. Macina⁴⁹, R. Mackeprang³⁵, R.J. Madaras¹⁴, W.F. Mader⁴³, R. Maenner^{58c}, T. Maeno²⁴, P. Mättig¹⁷⁴, S. Mättig⁴¹, P.J. Magalhaes Martins^{124a,h}, L. Magnoni²⁹, E. Magradze⁵¹, C.A. Magrath¹⁰⁴, Y. Mahalalel¹⁵³, K. Mahboubi⁴⁸, G. Mahout¹⁷, C. Maiani^{132a,132b}, C. Maidantchik^{23a}, A. Maio^{124a,q}, S. Majewski²⁴, Y. Makida⁶⁶, N. Makovec¹¹⁵, P. Mal⁶, Pa. Malecki³⁸, P. Malecki³⁸, V.P. Maleev¹²¹, F. Malek⁵⁵, U. Mallik⁶³, D. Malon⁵, S. Maltezos⁹, V. Malyshev¹⁰⁷, S. Malyukov⁶⁵, R. Mameghani⁹⁸, J. Mamuzic^{12b}, A. Manabe⁶⁶, L. Mandelli^{89a}, I. Mandić⁷⁴, R. Mandrysch¹⁵, J. Maneira^{124a}, P.S. Mangedard⁸⁸, I.D. Manjavidze⁶⁵, A. Mann⁵⁴, P.M. Manning¹³⁷, A. Manousakis-Katsikakis⁸, B. Mansoulie¹³⁶, A. Manz⁹⁹, A. Mapelli²⁹, L. Mapelli²⁹, L. March⁸⁰, J.F. Marchand²⁹, F. Marchese^{133a,133b}, M. Marchesotti²⁹, G. Marchiori⁷⁸, M. Marcisovsky¹²⁵, A. Marin^{21,*}, C.P. Marino⁶¹, F. Marroquin^{23a}, R. Marshall⁸², Z. Marshall^{34,ab}, F.K. Martens¹⁵⁸, S. Marti-Garcia¹⁶⁷, A.J. Martin¹⁷⁵, B. Martin²⁹, B. Martin⁸⁸, F.F. Martin¹²⁰, J.P. Martin⁹³, Ph. Martin⁵⁵, T.A. Martin¹⁷, B. Martin dit Latour⁴⁹, M. Martinez¹¹, V. Martinez Outschoorn⁵⁷, A.C. Martyniuk⁸², M. Marx⁸², F. Marzano^{132a}, A. Marzin¹¹¹, L. Masetti⁸¹, T. Mashimo¹⁵⁵, R. Mashinistov⁹⁴, J. Masik⁸², A.L. Maslennikov¹⁰⁷, M. Mab⁴², I. Massa^{19a,19b}, G. Massaro¹⁰⁵, N. Massol⁴, A. Mastroberardino^{36a,36b}, T. Masubuchi¹⁵⁵, M. Mathes²⁰, P. Matricon¹¹⁵, H. Matsumoto¹⁵⁵, H. Matsunaga¹⁵⁵, T. Matsushita⁶⁷, C. Mattravers^{118,ac}, J.M. Maugain²⁹, S.J. Maxfield⁷³, E.N. May⁵, A. Mayne¹³⁹, R. Mazini¹⁵¹, M. Mazur²⁰, M. Mazzanti^{89a}, E. Mazzoni^{122a,122b}, S.P. Mc Kee⁸⁷, A. McCarn¹⁶⁵, R.L. McCarthy¹⁴⁸, T.G. McCarthy²⁸, N.A. McCubbin¹²⁹, K.W. McFarlane⁵⁶, J.A. McFayden¹³⁹, H. McGlone⁵³, G. Mchedlidge⁵¹, R.A. McLaren²⁹, T. Mclaughlan¹⁷, S.J. McMahon¹²⁹, T.R. McMahon⁷⁶, T.J. McMahon¹⁷, R.A. McPherson^{169,k}, A. Meade⁸⁴, J. Mechnich¹⁰⁵, M. Mechtel¹⁷⁴, M. Medinnis⁴¹, R. Meera-Lebbai¹¹¹, T. Meguro¹¹⁶, R. Mehdiyev⁹³, S. Mehlhase⁴¹, A. Mehta⁷³, K. Meier^{58a}, J. Meinhardt⁴⁸, B. Meirose⁷⁹, C. Melachrinou³⁰, B.R. Mellado Garcia¹⁷², L. Mendoza Navas¹⁶², Z. Meng^{151,ad}, A. Mengarelli^{19a,19b}, S. Menke⁹⁹, C. Menot²⁹, E. Meoni¹¹, D. Merkl⁹⁸, P. Mermod¹¹⁸, L. Merola^{102a,102b}, C. Meroni^{89a}, F.S. Merritt³⁰, A. Messina²⁹, J. Metcalfe¹⁰³, A.S. Mete⁶⁴, S. Meuser²⁰, C. Meyer⁸¹, J-P. Meyer¹³⁶, J. Meyer¹⁷³, J. Meyer⁵⁴, T.C. Meyer²⁹, W.T. Meyer⁶⁴, J. Miao^{32d}, S. Michal²⁹, L. Micu^{25a}, R.P. Middleton¹²⁹, P. Miele²⁹, S. Migas⁷³, L. Mijovic⁴¹, G. Mikenberg¹⁷¹, M. Mikestikova¹²⁵, B. Mikulec⁴⁹, M. Mikuž⁷⁴, D.W. Miller¹⁴³, R.J. Miller⁸⁸, W.J. Mills¹⁶⁸, C. Mills⁵⁷, A. Milov¹⁷¹, D.A. Milstead^{146a,146b}, D. Milstein¹⁷¹, A.A. Minaenko¹²⁸, M. Miñano¹⁶⁷, I.A. Minashvili⁶⁵, A.I. Mincer¹⁰⁸, B. Mindur³⁷, M. Mineev⁶⁵, Y. Ming¹³⁰, L.M. Mir¹¹, G. Mirabelli^{132a}, L. Miralles Verge¹¹, A. Misiejuk⁷⁶, A. Mitra¹¹⁸, J. Mitrevski¹³⁷, G.Y. Mitrofanov¹²⁸, V.A. Mitsou¹⁶⁷, S. Mitsui⁶⁶, P.S. Miyagawa⁸², K. Miyazaki⁶⁷, J.U. Mjörnmark⁷⁹, T. Moa^{146a,146b}, P. Mockett¹³⁸, S. Moed⁵⁷, V. Moeller²⁷, K. Mönig⁴¹, N. Möser²⁰, S. Mohapatra¹⁴⁸, B. Mohn¹³, W. Mohr⁴⁸, S. Mohr dieck-Möck⁹⁹, A.M. Moiseev^{128,*}, R. Moles-Valls¹⁶⁷, J. Molina-Perez²⁹, L. Moneta⁴⁹, J. Monk⁷⁷, E. Monnier⁸³, S. Montesano^{89a,89b}, F. Monticelli⁷⁰, S. Monzani^{19a,19b}, R.W. Moore², G.F. Moorhead⁸⁶, C. Mora Herrera⁴⁹, A. Moraes⁵³, A. Morais^{124a,b}, N. Morange¹³⁶, J. Morel⁵⁴, G. Morello^{36a,36b}, D. Moreno⁸¹, M. Moreno Llácer¹⁶⁷, P. Morettini^{50a}, M. Morii⁵⁷, J. Morin⁷⁵, Y. Morita⁶⁶, A.K. Morley²⁹, G. Mornacchi²⁹, M-C. Morone⁴⁹, J.D. Morris⁷⁵, H.G. Moser⁹⁹, M. Mosidze⁵¹, J. Moss¹⁰⁹, R. Mount¹⁴³, E. Mountricha⁹, S.V. Mouraviev⁹⁴, E.J.W. Moyse⁸⁴, M. Mudrinic^{12b}, F. Mueller^{58a}, J. Mueller¹²³, K. Mueller²⁰, T.A. Müller⁹⁸, D. Muenstermann⁴², A. Muijs¹⁰⁵, A. Muir¹⁶⁸, Y. Munwes¹⁵³, K. Murakami⁶⁶, W.J. Murray¹²⁹, I. Mussche¹⁰⁵, E. Musto^{102a,102b}, A.G. Myagkov¹²⁸, M. Myska¹²⁵, J. Nadal¹¹, K. Nagai¹⁶⁰, K. Nagano⁶⁶, Y. Nagasaka⁶⁰, A.M. Nairz²⁹, Y. Nakahama¹¹⁵, K. Nakamura¹⁵⁵, I. Nakano¹¹⁰, G. Nanava²⁰, A. Napier¹⁶¹, M. Nash^{77,ae}, I. Nasteva⁸², N.R. Nation²¹, T. Nattermann²⁰, T. Naumann⁴¹, G. Navarro¹⁶², H.A. Neal⁸⁷, E. Nebot⁸⁰, P. Nechaeva⁹⁴, A. Negri^{119a,119b}, G. Negri²⁹, S. Nektarijevic⁴⁹, A. Nelson⁶⁴, S. Nelson¹⁴³, T.K. Nelson¹⁴³, S. Nemecek¹²⁵, P. Nemethy¹⁰⁸, A.A. Nepomuceno^{23a}, M. Nessi²⁹, S.Y. Nesterov¹²¹, M.S. Neubauer¹⁶⁵, A. Neusiedl⁸¹, R.M. Neves¹⁰⁸, P. Nevski²⁴, P.R. Newman¹⁷, R.B. Nickerson¹¹⁸, R. Nicolaidou¹³⁶, L. Nicolas¹³⁹, B. Nicquevert²⁹, F. Niedercorn¹¹⁵, J. Nielsen¹³⁷, T. Niinikoski²⁹, A. Nikiforov¹⁵, V. Nikolaenko¹²⁸, K. Nikolaev⁶⁵, I. Nikolic-Audit⁷⁸, K. Nikolopoulos²⁴, H. Nilsen⁴⁸, P. Nilsson⁷, Y. Ninomiya¹⁵⁵, A. Nisati^{132a}, T. Nishiyama⁶⁷, R. Nisius⁹⁹, L. Nodulman⁵, M. Nomachi¹¹⁶, I. Nomidis¹⁵⁴, H. Nomoto¹⁵⁵, M. Nordberg²⁹, B. Nordkvist^{146a,146b}, O. Norniella Francisco¹¹, P.R. Norton¹²⁹, J. Novakova¹²⁶, M. Nozaki⁶⁶, M. Nožička⁴¹, I.M. Nugent^{159a}, A.-E. Nuncio-Quiroz²⁰, G. Nunes Hanninger²⁰, T. Nunnemann⁹⁸, E. Nurse⁷⁷, T. Nyman²⁹, B.J. O'Brien⁴⁵, S.W. O'Neale^{17,*}, D.C. O'Neil¹⁴², V. O'Shea⁵³, F.G. Oakham^{28,af}, H. Oberlack⁹⁹, J. Ocariz⁷⁸, A. Ochi⁶⁷, S. Oda¹⁵⁵, S. Odaka⁶⁶, J. Odier⁸³, G.A. Odino^{50a,50b}, H. Ogren⁶¹, A. Oh⁸², S.H. Oh⁴⁴, C.C. Ohm^{146a,146b}, T. Ohshima¹⁰¹, H. Ohshita¹⁴⁰, T.K. Ohska⁶⁶, T. Ohsugi⁵⁹, S. Okada⁶⁷, H. Okawa¹⁶³, Y. Okumura¹⁰¹, T. Okuyama¹⁵⁵, M. Olcese^{50a}, A.G. Olchevski⁶⁵, M. Oliveira^{124a,h}, D. Oliveira Damazio²⁴, E. Oliver Garcia¹⁶⁷, D. Olivito¹²⁰, A. Olszewski³⁸, J. Olszowska³⁸, C. Omachi^{67,ag}, A. Onofre^{124a,ah},

P.U.E. Onyisi³⁰, C.J. Oram^{159a}, G. Ordóñez¹⁰⁴, M.J. Oreglia³⁰, F. Orellana⁴⁹, Y. Oren¹⁵³, D. Orestano^{134a,134b}, I. Orlov¹⁰⁷, C. Oropeza Barrera⁵³, R.S. Orr¹⁵⁸, E.O. Ortega¹³⁰, B. Osculati^{50a,50b}, R. Ospanov¹²⁰, C. Osuna¹¹, G. Otero y Garzon²⁶, J.P. Ottersbach¹⁰⁵, M. Ouchrif^{135c}, F. Ould-Saada¹¹⁷, A. Ouraou¹³⁶, Q. Ouyang^{32a}, M. Owen⁸², S. Owen¹³⁹, A. Oyarzun^{31b}, O.K. Øye¹³, V.E. Ozcan⁷⁷, N. Ozturk⁷, A. Pacheco Pages¹¹, C. Padilla Aranda¹¹, E. Paganis¹³⁹, F. Paige²⁴, K. Pajchel¹¹⁷, S. Palestini²⁹, D. Pallin³³, A. Palma^{124a,b}, J.D. Palmer¹⁷, Y.B. Pan¹⁷², E. Panagiotopoulou⁹, B. Panes^{31a}, N. Panikashvili⁸⁷, S. Panitkin²⁴, D. Pantea^{25a}, M. Panuskova¹²⁵, V. Paolone¹²³, A. Paoloni^{133a,133b}, Th.D. Papadopoulou⁹, A. Paramonov⁵, S.J. Park⁵⁴, W. Park^{24,ai}, M.A. Parker²⁷, F. Parodi^{50a,50b}, J.A. Parsons³⁴, U. Parzefall⁴⁸, E. Pasqualucci^{132a}, A. Passeri^{134a}, F. Pastore^{134a,134b}, Fr. Pastore²⁹, G. Pásztor^{49,aj}, S. Patariaia¹⁷², N. Patel¹⁵⁰, J.R. Pater⁸², S. Patricelli^{102a,102b}, T. Pauly²⁹, M. Pecsny^{144a}, M.I. Pedraza Morales¹⁷², S.V. Peleganchuk¹⁰⁷, H. Peng¹⁷², R. Pengo²⁹, A. Penson³⁴, J. Penwell⁶¹, M. Perantoni^{23a}, K. Perez^{34,ab}, T. Perez Cavalcanti⁴¹, E. Perez Codina¹¹, M.T. Pérez García-Estañ¹⁶⁷, V. Perez Reale³⁴, I. Peric²⁰, L. Perini^{89a,89b}, H. Pernegger²⁹, R. Perrino^{72a}, P. Perrodo⁴, S. Perseme^{3a}, P. Perus¹¹⁵, V.D. Peshekhonov⁶⁵, O. Peters¹⁰⁵, B.A. Petersen²⁹, J. Petersen²⁹, T.C. Petersen³⁵, E. Petit⁸³, A. Petridis¹⁵⁴, C. Petridou¹⁵⁴, E. Petrolo^{132a}, F. Petrucci^{134a,134b}, D. Petschull⁴¹, M. Petteni¹⁴², R. Pezoa^{31b}, A. Phan⁸⁶, A.W. Phillips²⁷, P.W. Phillips¹²⁹, G. Piacquadio²⁹, E. Piccaro⁷⁵, M. Piccinini^{19a,19b}, A. Pickford⁵³, R. Piegaiia²⁶, J.E. Pilcher³⁰, A.D. Pilkington⁸², J. Pina^{124a,q}, M. Pinamonti^{164a,164c}, J.L. Pinfold², J. Ping^{32c}, B. Pinto^{124a,b}, O. Pirotte²⁹, C. Pizio^{89a,89b}, R. Placakyte⁴¹, M. Plamondon¹⁶⁹, W.G. Plano⁸², M.-A. Pleier²⁴, A.V. Pleskach¹²⁸, A. Poblaguev²⁴, S. Poddar^{58a}, F. Podlyski³³, L. Poggioli¹¹⁵, T. Poghosyan²⁰, M. Pohl⁴⁹, F. Polci⁵⁵, G. Polesello^{119a}, A. Policicchio¹³⁸, A. Polini^{19a}, J. Poll⁷⁵, V. Polychronakos²⁴, D.M. Pomarede¹³⁶, D. Pomeroy²², K. Pommès²⁹, L. Pontecorvo^{132a}, B.G. Pope⁸⁸, G.A. Popeneciu^{25a}, D.S. Popovic^{12a}, A. Poppleton²⁹, X. Portell Bueso⁴⁸, R. Porter¹⁶³, C. Posch²¹, G.E. Pospelov⁹⁹, S. Pospisil¹²⁷, I.N. Potrap⁹⁹, C.J. Potter¹⁴⁹, C.T. Potter⁸⁵, G. Poulard²⁹, J. Poveda¹⁷², R. Prabhu⁷⁷, P. Pralavorio⁸³, S. Prasad⁵⁷, R. Pravahan⁷, S. Prell⁶⁴, K. Pretzl¹⁶, L. Pribl²⁹, D. Price⁶¹, L.E. Price²⁹, M.J. Price²⁹, P.M. Prichard⁷³, D. Prieur¹²³, M. Primavera^{72a}, K. Prokofiev²⁹, F. Prokoshin^{31b}, S. Protopopescu²⁴, J. Proudfoot⁵, X. Prudent⁴³, H. Przysieszniak⁴, S. Psoroulas²⁰, E. Ptacek¹¹⁴, J. Purdham⁸⁷, M. Purohit^{24,ak}, P. Puzo¹¹⁵, Y. Pylypchenko¹¹⁷, J. Qian⁸⁷, Z. Qian⁸³, Z. Qin⁴¹, A. Quadt⁵⁴, D.R. Quarrie¹⁴, W.B. Quayle¹⁷², F. Quinonez^{31a}, M. Raas¹⁰⁴, V. Radescu^{58b}, B. Radics²⁰, T. Rador^{18a}, F. Ragusa^{89a,89b}, G. Rahal¹⁷⁷, A.M. Rahimi¹⁰⁹, S. Rajagopalan²⁴, S. Rajek⁴², M. Rammensee⁴⁸, M. Rammes¹⁴¹, M. Ramstedt^{146a,146b}, K. Randrianarivony²⁸, P.N. Ratoff⁷¹, F. Rauscher⁹⁸, E. Rauter⁹⁹, M. Raymond²⁹, A.L. Read¹¹⁷, D.M. Rebuffi^{119a,119b}, A. Redelbach¹⁷³, G. Redlinger²⁴, R. Reece¹²⁰, K. Reeves⁴⁰, A. Reichold¹⁰⁵, E. Reinherz-Aronis¹⁵³, A. Reinsch¹¹⁴, I. Reisinger⁴², D. Reljic^{12a}, C. Rembser²⁹, Z.L. Ren¹⁵¹, A. Renaud¹¹⁵, P. Renkel³⁹, B. Rensch³⁵, M. Rescigno^{132a}, S. Resconi^{89a}, B. Resende¹³⁶, P. Reznicek⁹⁸, R. Rezvani¹⁵⁸, A. Richards⁷⁷, R. Richter⁹⁹, E. Richter-Was^{38,al}, M. Ridel⁷⁸, S. Rieke⁸¹, M. Rijpstra¹⁰⁵, M. Rijssenbeek¹⁴⁸, A. Rimoldi^{119a,119b}, L. Rinaldi^{19a}, R.R. Rios³⁹, I. Riu¹¹, G. Rivoltella^{89a,89b}, F. Rizatdinova¹¹², E. Rizvi⁷⁵, S.H. Robertson^{85,k}, A. Robichaud-Veronneau⁴⁹, D. Robinson²⁷, JEM Robinson⁷⁷, M. Robinson¹¹⁴, A. Robson⁵³, J.G. Rocha de Lima¹⁰⁶, C. Roda^{122a,122b}, D. Roda Dos Santos²⁹, S. Rodier⁸⁰, D. Rodriguez¹⁶², Y. Rodriguez Garcia¹⁵, A. Roe⁵⁴, S. Roe²⁹, O. Röhne¹¹⁷, V. Rojo¹, S. Rolli¹⁶¹, A. Romaniouk⁹⁶, V.M. Romanov⁶⁵, G. Romeo²⁶, D. Romero Maltrana^{31a}, L. Roos⁷⁸, E. Ros¹⁶⁷, S. Rosati¹³⁸, M. Rose⁷⁶, G.A. Rosenbaum¹⁵⁸, E.I. Rosenberg⁶⁴, P.L. Rosendahl¹³, L. Rossetlet⁴⁹, V. Rossetti¹¹, E. Rossi^{102a,102b}, L.P. Rossi^{50a}, L. Rossi^{89a,89b}, M. Rotaru^{25a}, I. Roth¹⁷¹, J. Rothberg¹³⁸, I. Rottländer²⁰, D. Rousseau¹¹⁵, C.R. Royon¹³⁶, A. Rozanov⁸³, Y. Rozen¹⁵², X. Ruan¹¹⁵, I. Rubinskiy⁴¹, B. Ruckert⁹⁸, N. Ruckstuhl¹⁰⁵, V.I. Rud⁹⁷, G. Rudolph⁶², F. Rühr⁶, A. Ruiz-Martinez⁶⁴, E. Rulikowska-Zarebska³⁷, V. Rumiantsev^{91,*}, L. Rumyantsev⁶⁵, K. Runge⁴⁸, O. Runolfsson²⁰, Z. Rurikova⁴⁸, N.A. Rusakovich⁶⁵, D.R. Rust⁶¹, J.P. Rutherford⁶, C. Ruwiedel¹⁴, P. Ruzicka¹²⁵, Y.F. Ryabov¹²¹, V. Ryadovikov¹²⁸, P. Ryan⁸⁸, M. Rybar¹²⁶, G. Rybkin¹¹⁵, N.C. Ryder¹¹⁸, S. Rzaeva¹⁰, A.F. Saavedra¹⁵⁰, I. Sadeh¹⁵³, H.F.-W. Sadrozinski¹³⁷, R. Sadykov⁶⁵, F. Safai Tehrani^{132a,132b}, H. Sakamoto¹⁵⁵, G. Salamanna¹⁰⁵, A. Salamon^{133a}, M. Saleem¹¹¹, D. Salihagic⁹⁹, A. Salnikov¹⁴³, J. Salt¹⁶⁷, B.M. Salvachua Ferrando⁵, D. Salvatore^{36a,36b}, F. Salvatore¹⁴⁹, A. Salzburger²⁹, D. Sampsonidis¹⁵⁴, B.H. Samset¹¹⁷, H. Sandaker¹³, H.G. Sander⁸¹, M.P. Sanders⁹⁸, M. Sandhoff¹⁷⁴, P. Sandhu¹⁵⁸, T. Sandoval²⁷, R. Sandstroem¹⁰⁵, S. Sandvoss¹⁷⁴, D.P.C. Sankey¹²⁹, A. Sansoni⁴⁷, C. Santamarina Rios⁸⁵, C. Santoni³³, R. Santonico^{133a,133b}, H. Santos^{124a}, J.G. Saraiva^{124a,q}, T. Sarangi¹⁷², E. Sarkisyan-Grinbaum⁷, F. Sarri^{122a,122b}, G. Sartisohn¹⁷⁴, O. Sasaki⁶⁶, T. Sasaki⁶⁶, N. Sasao⁶⁸, I. Satsounkevitch⁹⁰, G. Sauvage⁴, J.B. Sauvan¹¹⁵, P. Savard^{158,af}, V. Savinov¹²³, P. Savva⁹, L. Sawyer^{24,am}, D.H. Saxon⁵³, L.P. SAYS³³, C. Sbarra^{19a,19b}, A. Sbrizzi^{19a,19b}, O. Scallan⁹³, D.A. Scannicchio¹⁶³, J. Schaarschmidt⁴³, P. Schacht⁹⁹, U. Schäfer⁸¹, S. Schaetzel^{58b}, A.C. Schaffer¹¹⁵, D. Schaile⁹⁸, R.D. Schamberger¹⁴⁸, A.G. Schamov¹⁰⁷, V. Scharf^{58a}, V.A. Schegelsky¹²¹, D. Scheirich⁸⁷, M.I. Scherzer¹⁴, C. Schiavi^{50a,50b}, J. Schieck⁹⁸, M. Schioppa^{36a,36b}, S. Schlenker²⁹, J.L. Schlereth⁵, E. Schmidt⁴⁸, M.P. Schmidt^{175,*}, K. Schmieden²⁰, C. Schmitt⁸¹, M. Schmitz²⁰, A. Schöning^{58b}, M. Schott²⁹, D. Schouten¹⁴², J. Schovancova¹²⁵, M. Schram⁸⁵, A. Schreiner⁶³, C. Schroeder⁸¹, N. Schroer^{58c}, S. Schuh²⁹, G. Schuler²⁹, J. Schultes¹⁷⁴, H.-C. Schultz-Coulon^{58a}, H. Schulz¹⁵, J.W. Schumacher²⁰, M. Schumacher⁴⁸, B.A. Schumm¹³⁷, Ph. Schune¹³⁶, C. Schwanenberger⁸², A. Schwartzman¹⁴³, Ph. Schwemling⁷⁸, R. Schwienhorst⁸⁸, R. Schwierz⁴³, J. Schwindling¹³⁶, W.G. Scott¹²⁹, J. Searcy¹¹⁴, E. Sedkyh¹²¹,

E. Segura¹¹, S.C. Seidel¹⁰³, A. Seiden¹³⁷, F. Seifert⁴³, J.M. Seixas^{23a}, G. Sekhniadze^{102a}, D.M. Seliverstov¹²¹,
 B. Sellden^{146a}, G. Sellers⁷³, M. Seman^{144b}, N. Semprini-Cesari^{19a,19b}, C. Serfon⁹⁸, L. Serin¹¹⁵, R. Seuster⁹⁹,
 H. Severini¹¹¹, M.E. Seviour⁸⁶, A. Sfyrla²⁹, E. Shabalina⁵⁴, M. Shamim¹¹⁴, L.Y. Shan^{32a}, J.T. Shank²¹, Q.T. Shao⁸⁶,
 M. Shapiro¹⁴, P.B. Shatalov⁹⁵, L. Shaver⁶, C. Shaw⁵³, K. Shaw^{164a,164c}, D. Sherman¹⁷⁵, P. Sherwood⁷⁷,
 A. Shibata¹⁰⁸, S. Shimizu²⁹, M. Shimojima¹⁰⁰, T. Shin⁵⁶, A. Shmeleva⁹⁴, M.J. Shochet³⁰, D. Short¹¹⁸, M.A. Shupe⁶,
 P. Sicho¹²⁵, A. Sidoti¹⁵, A. Siebel¹⁷⁴, F. Siegert⁴⁸, J. Siegrist¹⁴, Dj. Sijacki^{12a}, O. Silbert¹⁷¹, Y. Silver¹⁵³,
 D. Silverstein¹⁴³, S.B. Silverstein^{146a}, V. Simak¹²⁷, Lj. Simic^{12a}, S. Simion¹¹⁵, B. Simmons⁷⁷, M. Simonyan³⁵,
 P. Sinervo¹⁵⁸, N.B. Sinev¹¹⁴, V. Sipica¹⁴¹, G. Siragusa⁸¹, A.N. Sisakyan⁶⁵, S.Yu. Sivoklokov⁹⁷, J. Sjölin^{146a,146b},
 T.B. Sjursen¹³, L.A. Skinnari¹⁴, K. Skovpen¹⁰⁷, P. Skubic¹¹¹, N. Skvorodnev²², M. Slater¹⁷, T. Slavicek¹²⁷,
 K. Sliwa¹⁶¹, T.J. Sloan⁷¹, J. Sloper²⁹, V. Smakhtin¹⁷¹, S.Yu. Smirnov⁹⁶, L.N. Smirnova⁹⁷, O. Smirnova⁷⁹,
 B.C. Smith⁵⁷, D. Smith¹⁴³, K.M. Smith⁵³, M. Smizanska⁷¹, K. Smolek¹²⁷, A.A. Snesarev⁹⁴, S.W. Snow⁸²,
 J. Snow¹¹¹, J. Snuverink¹⁰⁵, S. Snyder²⁴, M. Soares^{124a}, R. Sobie^{169,k}, J. Sodomka¹²⁷, A. Soffer¹⁵³, C.A. Solans¹⁶⁷,
 M. Solar¹²⁷, J. Solc¹²⁷, U. Soldevila¹⁶⁷, E. Solfaroli Camillocci^{132a,132b}, A.A. Solodkov¹²⁸, O.V. Solovyanov¹²⁸,
 J. Sondericker²⁴, N. Soni², V. Sopko¹²⁷, B. Sopko¹²⁷, M. Sorbi^{89a,89b}, M. Sosebee⁷, A. Soukharev¹⁰⁷,
 S. Spagnolo^{72a,72b}, F. Spano³⁴, R. Spighi^{19a}, G. Spigo²⁹, F. Spila^{132a,132b}, E. Spiriti^{134a}, R. Spiwoks²⁹,
 M. Spousta¹²⁶, T. Spreitzer¹⁵⁸, B. Spurlock⁷, R.D. St. Denis⁵³, T. Stahl¹⁴¹, J. Stahlman¹²⁰, R. Stamen^{58a},
 E. Stanecka²⁹, R.W. Stanek⁵, C. Stanescu^{134a}, S. Stapnes¹¹⁷, E.A. Starchenko¹²⁸, J. Stark⁵⁵, P. Staroba¹²⁵,
 P. Starovoitov⁹¹, A. Staude⁹⁸, P. Stavina^{144a}, G. Stavropoulos¹⁴, G. Steele⁵³, P. Steinbach⁴³, P. Steinberg²⁴,
 I. Stekl¹²⁷, B. Stelzer¹⁴², H.J. Stelzer⁴¹, O. Stelzer-Chilton^{159a}, H. Stenzel⁵², K. Stevenson⁷⁵, G.A. Stewart⁵³,
 T. Stockmanns²⁰, M.C. Stockton²⁹, K. Stoerig⁴⁸, G. Stoica^{25a}, S. Stonjek⁹⁹, P. Strachota¹²⁶, A.R. Stradling⁷,
 A. Straessner⁴³, J. Strandberg⁸⁷, S. Strandberg^{146a,146b}, A. Strandlie¹¹⁷, M. Strang¹⁰⁹, E. Strauss¹⁴³, M. Strauss¹¹¹,
 P. Strizenec^{144b}, R. Ströhrmer¹⁷³, D.M. Strom¹¹⁴, J.A. Strong^{76,*}, R. Stroynowski³⁹, J. Strube¹²⁹, B. Stugu¹³,
 I. Stumer^{24,*}, J. Stupak¹⁴⁸, P. Sturm¹⁷⁴, D.A. Soh^{151,y}, D. Su¹⁴³, S. Subramania², Y. Sugaya¹¹⁶, T. Sugimoto¹⁰¹,
 C. Suhr¹⁰⁶, K. Suita⁶⁷, M. Suk¹²⁶, V.V. Sulin⁹⁴, S. Sultansoy^{3d}, T. Sumida²⁹, X. Sun⁵⁵, J.E. Sundermann⁴⁸,
 K. Suruliz^{164a,164b}, S. Sushkov¹¹, G. Susinno^{36a,36b}, M.R. Sutton¹³⁹, Y. Suzuki⁶⁶, Yu.M. Sviridov¹²⁸, S. Swedish¹⁶⁸,
 I. Sykora^{144a}, T. Sykora¹²⁶, B. Szeless²⁹, J. Sánchez¹⁶⁷, D. Ta¹⁰⁵, K. Tackmann²⁹, A. Taffard¹⁶³, R. Tafirout^{159a},
 A. Taga¹¹⁷, N. Taiblum¹⁵³, Y. Takahashi¹⁰¹, H. Takai²⁴, R. Takashima⁶⁹, H. Takeda⁶⁷, T. Takeshita¹⁴⁰, M. Talby⁸³,
 A. Talyshev¹⁰⁷, M.C. Tamsett²⁴, J. Tanaka¹⁵⁵, R. Tanaka¹¹⁵, S. Tanaka¹³¹, S. Tanaka⁶⁶, Y. Tanaka¹⁰⁰, K. Tani⁶⁷,
 N. Tannoury⁸³, G.P. Tappern²⁹, S. Tapprogge⁸¹, D. Tardif¹⁵⁸, S. Tarem¹⁵², F. Tarrade²⁴, G.F. Tartarelli^{89a},
 P. Tas¹²⁶, M. Tasevsky¹²⁵, E. Tassi^{36a,36b}, M. Tatarkhanov¹⁴, C. Taylor⁷⁷, F.E. Taylor⁹², G. Taylor¹³⁷,
 G.N. Taylor⁸⁶, W. Taylor^{159b}, M. Teixeira Dias Castanheira⁷⁵, P. Teixeira-Dias⁷⁶, K.K. Temming⁴⁸, H. Ten Kate²⁹,
 P.K. Teng¹⁵¹, Y.D. Tennenbaum-Katan¹⁵², S. Terada⁶⁶, K. Terashi¹⁵⁵, J. Terron⁸⁰, M. Terwort^{41,an}, M. Testa⁴⁷,
 R.J. Teuscher^{158,k}, C.M. Tevlin⁸², J. Thadome¹⁷⁴, J. Therhaag²⁰, T. Theveneaux-Pelzer⁷⁸, M. Thioye¹⁷⁵,
 S. Thoma⁴⁸, J.P. Thomas¹⁷, E.N. Thompson⁸⁴, P.D. Thompson¹⁷, P.D. Thompson¹⁵⁸, A.S. Thompson⁵³,
 E. Thomson¹²⁰, M. Thomson²⁷, R.P. Thun⁸⁷, T. Tic¹²⁵, V.O. Tikhomirov⁹⁴, Y.A. Tikhonov¹⁰⁷,
 C.J.W.P. Timmermans¹⁰⁴, P. Tipton¹⁷⁵, F.J. Tique Aires Viegas²⁹, S. Tisserant⁸³, J. Tobias⁴⁸, B. Toczec³⁷,
 T. Todorov⁴, S. Todorova-Nova¹⁶¹, B. Toggerson¹⁶³, J. Tojo⁶⁶, S. Tokár^{144a}, K. Tokunaga⁶⁷, K. Tokushuku⁶⁶,
 K. Tollefson⁸⁸, M. Tomoto¹⁰¹, L. Tompkins¹⁴, K. Toms¹⁰³, A. Tonazzo^{134a,134b}, G. Tong^{32a}, A. Tonoyan¹³,
 C. Topfel¹⁶, N.D. Topilin⁶⁵, I. Torchiani²⁹, E. Torrence¹¹⁴, E. Torró Pastor¹⁶⁷, J. Toth^{83,aj}, F. Touchard⁸³,
 D.R. Tovey¹³⁹, D. Traynor⁷⁵, T. Trefzger¹⁷³, J. Treis²⁰, L. Tremblet²⁹, A. Tricoli²⁹, I.M. Trigger^{159a},
 S. Trincaz-Duvoid⁷⁸, T.N. Trinh⁷⁸, M.F. Tripiana⁷⁰, N. Triplett⁶⁴, W. Trischuk¹⁵⁸, A. Trivedi^{24,ao}, B. Trocmé⁵⁵,
 C. Troncon^{89a}, M. Trottier-McDonald¹⁴², A. Trzupek³⁸, C. Tsarouchas²⁹, J.C-L. Tseng¹¹⁸, M. Tsiakiris¹⁰⁵,
 P.V. Tsiareshka⁹⁰, D. Tsionou¹³⁹, G. Tsipolitis⁹, V. Tsiskaridze⁴⁸, E.G. Tskhadadze⁵¹, I.I. Tsukerman⁹⁵,
 V. Tsulaia¹²³, J.-W. Tsung²⁰, S. Tsuno⁶⁶, D. Tsybychev¹⁴⁸, A. Tua¹³⁹, J.M. Tuggle³⁰, M. Turala³⁸, D. Turecek¹²⁷,
 I. Turk Cakir^{3e}, E. Turlay¹⁰⁵, P.M. Tuts³⁴, A. Tykhonov⁷⁴, M. Tylmad^{146a,146b}, M. Tyndel¹²⁹, D. TYPDaldos¹⁷,
 H. Tyrvaivenen²⁹, G. Tzanakos⁸, K. Uchida²⁰, I. Ueda¹⁵⁵, R. Ueno²⁸, M. Uglan¹³, M. Uhlenbrock²⁰,
 M. Uhrmacher⁵⁴, F. Ukegawa¹⁶⁰, G. Unal²⁹, D.G. Underwood⁵, A. Undrus²⁴, G. Unel¹⁶³, Y. Unno⁶⁶, D. Urbaniec³⁴,
 E. Urkovsky¹⁵³, P. Urquijo^{49,ap}, P. Urrejola^{31a}, G. Usai⁷, M. Uslenghi^{119a,119b}, L. Vacavant⁸³, V. Vacek¹²⁷,
 B. Vachon⁸⁵, S. Vahsen¹⁴, C. Valderanis⁹⁹, J. Valenta¹²⁵, P. Valente^{132a}, S. Valentinetti^{19a,19b}, S. Valkar¹²⁶,
 E. Valladolid Gallego¹⁶⁷, S. Vallecorsa¹⁵², J.A. Valls Ferrer¹⁶⁷, H. van der Graaf¹⁰⁵, E. van der Kraaij¹⁰⁵,
 E. van der Poel¹⁰⁵, D. van der Ster²⁹, B. Van Eijk¹⁰⁵, N. van Eldik⁸⁴, P. van Gemmeren⁵, Z. van Kesteren¹⁰⁵,
 I. van Vulpen¹⁰⁵, W. Vandelli²⁹, G. Vandoni²⁹, A. Vaniachine⁵, P. Vankov⁴¹, F. Vannucci⁷⁸, F. Varela Rodriguez²⁹,
 R. Vari^{132a}, E.W. Varnes⁶, D. Varouchas¹⁴, A. Vartapetian⁷, K.E. Varvell¹⁵⁰, V.I. Vassilakopoulos⁵⁶, F. Vazeille³³,
 G. Vegni^{89a,89b}, J.J. Veillet¹¹⁵, C. Vellidis⁸, F. Veloso^{124a}, R. Veness²⁹, S. Veneziano^{132a}, A. Ventura^{72a,72b},
 D. Ventura¹³⁸, S. Ventura⁴⁷, M. Venturi⁴⁸, N. Venturi¹⁶, V. Vercesi^{119a}, M. Verducci¹³⁸, W. Verkerke¹⁰⁵,
 J.C. Vermeulen¹⁰⁵, A. Vest⁴³, M.C. Vetterli^{142,af}, I. Vichou¹⁶⁵, T. Vickey^{145b,aq}, G.H.A. Viehhauser¹¹⁸, S. Viel¹⁶⁸,
 M. Villa^{19a,19b}, M. Villaplana Perez¹⁶⁷, E. Vilucchi⁴⁷, M.G. Vincter²⁸, E. Vinek²⁹, V.B. Vinogradov⁶⁵,
 M. Virchaux^{136,*}, S. Viret³³, J. Virzi¹⁴, A. Vitale^{19a,19b}, O. Vitells¹⁷¹, I. Vivarelli⁴⁸, F. Vives Vaque¹¹, S. Vlachos⁹,

M. Vlasak¹²⁷, N. Vlasov²⁰, A. Vogel²⁰, P. Vokac¹²⁷, M. Volpi¹¹, G. Volpini^{89a}, H. von der Schmitt⁹⁹, J. von Loeben⁹⁹, H. von Radziewski⁴⁸, E. von Toerne²⁰, V. Vorobel¹²⁶, A.P. Vorobiev¹²⁸, V. Vorwerk¹¹, M. Vos¹⁶⁷, R. Voss²⁹, T.T. Voss¹⁷⁴, J.H. Vossebeld⁷³, A.S. Vovenko¹²⁸, N. Vranjes^{12a}, M. Vranjes Milosavljevic^{12a}, V. Vrba¹²⁵, M. Vreeswijk¹⁰⁵, T. Vu Anh⁸¹, R. Vuillermet²⁹, I. Vukotic¹¹⁵, W. Wagner¹⁷⁴, P. Wagner¹²⁰, H. Wahlen¹⁷⁴, J. Wakabayashi¹⁰¹, J. Walbersloh⁴², S. Walch⁸⁷, J. Walder⁷¹, R. Walker⁹⁸, W. Walkowiak¹⁴¹, R. Wall¹⁷⁵, P. Waller⁷³, C. Wang⁴⁴, H. Wang¹⁷², J. Wang¹⁵¹, J. Wang^{32d}, J.C. Wang¹³⁸, S.M. Wang¹⁵¹, A. Warburton⁸⁵, C.P. Ward²⁷, M. Warsinsky⁴⁸, P.M. Watkins¹⁷, A.T. Watson¹⁷, M.F. Watson¹⁷, G. Watts¹³⁸, S. Watts⁸², A.T. Waugh¹⁵⁰, B.M. Waugh⁷⁷, J. Weber⁴², M. Weber¹²⁹, M.S. Weber¹⁶, P. Weber⁵⁴, A.R. Weidberg¹¹⁸, J. Weingarten⁵⁴, C. Weiser⁴⁸, H. Wellenstein²², P.S. Wells²⁹, M. Wen⁴⁷, T. Wenaus²⁴, S. Wendler¹²³, Z. Weng^{151,ar}, T. Wengler²⁹, S. Wenig²⁹, N. Wermes²⁰, M. Werner⁴⁸, P. Werner²⁹, M. Werth¹⁶³, M. Wessels^{58a}, K. Whalen²⁸, S.J. Wheeler-Ellis¹⁶³, S.P. Whitaker²¹, A. White⁷, M.J. White⁸⁶, S. White²⁴, S.R. Whitehead¹¹⁸, D. Whiteson¹⁶³, D. Whittington⁶¹, F. Wicke¹¹⁵, D. Wicke¹⁷⁴, F.J. Wickens¹²⁹, W. Wiedenmann¹⁷², M. Wielers¹²⁹, P. Wienemann²⁰, C. Wiglesworth⁷³, L.A.M. Wiik⁴⁸, A. Wildauer¹⁶⁷, M.A. Wildt^{41,an}, I. Wilhelm¹²⁶, H.G. Wilkens²⁹, J.Z. Will⁹⁸, E. Williams³⁴, H.H. Williams¹²⁰, W. Willis³⁴, S. Willocq⁸⁴, J.A. Wilson¹⁷, M.G. Wilson¹⁴³, A. Wilson⁸⁷, I. Wingerter-Seez⁴, S. Winkelmann⁴⁸, F. Winklmeier²⁹, M. Wittgen¹⁴³, M.W. Wolter³⁸, H. Wolters^{124a,h}, G. Wooden¹¹⁸, B.K. Wosiek³⁸, J. Wotschack²⁹, M.J. Woudstra⁸⁴, K. Wraight⁵³, C. Wright⁵³, B. Wrona⁷³, S.L. Wu¹⁷², X. Wu⁴⁹, Y. Wu^{32b,as}, E. Wulf³⁴, R. Wunstorf⁴², B.M. Wynne⁴⁵, L. Xaplanteris⁹, S. Xella³⁵, S. Xie⁴⁸, Y. Xie^{32a}, C. Xu^{32b}, D. Xu¹³⁹, G. Xu^{32a}, B. Yabsley¹⁵⁰, M. Yamada⁶⁶, A. Yamamoto⁶⁶, K. Yamamoto⁶⁴, S. Yamamoto¹⁵⁵, T. Yamamura¹⁵⁵, J. Yamaoka⁴⁴, T. Yamazaki¹⁵⁵, Y. Yamazaki⁶⁷, Z. Yan²¹, H. Yang⁸⁷, U.K. Yang⁸², Y. Yang⁶¹, Y. Yang^{32a}, Z. Yang^{146a,146b}, S. Yanush⁹¹, W-M. Yao¹⁴, Y. Yao¹⁴, Y. Yasu⁶⁶, J. Ye³⁹, S. Ye²⁴, M. Yilmaz^{3c}, R. Yoosofmiya¹²³, K. Yorita¹⁷⁰, R. Yoshida⁵, C. Young¹⁴³, S. Youssef²¹, D. Yu²⁴, J. Yu⁷, J. Yu^{32c,at}, L. Yuan^{32a,au}, A. Yurkewicz¹⁴⁸, V.G. Zaets¹²⁸, R. Zaidan⁶³, A.M. Zaitsev¹²⁸, Z. Zajacova²⁹, Yo.K. Zalite¹²¹, L. Zanello^{132a,132b}, P. Zarzhitsky³⁹, A. Zaytsev¹⁰⁷, M. Zdrzil¹⁴, C. Zeitnitz¹⁷⁴, M. Zeller¹⁷⁵, P.F. Zema²⁹, A. Zemla³⁸, C. Zendler²⁰, A.V. Zenin¹²⁸, O. Zenin¹²⁸, T. Ženiš^{144a}, Z. Zenonos^{122a,122b}, S. Zenz¹⁴, D. Zerwas¹¹⁵, G. Zevi della Porta⁵⁷, Z. Zhan^{32d}, D. Zhang^{32b,av}, H. Zhang⁸⁸, J. Zhang⁵, X. Zhang^{32d}, Z. Zhang¹¹⁵, L. Zhao¹⁰⁸, T. Zhao¹³⁸, Z. Zhao^{32b}, A. Zhemchugov⁶⁵, S. Zheng^{32a}, J. Zhong^{151,aw}, B. Zhou⁸⁷, N. Zhou¹⁶³, Y. Zhou¹⁵¹, C.G. Zhu^{32d}, H. Zhu⁴¹, Y. Zhu¹⁷², X. Zhuang⁹⁸, V. Zhuravlov⁹⁹, D. Zieminska⁶¹, B. Zilka^{144a}, R. Zimmermann²⁰, S. Zimmermann²⁰, S. Zimmermann⁴⁸, M. Ziolkowski¹⁴¹, R. Zitoun⁴, L. Živković³⁴, V.V. Zmouchko^{128,*}, G. Zobernig¹⁷², A. Zoccoli^{19a,19b}, Y. Zolnierowski⁴, A. Zsenei²⁹, M. zur Nedden¹⁵, V. Zutshi¹⁰⁶, L. Zwalinski²⁹.

¹ University at Albany, 1400 Washington Ave, Albany, NY 12222, United States of America

² University of Alberta, Department of Physics, Centre for Particle Physics, Edmonton, AB T6G 2G7, Canada

³ Ankara University^(a), Faculty of Sciences, Department of Physics, TR 061000 Tandogan, Ankara; Dumlupinar University^(b), Faculty of Arts and Sciences, Department of Physics, Kutahya; Gazi University^(c), Faculty of Arts and Sciences, Department of Physics, 06500, Teknikokullar, Ankara; TOBB University of Economics and Technology^(d), Faculty of Arts and Sciences, Division of Physics, 06560, Sogutozu, Ankara; Turkish Atomic Energy Authority^(e), 06530, Lodumlu, Ankara, Turkey

⁴ LAPP, Université de Savoie, CNRS/IN2P3, Annecy-le-Vieux, France

⁵ Argonne National Laboratory, High Energy Physics Division, 9700 S. Cass Avenue, Argonne IL 60439, United States of America

⁶ University of Arizona, Department of Physics, Tucson, AZ 85721, United States of America

⁷ The University of Texas at Arlington, Department of Physics, Box 19059, Arlington, TX 76019, United States of America

⁸ University of Athens, Nuclear & Particle Physics, Department of Physics, Panepistimiopouli, Zografou, GR 15771 Athens, Greece

⁹ National Technical University of Athens, Physics Department, 9-Iroon Polytechniou, GR 15780 Zografou, Greece

¹⁰ Institute of Physics, Azerbaijan Academy of Sciences, H. Javid Avenue 33, AZ 143 Baku, Azerbaijan

¹¹ Institut de Física d'Altes Energies, IFAE, Edifici Cn, Universitat Autònoma de Barcelona, ES - 08193 Bellaterra (Barcelona), Spain

¹² University of Belgrade^(a), Institute of Physics, P.O. Box 57, 11001 Belgrade; Vinca Institute of Nuclear Sciences^(b) M. Petrovica Alasa 12-14, 11000 Belgrade, Serbia, Serbia

¹³ University of Bergen, Department for Physics and Technology, Allegaten 55, NO - 5007 Bergen, Norway

¹⁴ Lawrence Berkeley National Laboratory and University of California, Physics Division, MS50B-6227, 1 Cyclotron Road, Berkeley, CA 94720, United States of America

¹⁵ Humboldt University, Institute of Physics, Berlin, Newtonstr. 15, D-12489 Berlin, Germany

¹⁶ University of Bern, Albert Einstein Center for Fundamental Physics, Laboratory for High Energy Physics, Sidlerstrasse 5, CH - 3012 Bern, Switzerland

- ¹⁷ University of Birmingham, School of Physics and Astronomy, Edgbaston, Birmingham B15 2TT, United Kingdom
- ¹⁸ Bogazici University^(a), Faculty of Sciences, Department of Physics, TR - 80815 Bebek-Istanbul; Dogus University^(b), Faculty of Arts and Sciences, Department of Physics, 34722, Kadikoy, Istanbul; ^(c)Gaziantep University, Faculty of Engineering, Department of Physics Engineering, 27310, Sehitkamil, Gaziantep, Turkey; Istanbul Technical University^(d), Faculty of Arts and Sciences, Department of Physics, 34469, Maslak, Istanbul, Turkey
- ¹⁹ INFN Sezione di Bologna^(a); Università di Bologna, Dipartimento di Fisica^(b), viale C. Berti Pichat, 6/2, IT - 40127 Bologna, Italy
- ²⁰ University of Bonn, Physikalisches Institut, Nussallee 12, D - 53115 Bonn, Germany
- ²¹ Boston University, Department of Physics, 590 Commonwealth Avenue, Boston, MA 02215, United States of America
- ²² Brandeis University, Department of Physics, MS057, 415 South Street, Waltham, MA 02454, United States of America
- ²³ Universidade Federal do Rio De Janeiro, COPPE/EE/IF ^(a), Caixa Postal 68528, Ilha do Fundao, BR - 21945-970 Rio de Janeiro; ^(b)Universidade de Sao Paulo, Instituto de Fisica, R.do Matao Trav. R.187, Sao Paulo - SP, 05508 - 900, Brazil
- ²⁴ Brookhaven National Laboratory, Physics Department, Bldg. 510A, Upton, NY 11973, United States of America
- ²⁵ National Institute of Physics and Nuclear Engineering^(a)Bucharest-Magurele, Str. Atomistilor 407, P.O. Box MG-6, R-077125, Romania; University Politehnica Bucharest^(b), Rectorat - AN 001, 313 Splaiul Independentei, sector 6, 060042 Bucuresti; West University^(c) in Timisoara, Bd. Vasile Parvan 4, Timisoara, Romania
- ²⁶ Universidad de Buenos Aires, FCEyN, Dto. Fisica, Pab I - C. Universitaria, 1428 Buenos Aires, Argentina
- ²⁷ University of Cambridge, Cavendish Laboratory, J J Thomson Avenue, Cambridge CB3 0HE, United Kingdom
- ²⁸ Carleton University, Department of Physics, 1125 Colonel By Drive, Ottawa ON K1S 5B6, Canada
- ²⁹ CERN, CH - 1211 Geneva 23, Switzerland
- ³⁰ University of Chicago, Enrico Fermi Institute, 5640 S. Ellis Avenue, Chicago, IL 60637, United States of America
- ³¹ Pontificia Universidad Católica de Chile, Facultad de Fisica, Departamento de Fisica^(a), Avda. Vicuna Mackenna 4860, San Joaquin, Santiago; Universidad Técnica Federico Santa María, Departamento de Física^(b), Avda. Española 1680, Casilla 110-V, Valparaíso, Chile
- ³² Institute of High Energy Physics, Chinese Academy of Sciences^(a), P.O. Box 918, 19 Yuquan Road, Shijing Shan District, CN - Beijing 100049; University of Science & Technology of China (USTC), Department of Modern Physics^(b), Hefei, CN - Anhui 230026; Nanjing University, Department of Physics^(c), Nanjing, CN - Jiangsu 210093; Shandong University, High Energy Physics Group^(d), Jinan, CN - Shandong 250100, China
- ³³ Laboratoire de Physique Corpusculaire, Clermont Université, Université Blaise Pascal, CNRS/IN2P3, FR - 63177 Aubiere Cedex, France
- ³⁴ Columbia University, Nevis Laboratory, 136 So. Broadway, Irvington, NY 10533, United States of America
- ³⁵ University of Copenhagen, Niels Bohr Institute, Blegdamsvej 17, DK - 2100 Kobenhavn 0, Denmark
- ³⁶ INFN Gruppo Collegato di Cosenza^(a); Università della Calabria, Dipartimento di Fisica^(b), IT-87036 Arcavacata di Rende, Italy
- ³⁷ Faculty of Physics and Applied Computer Science of the AGH-University of Science and Technology, (FPACS, AGH-UST), al. Mickiewicza 30, PL-30059 Cracow, Poland
- ³⁸ The Henryk Niewodniczanski Institute of Nuclear Physics, Polish Academy of Sciences, ul. Radzikowskiego 152, PL - 31342 Krakow, Poland
- ³⁹ Southern Methodist University, Physics Department, 106 Fondren Science Building, Dallas, TX 75275-0175, United States of America
- ⁴⁰ University of Texas at Dallas, 800 West Campbell Road, Richardson, TX 75080-3021, United States of America
- ⁴¹ DESY, Notkestr. 85, D-22603 Hamburg and Platanenallee 6, D-15738 Zeuthen, Germany
- ⁴² TU Dortmund, Experimentelle Physik IV, DE - 44221 Dortmund, Germany
- ⁴³ Technical University Dresden, Institut für Kern- und Teilchenphysik, Zellescher Weg 19, D-01069 Dresden, Germany
- ⁴⁴ Duke University, Department of Physics, Durham, NC 27708, United States of America
- ⁴⁵ University of Edinburgh, School of Physics & Astronomy, James Clerk Maxwell Building, The Kings Buildings, Mayfield Road, Edinburgh EH9 3JZ, United Kingdom
- ⁴⁶ Fachhochschule Wiener Neustadt; Johannes Gutenbergstrasse 3 AT - 2700 Wiener Neustadt, Austria
- ⁴⁷ INFN Laboratori Nazionali di Frascati, via Enrico Fermi 40, IT-00044 Frascati, Italy
- ⁴⁸ Albert-Ludwigs-Universität, Fakultät für Mathematik und Physik, Hermann-Herder Str. 3, D - 79104 Freiburg i.Br., Germany
- ⁴⁹ Université de Genève, Section de Physique, 24 rue Ernest Ansermet, CH - 1211 Geneve 4, Switzerland
- ⁵⁰ INFN Sezione di Genova^(a); Università di Genova, Dipartimento di Fisica^(b), via Dodecaneso 33, IT - 16146

Genova, Italy

⁵¹ Institute of Physics of the Georgian Academy of Sciences, 6 Tamarashvili St., GE - 380077 Tbilisi; Tbilisi State University, HEP Institute, University St. 9, GE - 380086 Tbilisi, Georgia

⁵² Justus-Liebig-Universität Giessen, II Physikalisches Institut, Heinrich-Buff Ring 16, D-35392 Giessen, Germany

⁵³ University of Glasgow, Department of Physics and Astronomy, Glasgow G12 8QQ, United Kingdom

⁵⁴ Georg-August-Universität, II. Physikalisches Institut, Friedrich-Hund Platz 1, D-37077 Göttingen, Germany

⁵⁵ LPSC, CNRS/IN2P3 and Univ. Joseph Fourier Grenoble, 53 avenue des Martyrs, FR-38026 Grenoble Cedex, France

⁵⁶ Hampton University, Department of Physics, Hampton, VA 23668, United States of America

⁵⁷ Harvard University, Laboratory for Particle Physics and Cosmology, 18 Hammond Street, Cambridge, MA 02138, United States of America

⁵⁸ Ruprecht-Karls-Universität Heidelberg: Kirchhoff-Institut für Physik^(a), Im Neuenheimer Feld 227, D-69120 Heidelberg; Physikalisches Institut^(b), Philosophenweg 12, D-69120 Heidelberg; ZITI Ruprecht-Karls-Universität Heidelberg^(c), Lehrstuhl für Informatik V, B6, 23-29, DE - 68131 Mannheim, Germany

⁵⁹ Hiroshima University, Faculty of Science, 1-3-1 Kagamiyama, Higashihiroshima-shi, JP - Hiroshima 739-8526, Japan

⁶⁰ Hiroshima Institute of Technology, Faculty of Applied Information Science, 2-1-1 Miyake Saeki-ku, Hiroshima-shi, JP - Hiroshima 731-5193, Japan

⁶¹ Indiana University, Department of Physics, Swain Hall West 117, Bloomington, IN 47405-7105, United States of America

⁶² Institut für Astro- und Teilchenphysik, Technikerstrasse 25, A - 6020 Innsbruck, Austria

⁶³ University of Iowa, 203 Van Allen Hall, Iowa City, IA 52242-1479, United States of America

⁶⁴ Iowa State University, Department of Physics and Astronomy, Ames High Energy Physics Group, Ames, IA 50011-3160, United States of America

⁶⁵ Joint Institute for Nuclear Research, JINR Dubna, RU-141980 Moscow Region, Russia, Russia

⁶⁶ KEK, High Energy Accelerator Research Organization, 1-1 Oho, Tsukuba-shi, Ibaraki-ken 305-0801, Japan

⁶⁷ Kobe University, Graduate School of Science, 1-1 Rokkodai-cho, Nada-ku, JP Kobe 657-8501, Japan

⁶⁸ Kyoto University, Faculty of Science, Oiwake-cho, Kitashirakawa, Sakyou-ku, Kyoto-shi, JP - Kyoto 606-8502, Japan

⁶⁹ Kyoto University of Education, 1 Fukakusa, Fujimori, fushimi-ku, Kyoto-shi, JP - Kyoto 612-8522, Japan

⁷⁰ Universidad Nacional de La Plata, FCE, Departamento de Física, IFLP (CONICET-UNLP), C.C. 67, 1900 La Plata, Argentina

⁷¹ Lancaster University, Physics Department, Lancaster LA1 4YB, United Kingdom

⁷² INFN Sezione di Lecce^(a); Università del Salento, Dipartimento di Fisica^(b) Via Arnesano IT - 73100 Lecce, Italy

⁷³ University of Liverpool, Oliver Lodge Laboratory, P.O. Box 147, Oxford Street, Liverpool L69 3BX, United Kingdom

⁷⁴ Jožef Stefan Institute and University of Ljubljana, Department of Physics, SI-1000 Ljubljana, Slovenia

⁷⁵ Queen Mary University of London, Department of Physics, Mile End Road, London E1 4NS, United Kingdom

⁷⁶ Royal Holloway, University of London, Department of Physics, Egham Hill, Egham, Surrey TW20 0EX, United Kingdom

⁷⁷ University College London, Department of Physics and Astronomy, Gower Street, London WC1E 6BT, United Kingdom

⁷⁸ Laboratoire de Physique Nucléaire et de Hautes Energies, Université Pierre et Marie Curie (Paris 6), Université Denis Diderot (Paris-7), CNRS/IN2P3, Tour 33, 4 place Jussieu, FR - 75252 Paris Cedex 05, France

⁷⁹ Fysiska institutionen, Lunds universitet, Box 118, SE - 221 00 Lund, Sweden

⁸⁰ Universidad Autonoma de Madrid, Facultad de Ciencias, Departamento de Física Teórica, ES - 28049 Madrid, Spain

⁸¹ Universität Mainz, Institut für Physik, Staudinger Weg 7, DE - 55099 Mainz, Germany

⁸² University of Manchester, School of Physics and Astronomy, Manchester M13 9PL, United Kingdom

⁸³ CPPM, Aix-Marseille Université, CNRS/IN2P3, Marseille, France

⁸⁴ University of Massachusetts, Department of Physics, 710 North Pleasant Street, Amherst, MA 01003, United States of America

⁸⁵ McGill University, High Energy Physics Group, 3600 University Street, Montreal, Quebec H3A 2T8, Canada

⁸⁶ University of Melbourne, School of Physics, AU - Parkville, Victoria 3010, Australia

⁸⁷ The University of Michigan, Department of Physics, 2477 Randall Laboratory, 500 East University, Ann Arbor, MI 48109-1120, United States of America

⁸⁸ Michigan State University, Department of Physics and Astronomy, High Energy Physics Group, East Lansing, MI 48824-2320, United States of America

- ⁸⁹ INFN Sezione di Milano^(a); Università di Milano, Dipartimento di Fisica^(b), via Celoria 16, IT - 20133 Milano, Italy
- ⁹⁰ B.I. Stepanov Institute of Physics, National Academy of Sciences of Belarus, Independence Avenue 68, Minsk 220072, Republic of Belarus
- ⁹¹ National Scientific & Educational Centre for Particle & High Energy Physics, NC PHEP BSU, M. Bogdanovich St. 153, Minsk 220040, Republic of Belarus
- ⁹² Massachusetts Institute of Technology, Department of Physics, Room 24-516, Cambridge, MA 02139, United States of America
- ⁹³ University of Montreal, Group of Particle Physics, C.P. 6128, Succursale Centre-Ville, Montreal, Quebec, H3C 3J7, Canada
- ⁹⁴ P.N. Lebedev Institute of Physics, Academy of Sciences, Leninsky pr. 53, RU - 117 924 Moscow, Russia
- ⁹⁵ Institute for Theoretical and Experimental Physics (ITEP), B. Cheremushkinskaya ul. 25, RU 117 218 Moscow, Russia
- ⁹⁶ Moscow Engineering & Physics Institute (MEPhI), Kashirskoe Shosse 31, RU - 115409 Moscow, Russia
- ⁹⁷ Lomonosov Moscow State University Skobeltsyn Institute of Nuclear Physics (MSU SINP), 1(2), Leninskie gory, GSP-1, Moscow 119991 Russian Federation, Russia
- ⁹⁸ Ludwig-Maximilians-Universität München, Fakultät für Physik, Am Coulombwall 1, DE - 85748 Garching, Germany
- ⁹⁹ Max-Planck-Institut für Physik, (Werner-Heisenberg-Institut), Föhringer Ring 6, 80805 München, Germany
- ¹⁰⁰ Nagasaki Institute of Applied Science, 536 Aba-machi, JP Nagasaki 851-0193, Japan
- ¹⁰¹ Nagoya University, Graduate School of Science, Furo-Cho, Chikusa-ku, Nagoya, 464-8602, Japan
- ¹⁰² INFN Sezione di Napoli^(a); Università di Napoli, Dipartimento di Scienze Fisiche^(b), Complesso Universitario di Monte Sant'Angelo, via Cinthia, IT - 80126 Napoli, Italy
- ¹⁰³ University of New Mexico, Department of Physics and Astronomy, MSC07 4220, Albuquerque, NM 87131 USA, United States of America
- ¹⁰⁴ Radboud University Nijmegen/NIKHEF, Department of Experimental High Energy Physics, Heyendaalseweg 135, NL-6525 AJ, Nijmegen, Netherlands
- ¹⁰⁵ Nikhef National Institute for Subatomic Physics, and University of Amsterdam, Science Park 105, 1098 XG Amsterdam, Netherlands
- ¹⁰⁶ Department of Physics, Northern Illinois University, LaTourette Hall Normal Road, DeKalb, IL 60115, United States of America
- ¹⁰⁷ Budker Institute of Nuclear Physics (BINP), RU - Novosibirsk 630 090, Russia
- ¹⁰⁸ New York University, Department of Physics, 4 Washington Place, New York NY 10003, USA, United States of America
- ¹⁰⁹ Ohio State University, 191 West Woodruff Ave, Columbus, OH 43210-1117, United States of America
- ¹¹⁰ Okayama University, Faculty of Science, Tsushimanaka 3-1-1, Okayama 700-8530, Japan
- ¹¹¹ University of Oklahoma, Homer L. Dodge Department of Physics and Astronomy, 440 West Brooks, Room 100, Norman, OK 73019-0225, United States of America
- ¹¹² Oklahoma State University, Department of Physics, 145 Physical Sciences Building, Stillwater, OK 74078-3072, United States of America
- ¹¹³ Palacký University, 17.listopadu 50a, 772 07 Olomouc, Czech Republic
- ¹¹⁴ University of Oregon, Center for High Energy Physics, Eugene, OR 97403-1274, United States of America
- ¹¹⁵ LAL, Univ. Paris-Sud, IN2P3/CNRS, Orsay, France
- ¹¹⁶ Osaka University, Graduate School of Science, Machikaneyama-machi 1-1, Toyonaka, Osaka 560-0043, Japan
- ¹¹⁷ University of Oslo, Department of Physics, P.O. Box 1048, Blindern, NO - 0316 Oslo 3, Norway
- ¹¹⁸ Oxford University, Department of Physics, Denys Wilkinson Building, Keble Road, Oxford OX1 3RH, United Kingdom
- ¹¹⁹ INFN Sezione di Pavia^(a); Università di Pavia, Dipartimento di Fisica Nucleare e Teorica^(b), Via Bassi 6, IT-27100 Pavia, Italy
- ¹²⁰ University of Pennsylvania, Department of Physics, High Energy Physics Group, 209 S. 33rd Street, Philadelphia, PA 19104, United States of America
- ¹²¹ Petersburg Nuclear Physics Institute, RU - 188 300 Gatchina, Russia
- ¹²² INFN Sezione di Pisa^(a); Università di Pisa, Dipartimento di Fisica E. Fermi^(b), Largo B. Pontecorvo 3, IT - 56127 Pisa, Italy
- ¹²³ University of Pittsburgh, Department of Physics and Astronomy, 3941 O'Hara Street, Pittsburgh, PA 15260, United States of America
- ¹²⁴ Laboratorio de Instrumentacao e Fisica Experimental de Particulas - LIP^(a), Avenida Elias Garcia 14-1, PT - 1000-149 Lisboa, Portugal; Universidad de Granada, Departamento de Fisica Teorica y del Cosmos and CAFPE^(b),

E-18071 Granada, Spain

¹²⁵ Institute of Physics, Academy of Sciences of the Czech Republic, Na Slovance 2, CZ - 18221 Praha 8, Czech Republic

¹²⁶ Charles University in Prague, Faculty of Mathematics and Physics, Institute of Particle and Nuclear Physics, V Holesovickach 2, CZ - 18000 Praha 8, Czech Republic

¹²⁷ Czech Technical University in Prague, Zikova 4, CZ - 166 35 Praha 6, Czech Republic

¹²⁸ State Research Center Institute for High Energy Physics, Moscow Region, 142281, Protvino, Pobeda street, 1, Russia

¹²⁹ Rutherford Appleton Laboratory, Science and Technology Facilities Council, Harwell Science and Innovation Campus, Didcot OX11 0QX, United Kingdom

¹³⁰ University of Regina, Physics Department, Canada

¹³¹ Ritsumeikan University, Noji Higashi 1 chome 1-1, JP - Kusatsu, Shiga 525-8577, Japan

¹³² INFN Sezione di Roma I^(a); Università La Sapienza, Dipartimento di Fisica^(b), Piazzale A. Moro 2, IT- 00185 Roma, Italy

¹³³ INFN Sezione di Roma Tor Vergata^(a); Università di Roma Tor Vergata, Dipartimento di Fisica^(b), via della Ricerca Scientifica, IT-00133 Roma, Italy

¹³⁴ INFN Sezione di Roma Tre^(a); Università Roma Tre, Dipartimento di Fisica^(b), via della Vasca Navale 84, IT-00146 Roma, Italy

¹³⁵ Réseau Universitaire de Physique des Hautes Energies (RUPHE): Université Hassan II, Faculté des Sciences Ain Chock^(a), B.P. 5366, MA - Casablanca; Centre National de l'Energie des Sciences Techniques Nucleaires (CNESTEN)^(b), B.P. 1382 R.P. 10001 Rabat 10001; Université Mohamed Premier^(c), LPTPM, Faculté des Sciences, B.P.717. Bd. Mohamed VI, 60000, Oujda ; Université Mohammed V, Faculté des Sciences^(d) 4 Avenue Ibn Battouta, BP 1014 RP, 10000 Rabat, Morocco

¹³⁶ CEA, DSM/IRFU, Centre d'Etudes de Saclay, FR - 91191 Gif-sur-Yvette, France

¹³⁷ University of California Santa Cruz, Santa Cruz Institute for Particle Physics (SCIPP), Santa Cruz, CA 95064, United States of America

¹³⁸ University of Washington, Seattle, Department of Physics, Box 351560, Seattle, WA 98195-1560, United States of America

¹³⁹ University of Sheffield, Department of Physics & Astronomy, Hounsfield Road, Sheffield S3 7RH, United Kingdom

¹⁴⁰ Shinshu University, Department of Physics, Faculty of Science, 3-1-1 Asahi, Matsumoto-shi, JP - Nagano 390-8621, Japan

¹⁴¹ Universität Siegen, Fachbereich Physik, D 57068 Siegen, Germany

¹⁴² Simon Fraser University, Department of Physics, 8888 University Drive, CA - Burnaby, BC V5A 1S6, Canada

¹⁴³ SLAC National Accelerator Laboratory, Stanford, California 94309, United States of America

¹⁴⁴ Comenius University, Faculty of Mathematics, Physics & Informatics^(a), Mlynska dolina F2, SK - 84248 Bratislava; Institute of Experimental Physics of the Slovak Academy of Sciences, Dept. of Subnuclear Physics^(b), Watsonova 47, SK - 04353 Kosice, Slovak Republic

¹⁴⁵ ^(a)University of Johannesburg, Department of Physics, PO Box 524, Auckland Park, Johannesburg 2006;

^(b)School of Physics, University of the Witwatersrand, Private Bag 3, Wits 2050, Johannesburg, South Africa, South Africa

¹⁴⁶ Stockholm University: Department of Physics^(a); The Oskar Klein Centre^(b), AlbaNova, SE - 106 91 Stockholm, Sweden

¹⁴⁷ Royal Institute of Technology (KTH), Physics Department, SE - 106 91 Stockholm, Sweden

¹⁴⁸ Stony Brook University, Department of Physics and Astronomy, Nicolls Road, Stony Brook, NY 11794-3800, United States of America

¹⁴⁹ University of Sussex, Department of Physics and Astronomy Pevensey 2 Building, Falmer, Brighton BN1 9QH, United Kingdom

¹⁵⁰ University of Sydney, School of Physics, AU - Sydney NSW 2006, Australia

¹⁵¹ Insitute of Physics, Academia Sinica, TW - Taipei 11529, Taiwan

¹⁵² Technion, Israel Inst. of Technology, Department of Physics, Technion City, IL - Haifa 32000, Israel

¹⁵³ Tel Aviv University, Raymond and Beverly Sackler School of Physics and Astronomy, Ramat Aviv, IL - Tel Aviv 69978, Israel

¹⁵⁴ Aristotle University of Thessaloniki, Faculty of Science, Department of Physics, Division of Nuclear & Particle Physics, University Campus, GR - 54124, Thessaloniki, Greece

¹⁵⁵ The University of Tokyo, International Center for Elementary Particle Physics and Department of Physics, 7-3-1 Hongo, Bunkyo-ku, JP - Tokyo 113-0033, Japan

¹⁵⁶ Tokyo Metropolitan University, Graduate School of Science and Technology, 1-1 Minami-Osawa, Hachioji, Tokyo

192-0397, Japan

¹⁵⁷ Tokyo Institute of Technology, Department of Physics, 2-12-1 O-Okayama, Meguro, Tokyo 152-8551, Japan

¹⁵⁸ University of Toronto, Department of Physics, 60 Saint George Street, Toronto M5S 1A7, Ontario, Canada

¹⁵⁹ TRIUMF^(a), 4004 Wesbrook Mall, Vancouver, B.C. V6T 2A3; ^(b)York University, Department of Physics and Astronomy, 4700 Keele St., Toronto, Ontario, M3J 1P3, Canada

¹⁶⁰ University of Tsukuba, Institute of Pure and Applied Sciences, 1-1-1 Tennoudai, Tsukuba-shi, JP - Ibaraki 305-8571, Japan

¹⁶¹ Tufts University, Science & Technology Center, 4 Colby Street, Medford, MA 02155, United States of America

¹⁶² Universidad Antonio Narino, Centro de Investigaciones, Cra 3 Este No.47A-15, Bogota, Colombia

¹⁶³ University of California, Irvine, Department of Physics & Astronomy, CA 92697-4575, United States of America

¹⁶⁴ INFN Gruppo Collegato di Udine^(a); ICTP^(b), Strada Costiera 11, IT-34014, Trieste; Università di Udine, Dipartimento di Fisica^(c), via delle Scienze 208, IT - 33100 Udine, Italy

¹⁶⁵ University of Illinois, Department of Physics, 1110 West Green Street, Urbana, Illinois 61801, United States of America

¹⁶⁶ University of Uppsala, Department of Physics and Astronomy, P.O. Box 516, SE -751 20 Uppsala, Sweden

¹⁶⁷ Instituto de Física Corpuscular (IFIC) Centro Mixto UVEG-CSIC, Apdo. 22085 ES-46071 Valencia, Dept. Física At. Mol. y Nuclear; Dept. Ing. Electrónica; Univ. of Valencia, and Inst. de Microelectrónica de Barcelona (IMB-CNM-CSIC) 08193 Bellaterra, Spain

¹⁶⁸ University of British Columbia, Department of Physics, 6224 Agricultural Road, CA - Vancouver, B.C. V6T 1Z1, Canada

¹⁶⁹ University of Victoria, Department of Physics and Astronomy, P.O. Box 3055, Victoria B.C., V8W 3P6, Canada

¹⁷⁰ Waseda University, WISE, 3-4-1 Okubo, Shinjuku-ku, Tokyo, 169-8555, Japan

¹⁷¹ The Weizmann Institute of Science, Department of Particle Physics, P.O. Box 26, IL - 76100 Rehovot, Israel

¹⁷² University of Wisconsin, Department of Physics, 1150 University Avenue, WI 53706 Madison, Wisconsin, United States of America

¹⁷³ Julius-Maximilians-University of Würzburg, Physikalisches Institute, Am Hubland, 97074 Würzburg, Germany

¹⁷⁴ Bergische Universität, Fachbereich C, Physik, Postfach 100127, Gauss-Strasse 20, D- 42097 Wuppertal, Germany

¹⁷⁵ Yale University, Department of Physics, PO Box 208121, New Haven CT, 06520-8121, United States of America

¹⁷⁶ Yerevan Physics Institute, Alikhanian Brothers Street 2, AM - 375036 Yerevan, Armenia

¹⁷⁷ Centre de Calcul CNRS/IN2P3, Domaine scientifique de la Doua, 27 bd du 11 Novembre 1918, 69622 Villeurbanne Cedex, France

^a Also at LIP, Portugal

^b Also at Faculdade de Ciencias, Universidade de Lisboa, Portugal

^c Also at CPPM, Marseille, France.

^d Also at Centro de Física Nuclear da Universidade de Lisboa, Portugal

^e Also at TRIUMF, Vancouver, Canada

^f Also at FPACS, AGH-UST, Cracow, Poland

^g Now at Università dell'Insubria, Dipartimento di Fisica e Matematica

^h Also at Department of Physics, University of Coimbra, Portugal

ⁱ Now at CERN

^j Also at Università di Napoli Parthenope, Napoli, Italy

^k Also at Institute of Particle Physics (IPP), Canada

^l Also at Università di Napoli Parthenope, via A. Acton 38, IT - 80133 Napoli, Italy

^m Louisiana Tech University, 305 Wisteria Street, P.O. Box 3178, Ruston, LA 71272, United States of America

ⁿ Also at Universidade de Lisboa, Portugal

^o At California State University, Fresno, USA

^p Also at TRIUMF, 4004 Wesbrook Mall, Vancouver, B.C. V6T 2A3, Canada

^q Also at Faculdade de Ciencias, Universidade de Lisboa, Portugal and at Centro de Física Nuclear da Universidade de Lisboa, Portugal

^r Also at FPACS, AGH-UST, Cracow, Poland

^s Also at California Institute of Technology, Pasadena, USA

^t Louisiana Tech University, Ruston, USA

^u Also at University of Montreal, Montreal, Canada

^v Now at Chonnam National University, Chonnam, Korea 500-757

^w Also at Institut für Experimentalphysik, Universität Hamburg, Luruper Chaussee 149, 22761 Hamburg, Germany

^x Also at Manhattan College, NY, USA

^y Also at School of Physics and Engineering, Sun Yat-sen University, China

^z Also at Taiwan Tier-1, ASGC, Academia Sinica, Taipei, Taiwan

- aa* Also at School of Physics, Shandong University, Jinan, China
- ab* Also at California Institute of Technology, Pasadena, USA
- ac* Also at Rutherford Appleton Laboratory, Didcot, UK
- ad* Also at school of physics, Shandong University, Jinan
- ae* Also at Rutherford Appleton Laboratory, Didcot , UK
- af* Also at TRIUMF, Vancouver, Canada
- ag* Now at KEK
- ah* Also at Departamento de Fisica, Universidade de Minho, Portugal
- ai* University of South Carolina, Columbia, USA
- aj* Also at KFKI Research Institute for Particle and Nuclear Physics, Budapest, Hungary
- ak* University of South Carolina, Dept. of Physics and Astronomy, 700 S. Main St, Columbia, SC 29208, United States of America
- al* Also at Institute of Physics, Jagiellonian University, Cracow, Poland
- am* Louisiana Tech University, Ruston, USA
- an* Also at Institut für Experimentalphysik, Universität Hamburg, Hamburg, Germany
- ao* University of South Carolina, Columbia, USA
- ap* Transfer to LHCb 31.01.2010
- aq* Also at Oxford University, Department of Physics, Denys Wilkinson Building, Keble Road, Oxford OX1 3RH, United Kingdom
- ar* Also at school of physics and engineering, Sun Yat-sen University, China
- as* Determine the Muon T0s using 2009 and 2010 beam splash events for MDT chambers and for each mezzanine card, starting from 2009/09/15
- at* Also at CEA
- au* Also at LPNHE, Paris, France
- av* has been working on Muon MDT noise study and calibration since 2009/10, contact as Tiesheng Dai and Muon convener
- aw* Also at Nanjing University, China
- * Deceased